Imperial College London

Boundary layer control

Summer School on Sustainable Aviation

UTIAS

May 16-17, 2016

Jonathan Morrison
Department of Aeronautics
Imperial College
http://www.imperial.ac.uk/people/j.morrison
http://www.imperial.ac.uk/aeflowcontrol
http://www.smartwingdesign.org/
http://www.nwtf.ac.uk/html/index.html

Drag reduction

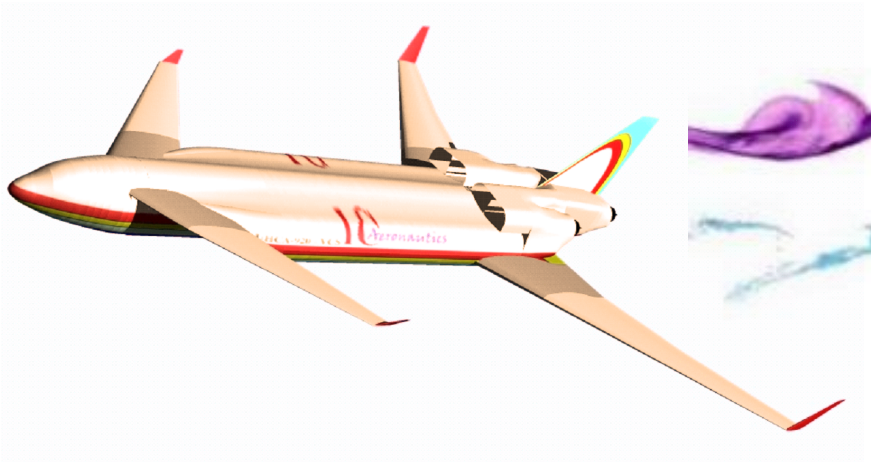

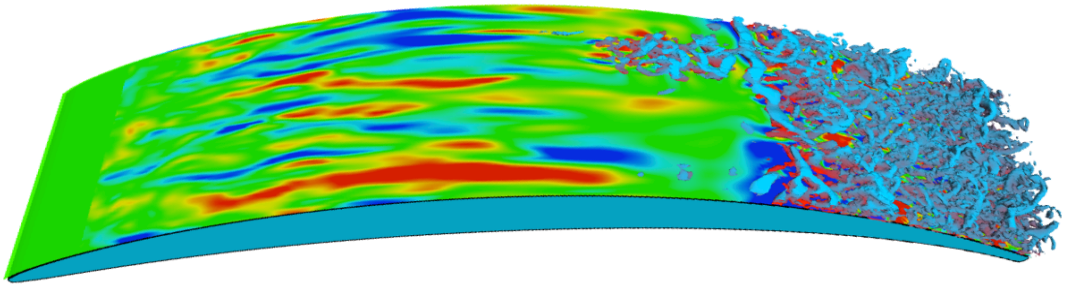

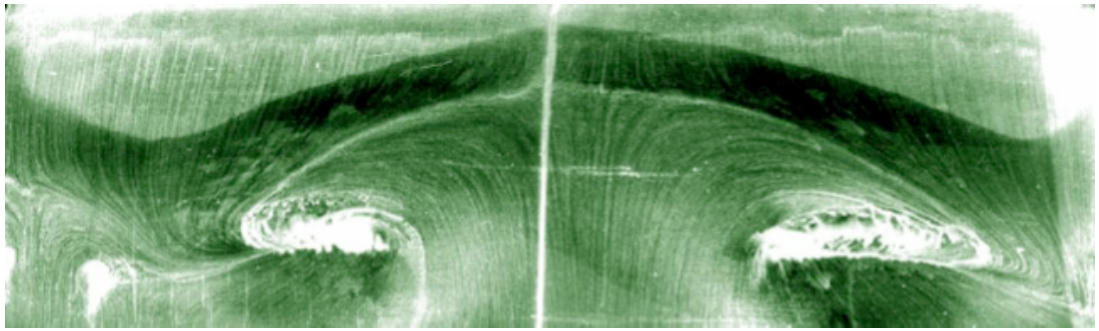

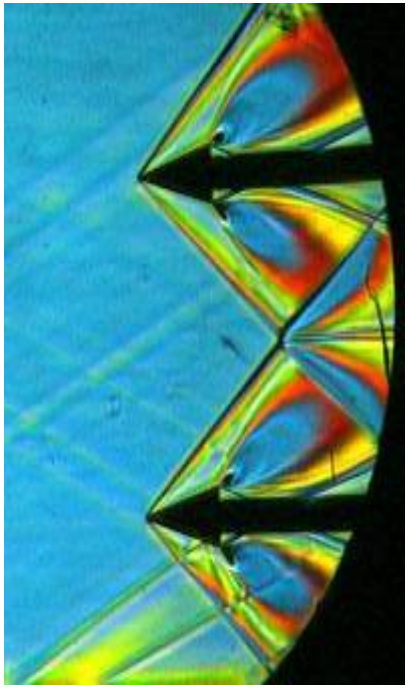

Friction drag reduction

Acknowledgements:

Hari Vemuri
Richard Bosworth
Eric Kerrigan
Mike Gaster (City University)

Kevin Gouder
Phil Lavoie (UTIAS)
Ahmed Naguib (Michigan State U.)

Kamthon Septham
Ati Sharma (Southampton U.)

James Bird
Matthew Santer

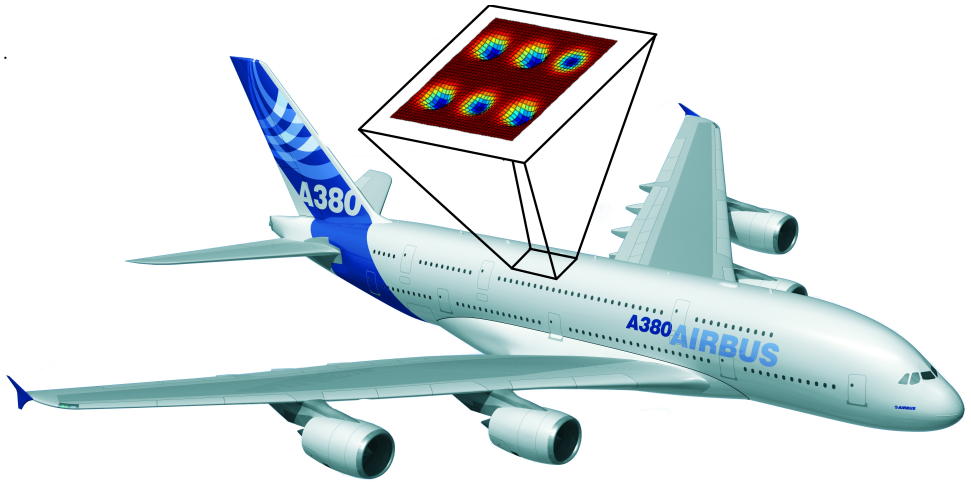

EPSRC
Engineering and Physical Sciences Research Council

Royal Thai Government

Outline

Four control challenges:

- Tollmien-Schlichting (TS) wave cancellation
- Transient growth: a linear paradigm for near-wall turbulence control
- Role of linear feedback in the control of turbulent channel flow
- Open-loop control and travelling surface waves for turbulent skin-friction reduction

Some preliminaries

- Why use feedback control?
- How far can we take linear control?
- Why have a physical model?
- Can we use wall shear stress or wall pressure for estimation?

Requirements for effective control: linear control

- Feedback control to improve the efficiency of fluid-based systems – in this course, the driver is the reduction of drag and CO_2.
- Feedback control provides a theoretical framework for dealing with the effects of uncertainty, energy efficiency (e.g. minimal actuator duty cycle) and system retuning for given conditions.
- Navier-Stokes equations are inherently nonlinear
  - Require small perturbations to linearise
  - Or make use of nonlinear terms being conservative (with restrictions)

Linear control

- At its simplest we have a Plant (the NS equations + the input $u(t)$) with output $y(t)$ and controller, K.
- We approximate P using a state space matrix A, vector $x(t)$, where A models the flow and B models the input from K. C is a sensor transfer function, $y(t)=Cx(t)$.

$$\dot{x} = Ax + Bu$$

$$y = Cx$$

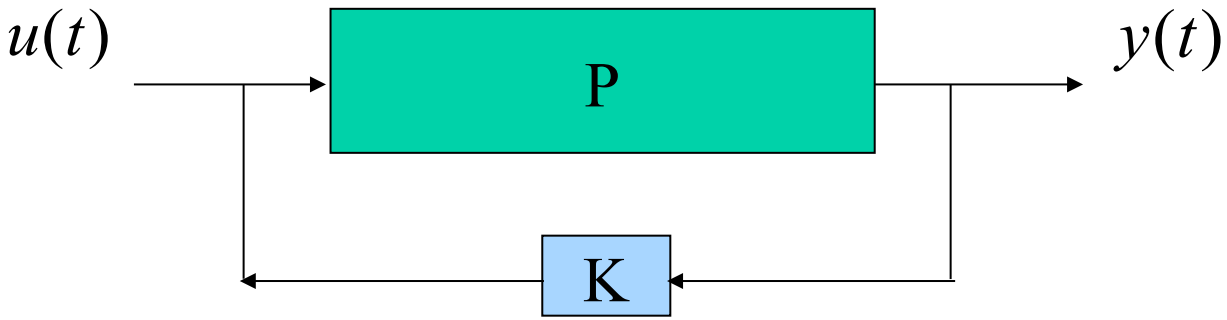

Feedforward / feedback control

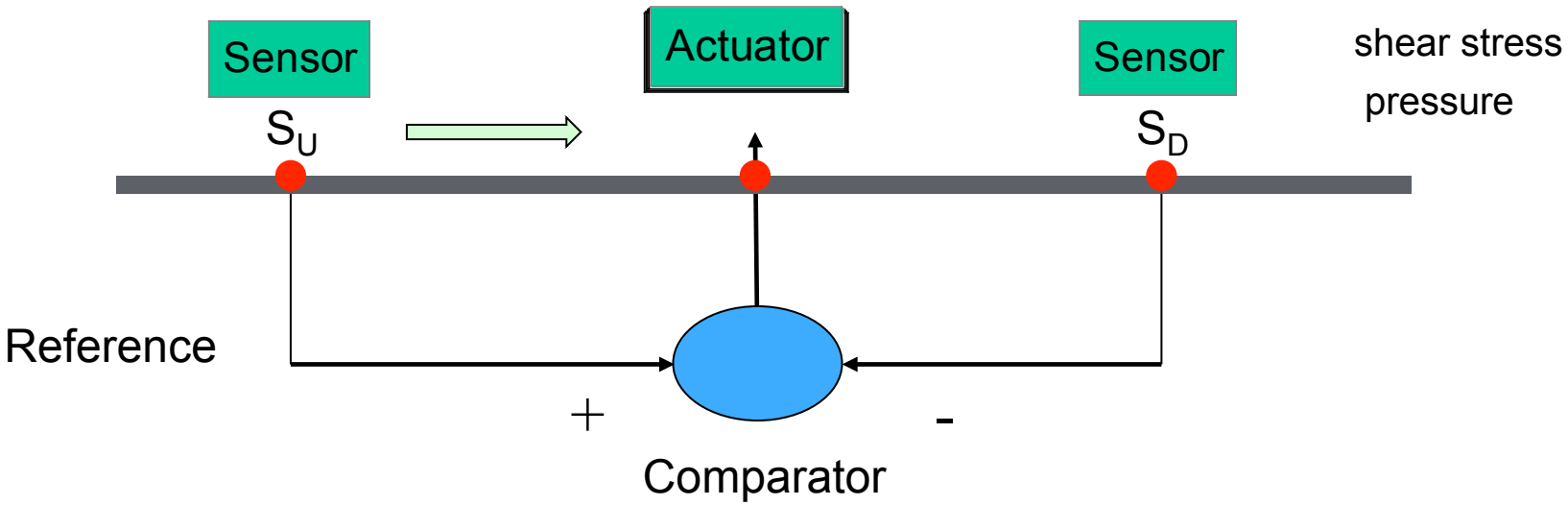

- Require some means of assessing flow at actuator based on measurement at upstream sensor, S_U.
- Information from S_D fed back to compare with reference.

Why feedback control?

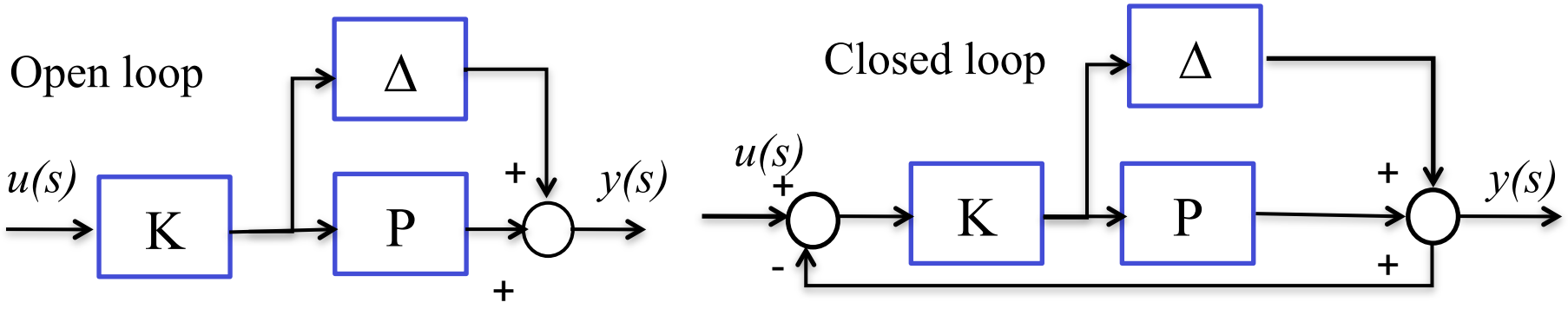

$$y(s) = \int_0^\infty y(t)e^{-st}dt$$

- Plant P, to be controlled by controller K.
- Transfer function $G(s)=y(s)/u(s)$
- Open loop: $G(s)=K(P+\Delta)$ Closed loop: $G(s) = \frac{K(P+\Delta)}{1+K(P+\Delta)}$
- Good tracking requires $G(s)=1$.
- Open loop: $K=1/(P+\Delta)$ Closed loop: $K>>1$
- Feedback control provides control in spite of system uncertainty.

Requirements for effective control: a model

- "No-free-lunch" theorem (Ho & Pepyne 2002): without the benefit of prior knowledge (i.e. a physically based model), no control strategy can be expected to out-perform any other.
- In the case of TS waves, model is straightforward
  - They are deterministic and completely described by the linear Orr – Sommerfeld equation
  - With some limitations: receptivity is a challenge – a resonance condition between any two of three possible types of disturbance
    - Vorticity
    - Noise
    - Roughness
- For larger disturbances, modal transition is "bypassed" – use of a linear, reduced-order equation.

TS waves and Orr-Sommerfeld (OS) equation

- 2D small perturbation velocity in 2D base flow (Blasius boundary layer): $\mathbf{u}' = \left(u'(x,y), v'(x,y), 0\right) = \nabla \times \boldsymbol{\psi}'$

  where stream function is $u' = \dfrac{\partial \boldsymbol{\psi}'}{\partial y}$, $v' = -\dfrac{\partial \boldsymbol{\psi}'}{\partial x}$
- Parallel flow approximation
- Decompose $\boldsymbol{\psi}'$ using normal modes $\boldsymbol{\psi}' = \boldsymbol{\phi}(y)\exp\left(i(\boldsymbol{\alpha}x - \boldsymbol{\omega}t)\right)$
- Spatially stability more relevant to practical problems for flow control
- Assume ω and R are given and real
- Linear, 4th – order ODE in $\alpha=\omega/c$:

$$(U-c)(\boldsymbol{\phi}'' - \boldsymbol{\alpha}^2\boldsymbol{\phi}) - U''\boldsymbol{\phi} = -\frac{i}{\boldsymbol{\alpha}R}\left(\boldsymbol{\phi}'''' - 2\boldsymbol{\alpha}^2\boldsymbol{\phi}'' + \boldsymbol{\alpha}^4\boldsymbol{\phi}\right)$$

Boundary layer – 2D spatial stability

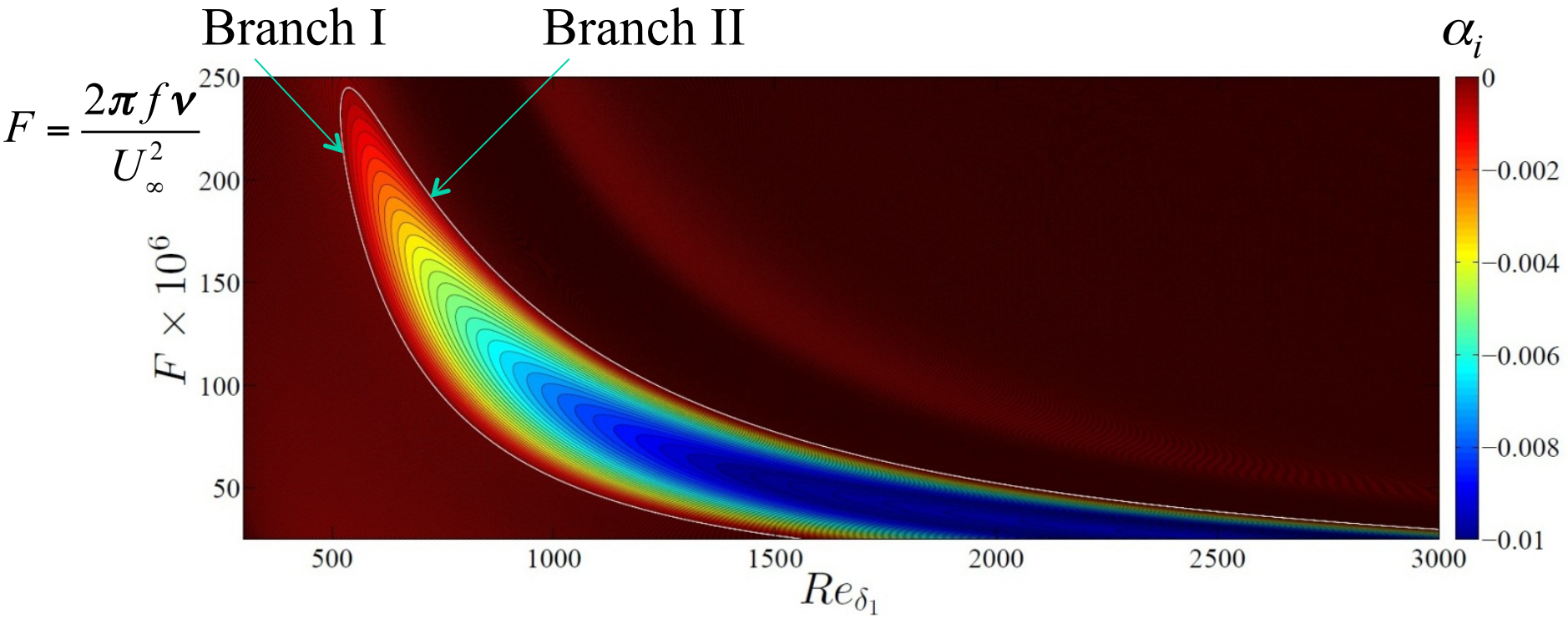

- Eigenvalue problem: find complex α for given real ω and R
- Above curves are contours of α_i: branches I and II denote neutral growth, $\alpha_i = 0$, unstable growth $\alpha_i < 0$.
- Dispersion relation $D(\alpha, \omega, R) = 0$, $c = \omega/\alpha$

Numerical Results: TS waves – 2D

2D source:150 Hz sinusoidal forcing, Re_{δ_1}(source) = 875

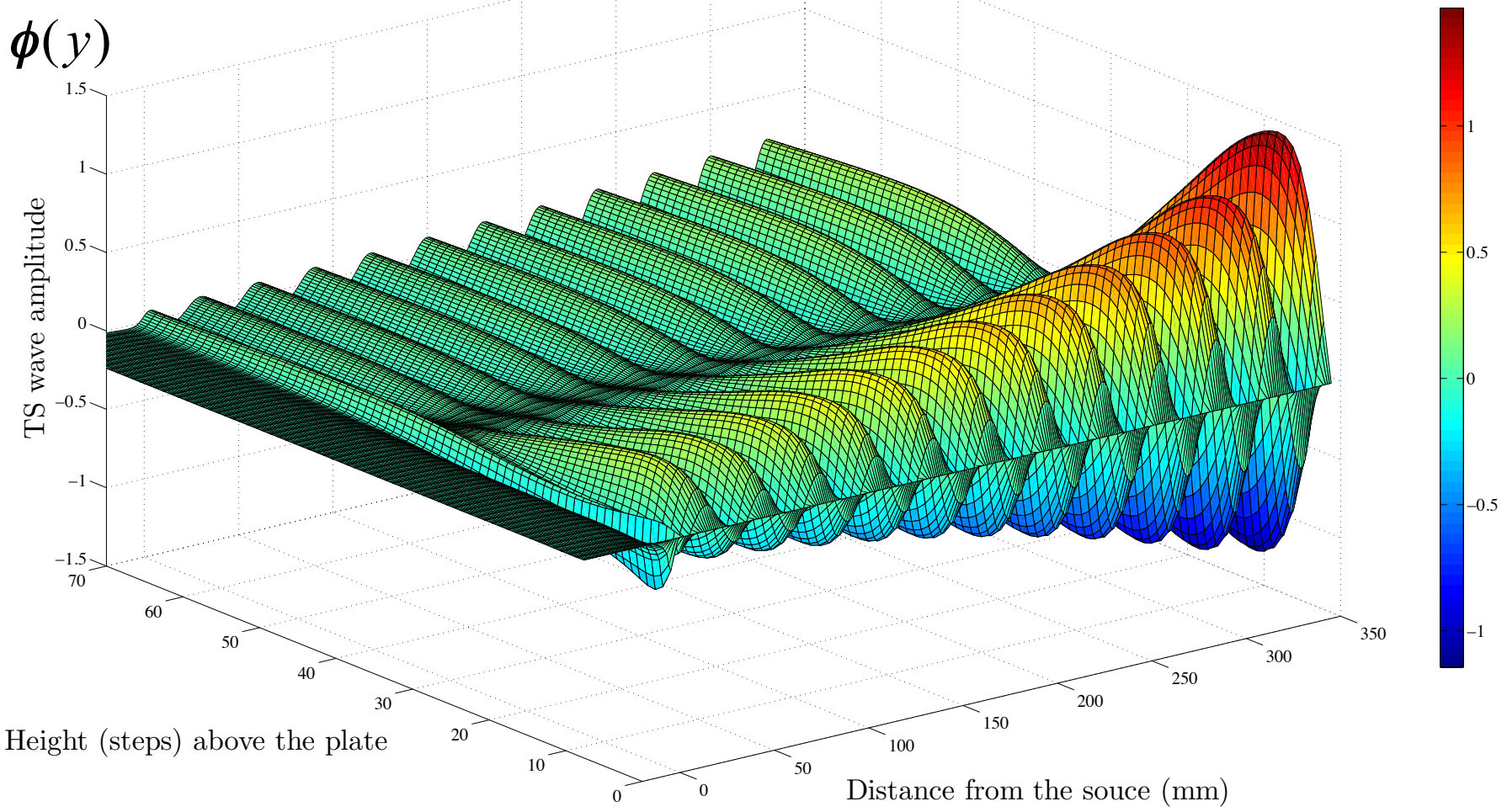

Numerical Results: TS waves – 3D

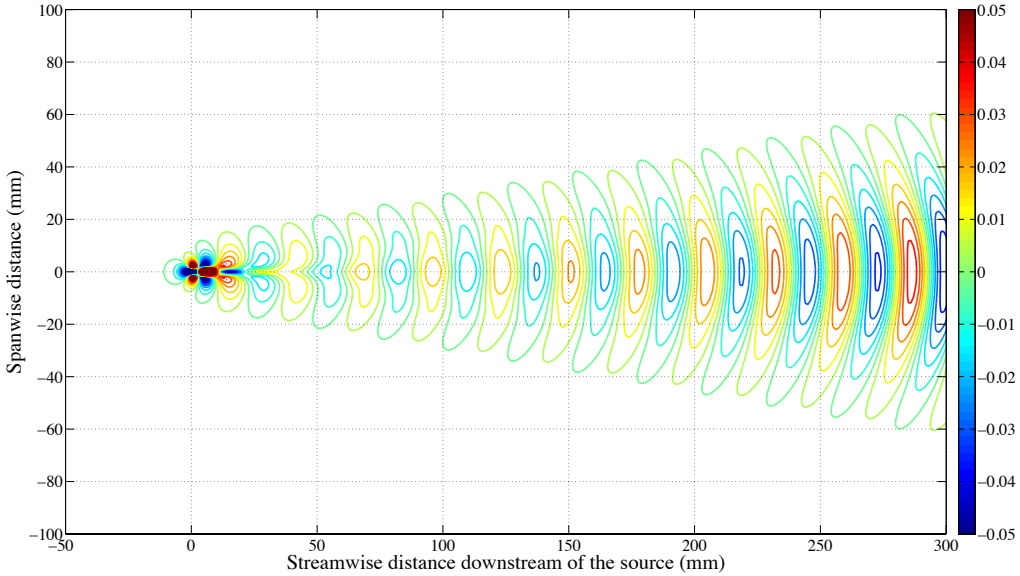

Squire's theorem: as Re increases, first appearance of instability occurs in 2D before 3D

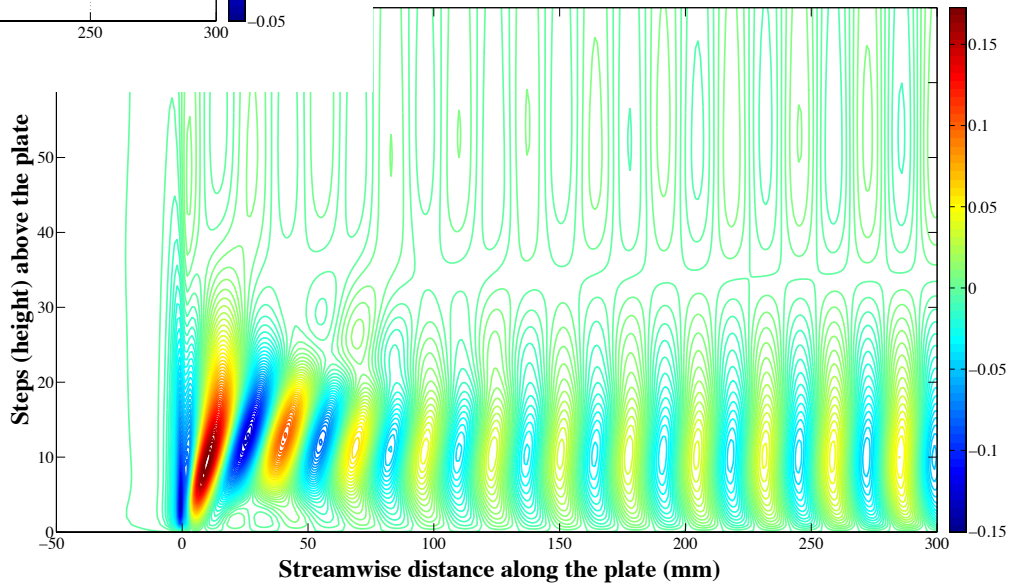

3D sinusoidal forcing: 159 Hz
12 ms^{-1} Re_{δ_1}(source) = 695

Requirements for effective control

- Is there a role for linear control in more complicated flows?
- Is coherent-structure based modelling useful?
- Would such a model still be useful at high Re?
- A pragmatic requirement that all sensing and actuation is performed in a wall – observability & controllability.
- Estimation: is drag reduction possible with wall control alone?
- What are the requirements for sensing and actuation at high Re?

Nonlinear 3D disturbance equations

- The evolution equation for disturbance u_i, p' growing on a base flow U_i, p :

$$\frac{\partial u_i}{\partial t} = -U_j \frac{\partial u_i}{\partial x_j} - u_j \frac{\partial U_i}{\partial x_j} - \frac{\partial p'}{\partial x_i} + \frac{1}{\mathrm{Re}} \nabla^2 u_i - u_j \frac{\partial u_i}{\partial x_j}$$

- Define disturbance energy: $E_V = \frac{1}{2} \int_V u_i u_i dV$

- A solution to the NS equations is stable to perturbations if its energy satisfies:

$$\lim_{t \to \infty} \frac{E_V(t)}{E_V(0)} \to 0$$

- $\frac{1}{E_V} \frac{dE_V}{dt}$ is independent of the size of the initial disturbance.
- Neglect of nonlinear term and assumption of parallel base flow leads to OS equation.

The Reynolds-Orr equation for energy

- Using the disturbance equation, evaluate $u_i \partial u_i / \partial t$
- Integration over volume V for localised disturbance:

$$\frac{dE_V}{dt} = -\oint_V u_i u_j \frac{\partial U_i}{\partial x_j} dV - \frac{1}{\mathrm{Re}} \oint_V \frac{\partial u_i}{\partial x_j} \frac{\partial u_i}{\partial x_j} dV$$

- This is the Reynolds-Orr equation, the evolution equation for the energy of a disturbance.
- Simplify for a parallel base flow: $U_i = U(y)\delta_{1i}$

$$\frac{dE_V}{dt} = -\oint_V \left\{ uvU'(y) + \frac{1}{\mathrm{Re}} D \right\} dV$$

Nonlinear terms are conservative!

- Two terms on RHS describe, respectively, the exchange of energy with the base flow and energy dissipation, D, due to viscous effects – both originate from linear terms in the original disturbance equation.

Linearised Navier-Stokes equations

- The 3D linear disturbance equations (in real space) are:

$$\left(\frac{\partial}{\partial t}+U\frac{\partial}{\partial x}\right)\nabla^2 v - U''\frac{\partial v}{\partial x} - \frac{\nabla^4 v}{\mathrm{Re}} = 0 \qquad (1)$$

$$\left(\frac{\partial}{\partial t}+U\frac{\partial}{\partial x}\right)\omega_y - \frac{\nabla^2 \omega_y}{\mathrm{Re}} = -U'\frac{\partial v}{\partial z} \qquad (2)$$

- These are the Orr-Sommerfeld (1) and Squire (2) equations: v evolves via OS operator, ω_y evolves via the Squire operator. The coupling of the two equations appears through the LHS of (2), the v-forcing of ω_y. It is taken to represent the "lift-up" phenomenon in wall turbulence by which v causes movement across the mean gradient, $U' = \frac{dU}{dy}$
- We write v and ω_y as wave-like solutions with wavenumber pair (α, β):

$$v(x,y,z,t) = \hat{v}(y)e^{i(\alpha x+\beta z-\varpi t)}$$

$$\omega_y(x,y,z,t) = \hat{\omega}_y(y)e^{i(\alpha x+\beta z-\varpi t)}$$

State-space representation of NS equations

- With v and ω_y written in terms of (x,z) Fourier modes, N–S equations can be written in operator form:

$$\frac{d}{dt}\begin{bmatrix}\hat{v}\\ \hat{\omega}_y\end{bmatrix}=[A]\begin{bmatrix}\hat{v}\\ \hat{\omega}_y\end{bmatrix} \qquad (1)$$

where ^ denotes the Fourier-transformed quantity, and

$$[A]=\begin{bmatrix}L_{os} & 0\\ L_c & L_{sq}\end{bmatrix} \qquad (2)$$

- (1) is in "state-space" form:

$$\frac{d\mathbf{x}}{dt}=A\mathbf{x}+B\mathbf{u}$$

where the state vector, $\mathbf{x}$, of the system consists of the Fourier coefficients, $\hat{v}$, $\hat{\omega}_y$, and $\mathbf{u}$ is the control input

Outline

- Tollmien-Schlichting (TS) wave cancellation
- Transient growth: a linear paradigm for near-wall turbulence control
- Role of linear feedback in the control of turbulent channel flow
- Open-loop control and travelling surface waves for turbulent skin-friction reduction

3’ x 3’ Tunnel

- Free-stream turbulence intensity ~ 0.05%
- 1.5 m long flat plate with trailing edge flap
- Asymmetric MSE leading edge to reduce pressure gradient and eliminate join discontinuity
- Feedback control: 3D point-source mini- speaker as trigger
- Receptivity: ribbon spanning test section, forced by voice-coil actuators creating single-frequency free-stream disturbance
  - Roughness height ≈ 95 μm ≈ inner layer from Triple Deck theory

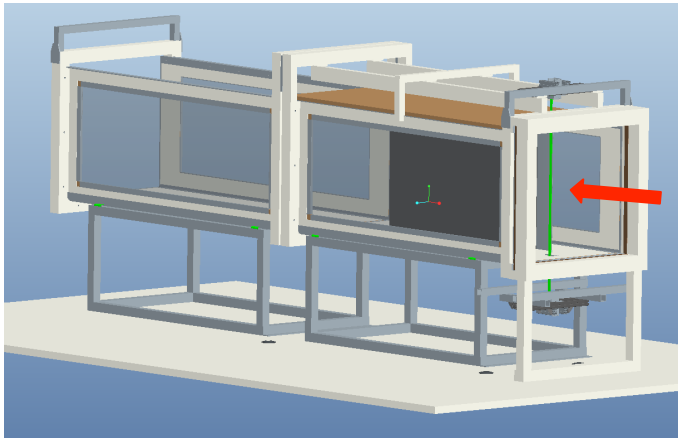

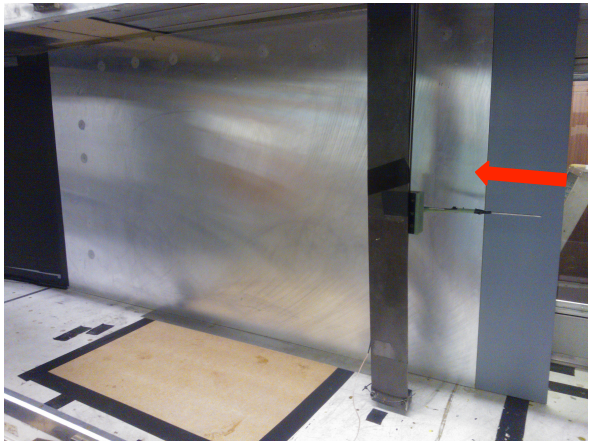

Experimental boundary layer profiles

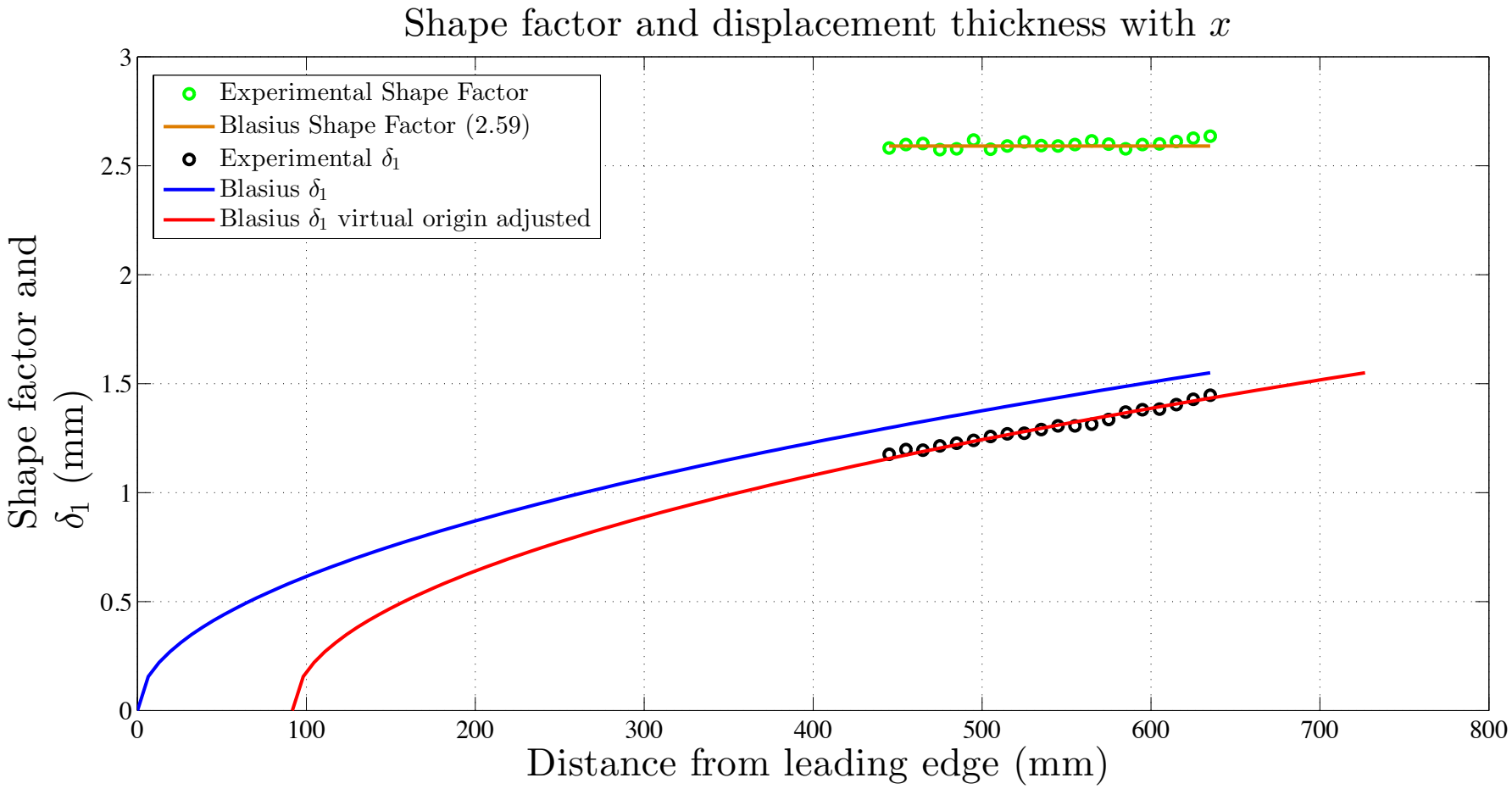

Feedback control

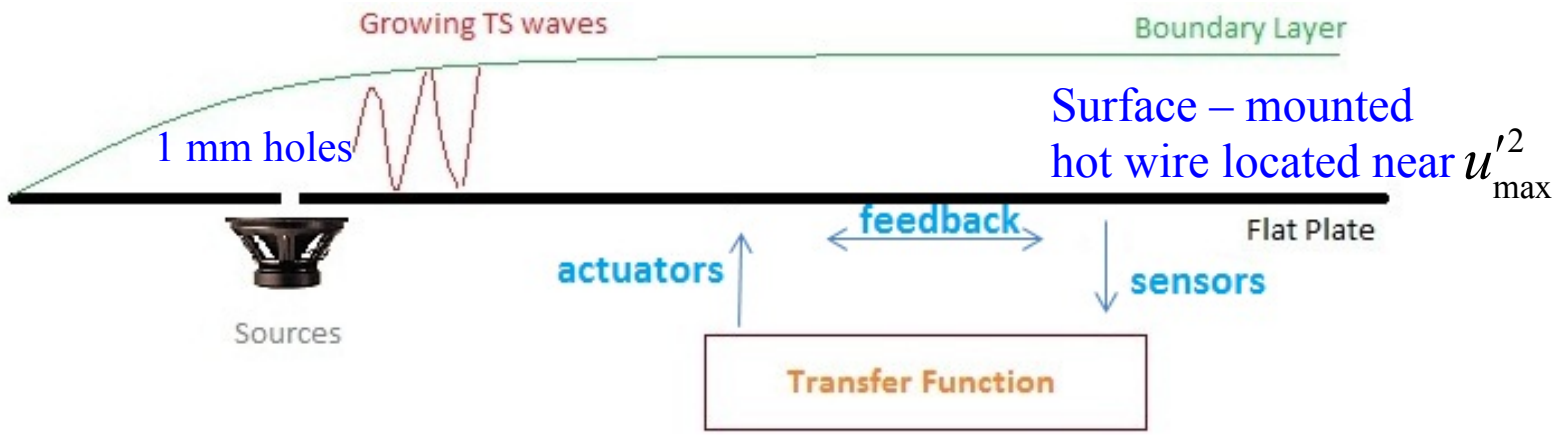

- The OS equation is a 4th order ode in space – no straight-forward way to obtain the numerical model
- Controller design based on experimental frequency response data – FRD models of the system
- Important considerations for controller design:
  - Stability of the closed-loop
  - Non-minimum phase system
  - Sensors should avoid the near-field of the actuator

Feedback Control Approach

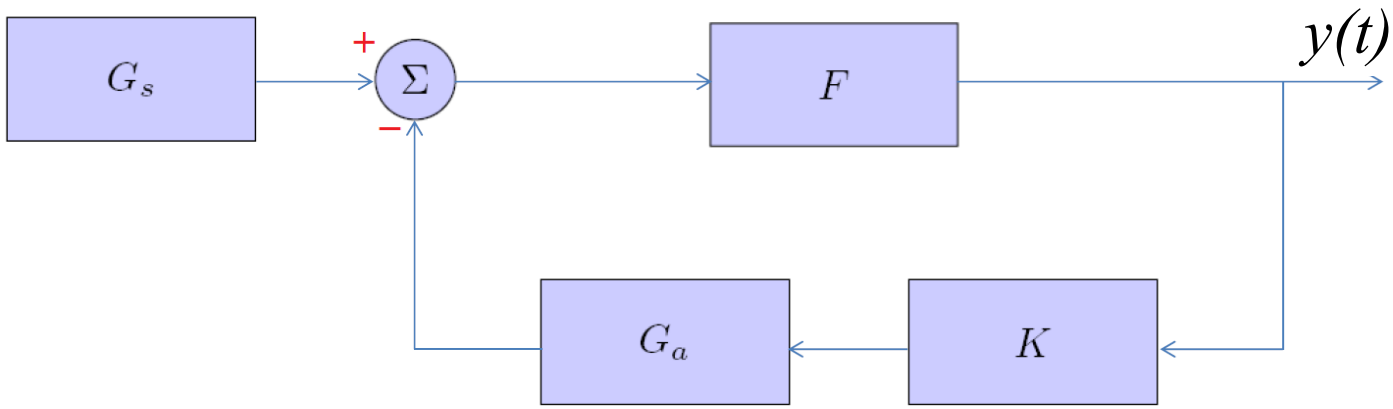

- G_s: Original unstable wave generated by the source
- G_a: Cancelling waves generated by actuators
- K : Controller
- F : Krohn-Hite Filter
- $y(t)$: Residual time signal measured by sensors

$$G(s) = \frac{F G_s}{\left(1 + K G_a F\right)}$$

Sensor – actuator separation effects
Nyquist plot

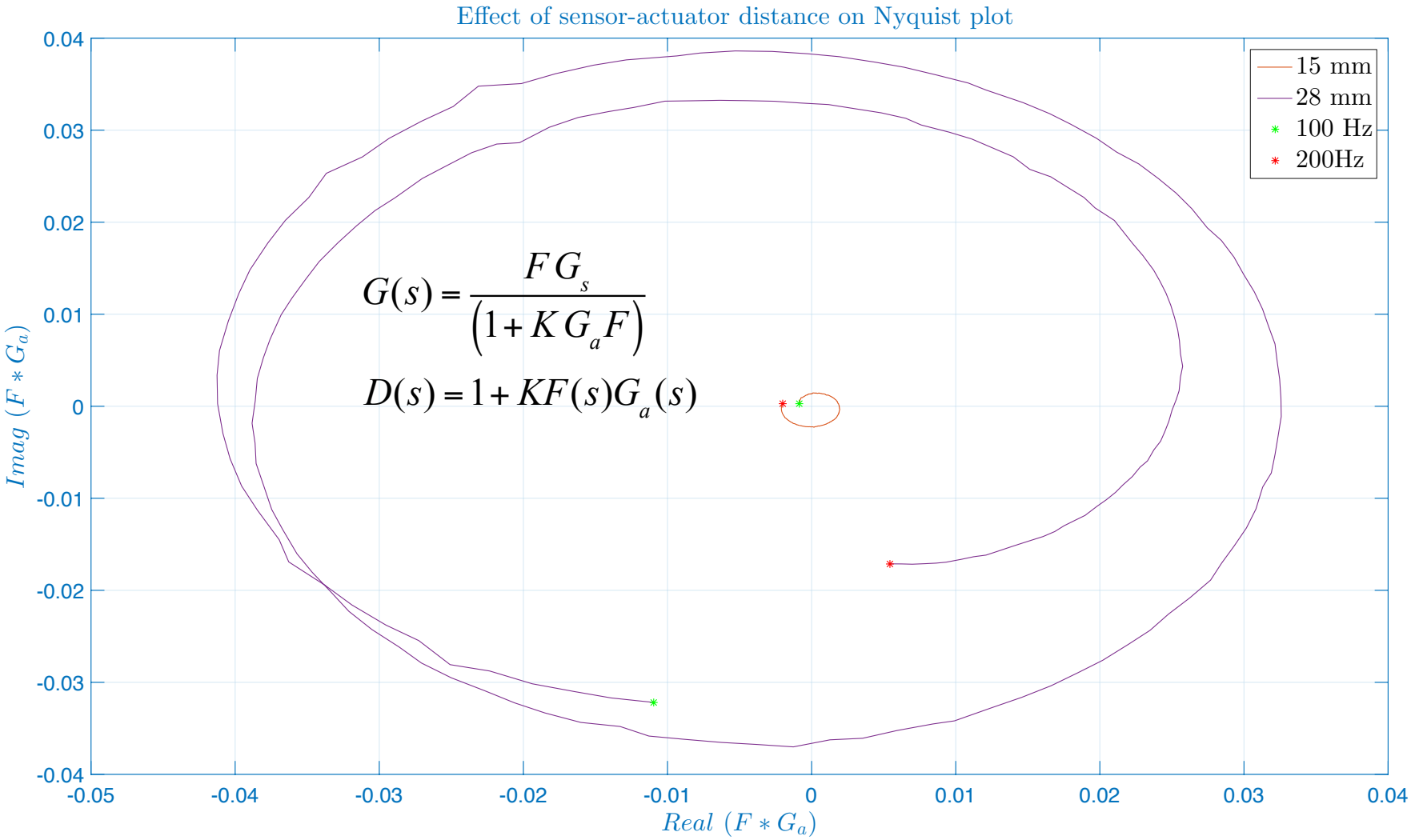

Transfer functions

15 mm sensor – actuator separation

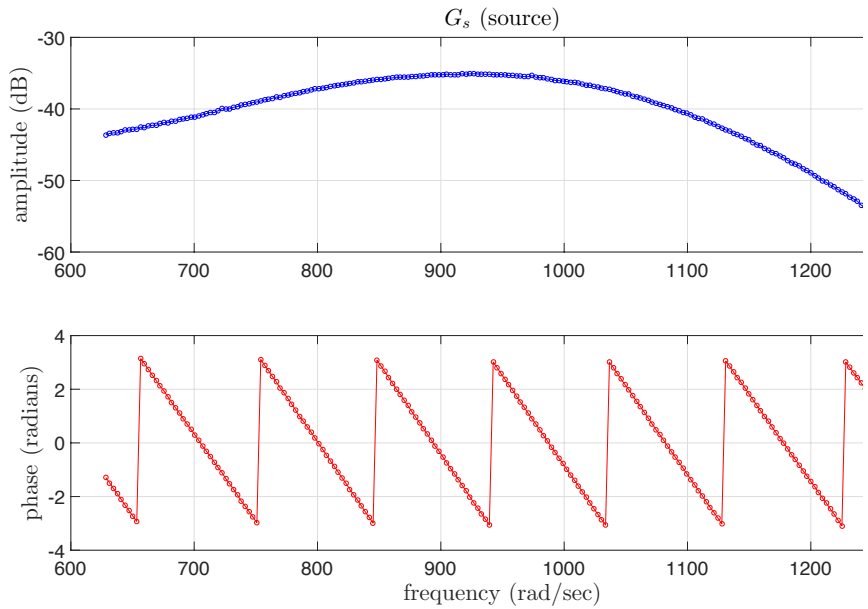

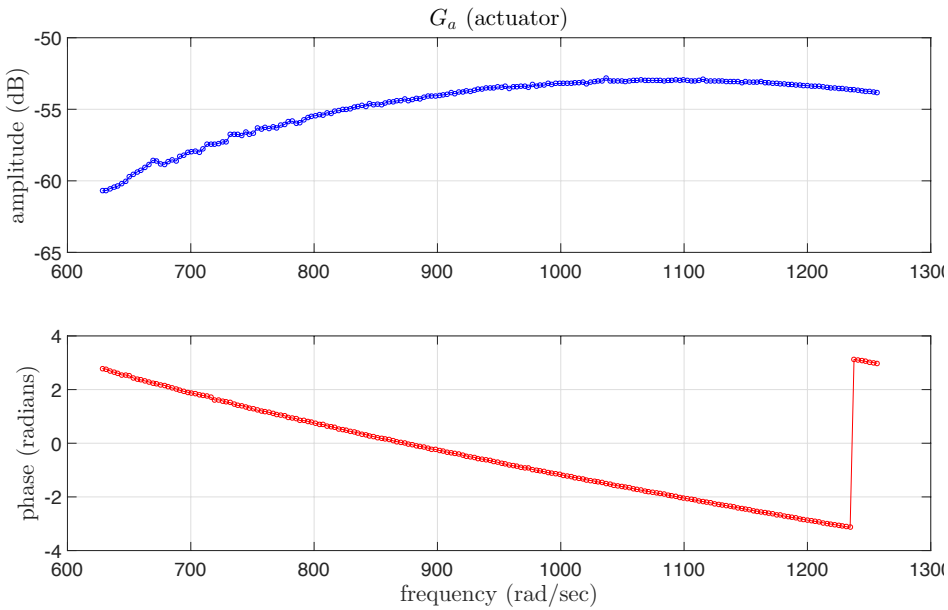

Effect of controller order

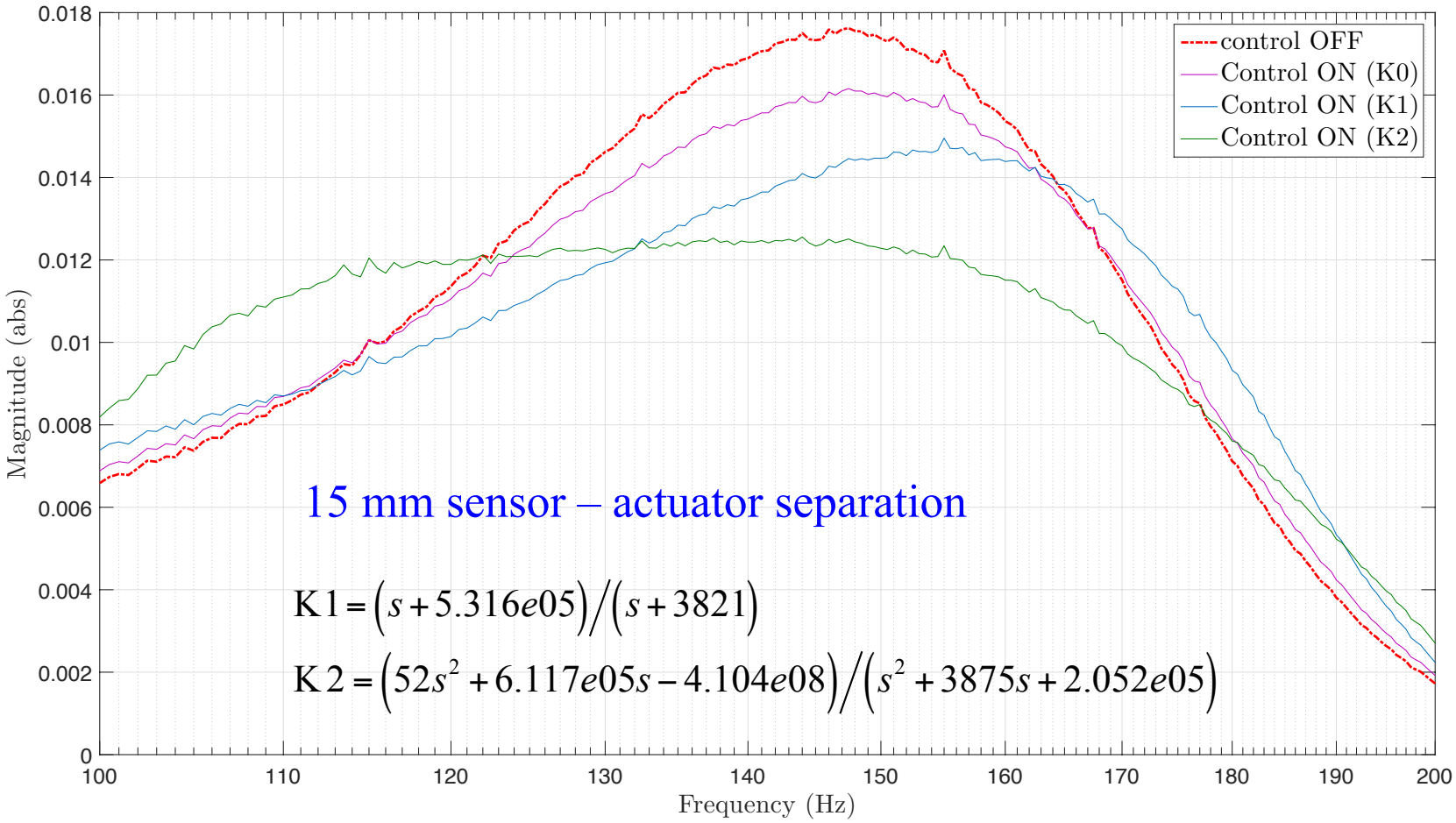

K2: 145 Hz attenuation

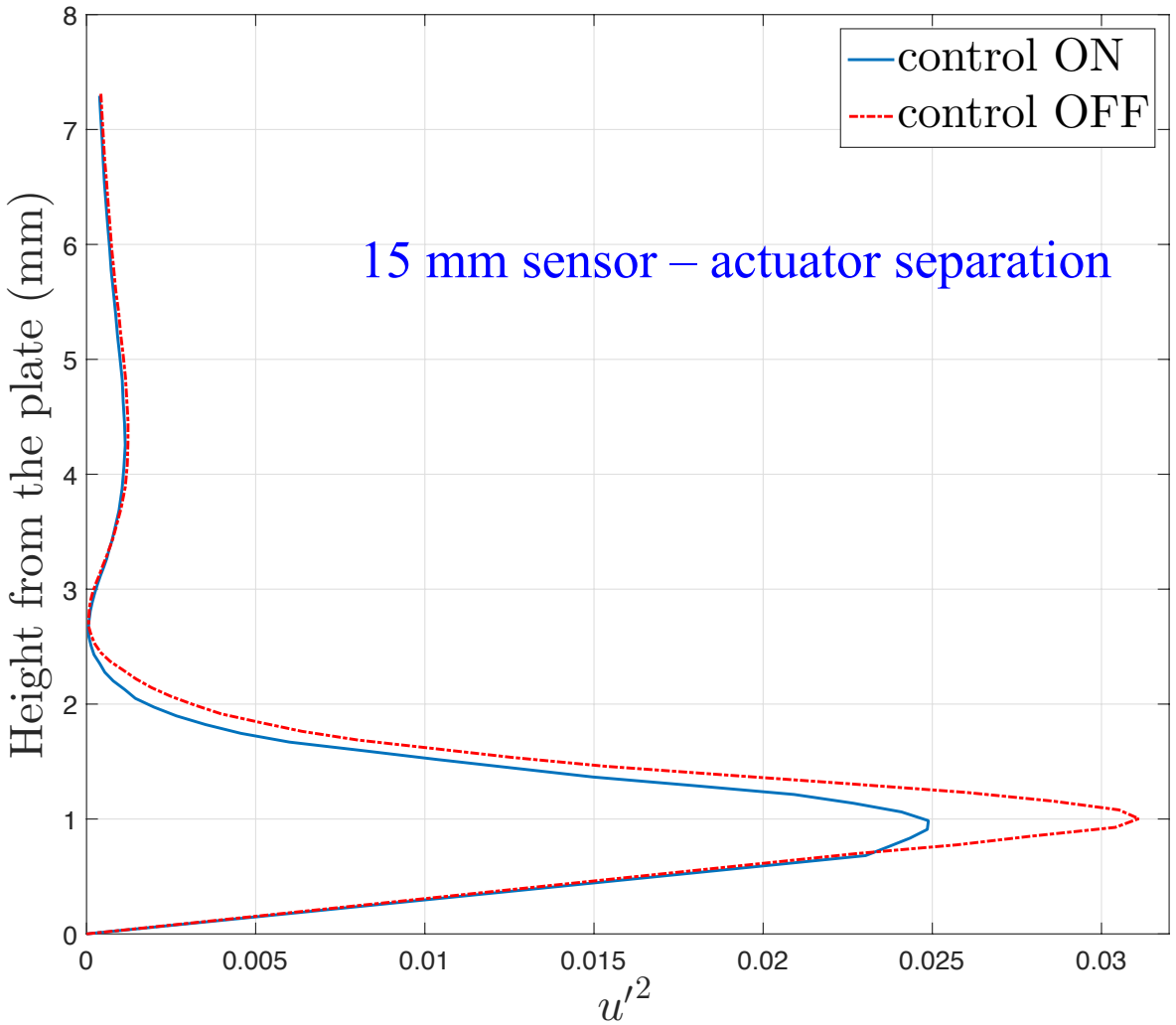

K2: wave packet attenuation

15 mm sensor – actuator separation

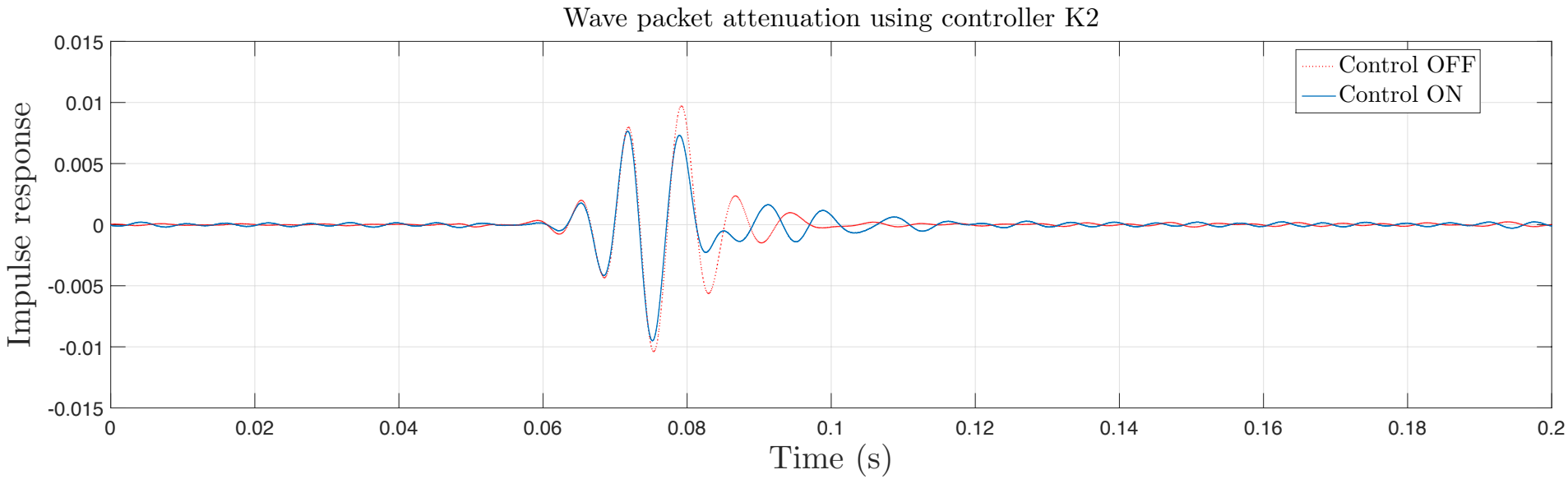

Summary

- One actuator driven out-of-phase with the source is able to produce cancellation
- Real-time feedback control
  - Sensor – actuator distance crucial
  - Controllers designed using frequency – response data perform well
  - Second-order controller provides significant attenuation of wave packets and single – frequency TS waves
  - Controllers appear robust
  - System data show a non-minimum phase system
- Next steps: replace controlled source with wave packet generation via roughness receptivity to free-stream disturbances.

Receptivity to free-stream vorticity

- Asymptotic theory – Wu (2001), Duck & Ruban (1996) – suggest free-stream disturbances will not penetrate a Blasius boundary layer without some scale conversion mechanism
- Investigate penetration of controlled free-stream disturbances with & without localised roughness
- Setup experiment: vibrating ribbon – Dietz (1999)
- Can exploit different roughness geometries – 3D effects
- Second control experiment: Exploit TS wave initiation by variable free-stream perturbations and provide feedback control downstream of near field.

Receptivity experiment

- Consider here only vortical disturbances
- Dietz (1999) showed experimentally the effect of roughness on receptivity to vorticity
- Use of vibrating ribbon, or wire, in the free stream as source of controllable disturbance

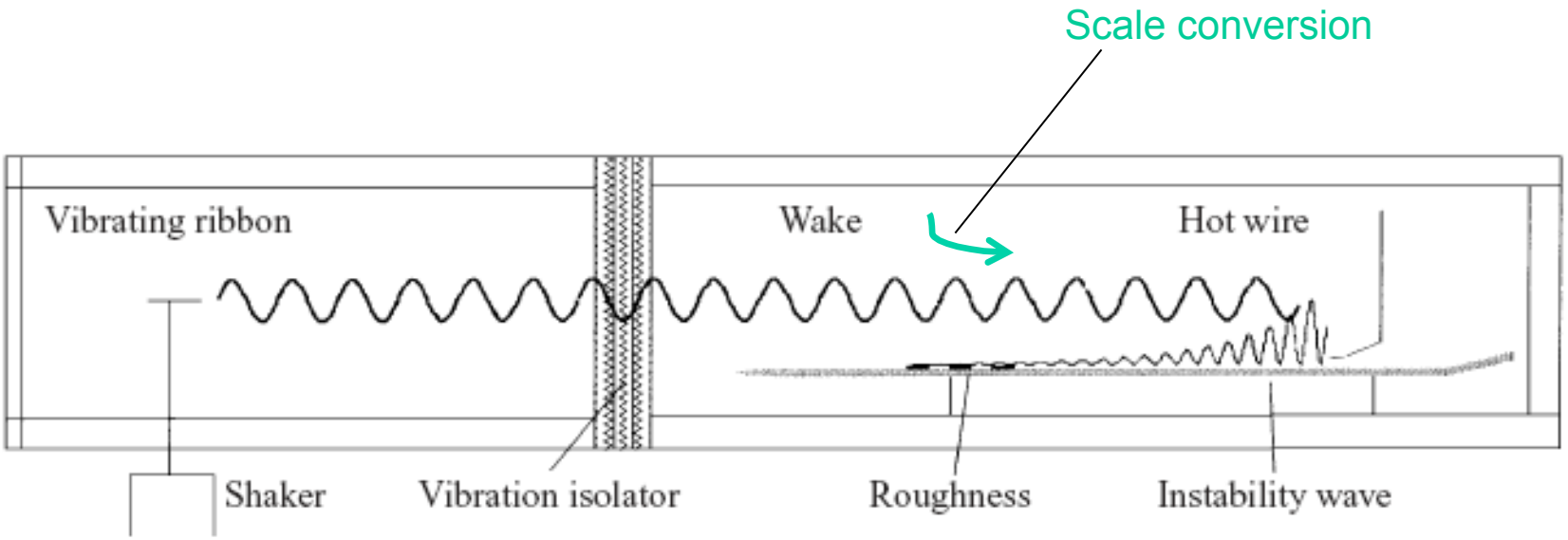

Receptivity experiment

- Ribbon forcing at 127 Hz
- Voice-coil actuators isolated from tunnel
- Roughness position determined by branch I of neutral stability curve
- Roughness strips 60 μm

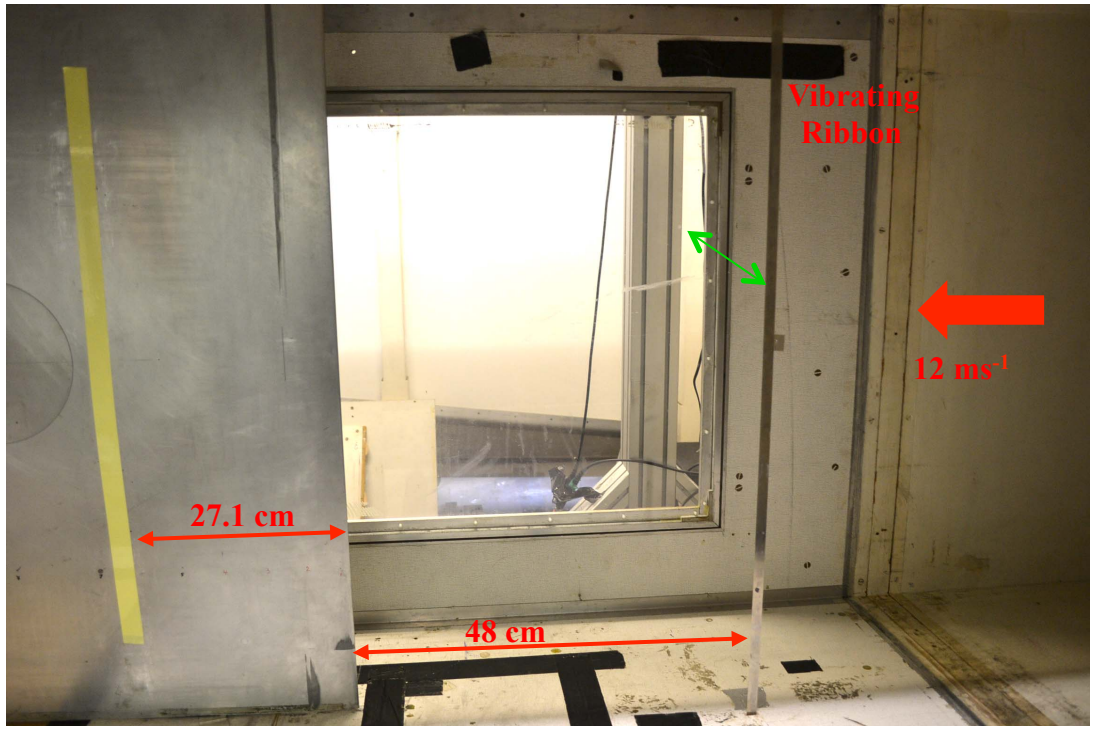

Effect of roughness

- Clear TS signal requires both roughness and forcing
- Addition of roughness clearly excites a sinusoidal disturbance

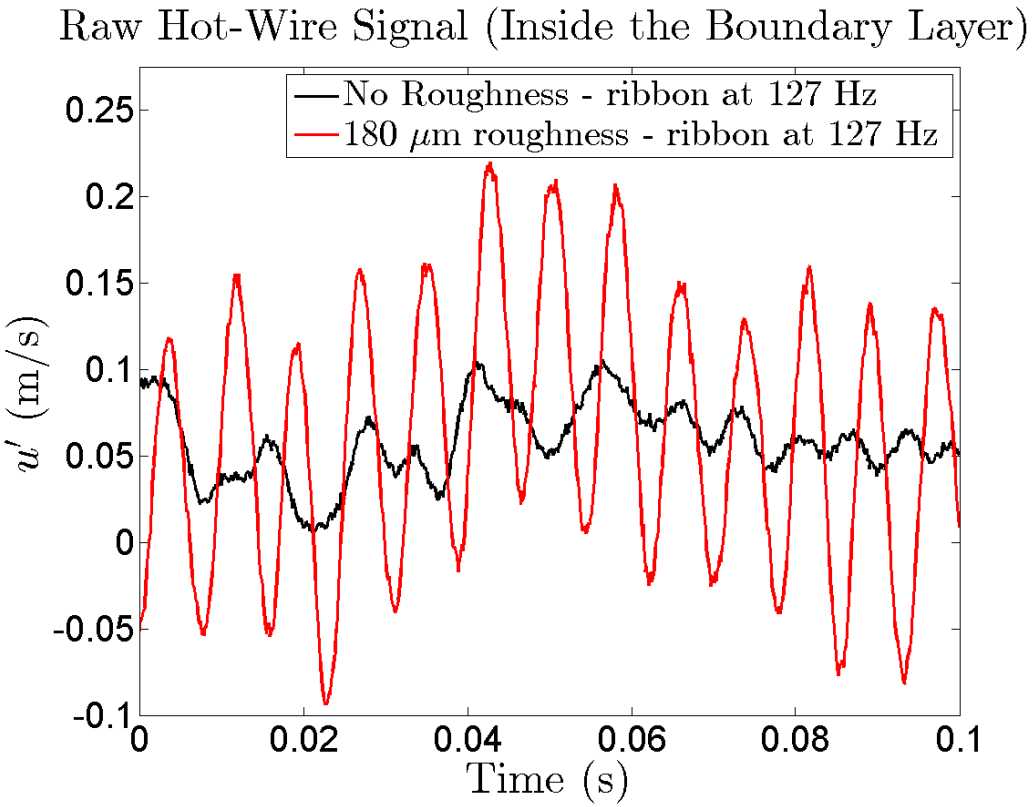

Summary

- At small forcing amplitudes
  - Free-stream disturbances generate TS waves in the boundary layer only when roughness strip is present – in line with theoretical predictions
- Boundary layer response is:
  - Linear with free-stream forcing amplitude to ~0.8%
  - Nonlinear for roughness heights above triple deck inner layer
- At high forcing amplitudes and with / without roughness
  - TS waves begin to break down
  - Energy spreads across nearby frequencies and then becomes prevalent at low frequencies – streaks, vortices – Klebanoff distortions – "bypass" – shear sheltering

Outline

- Tollmien-Schlichting (TS) wave cancellation
- Transient (non-modal) growth: a linear paradigm for near-wall turbulence control
- Role of linear feedback in the control of turbulent channel flow
- Open-loop control and travelling surface waves for turbulent skin-friction reduction

Turbulence – structure fundamentals

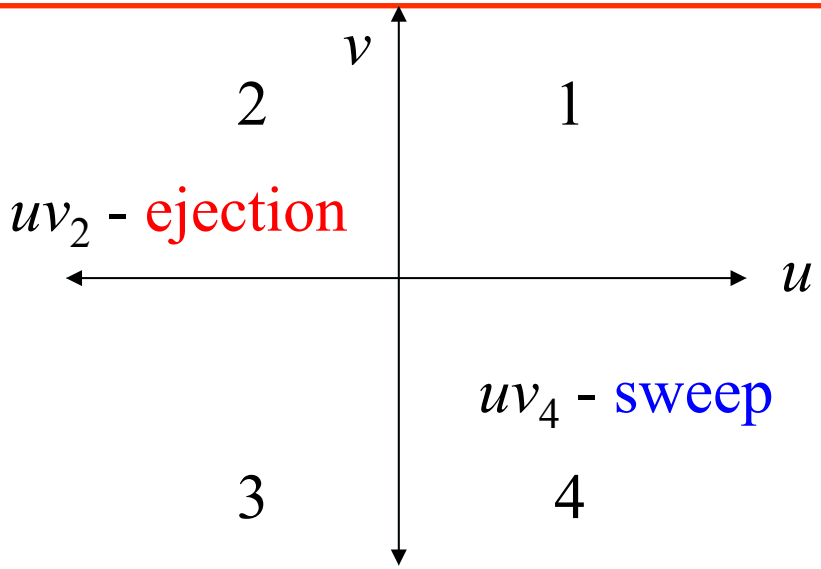

Unlike a channel or pipe flow, a boundary layer is highly intermittent in the outer region. Both pictures show that there are deep irrotational fissures in the boundary, and that the predominant component of vorticity in the outer layer is in the spanwise (negative) direction.

The key difference between laminar and turbulent flow is $\overline{\frac{\partial uv}{\partial y}}$

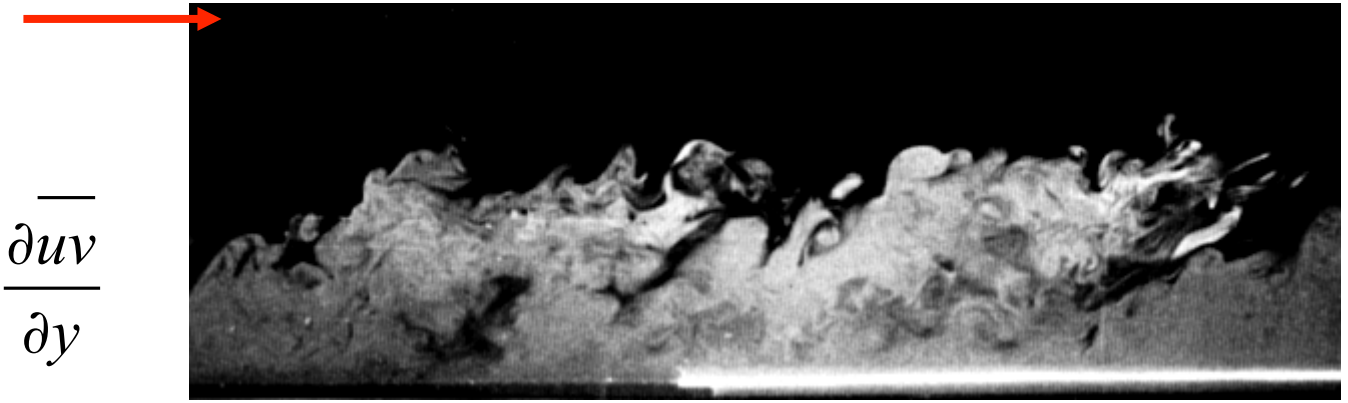

Model-based friction drag reduction

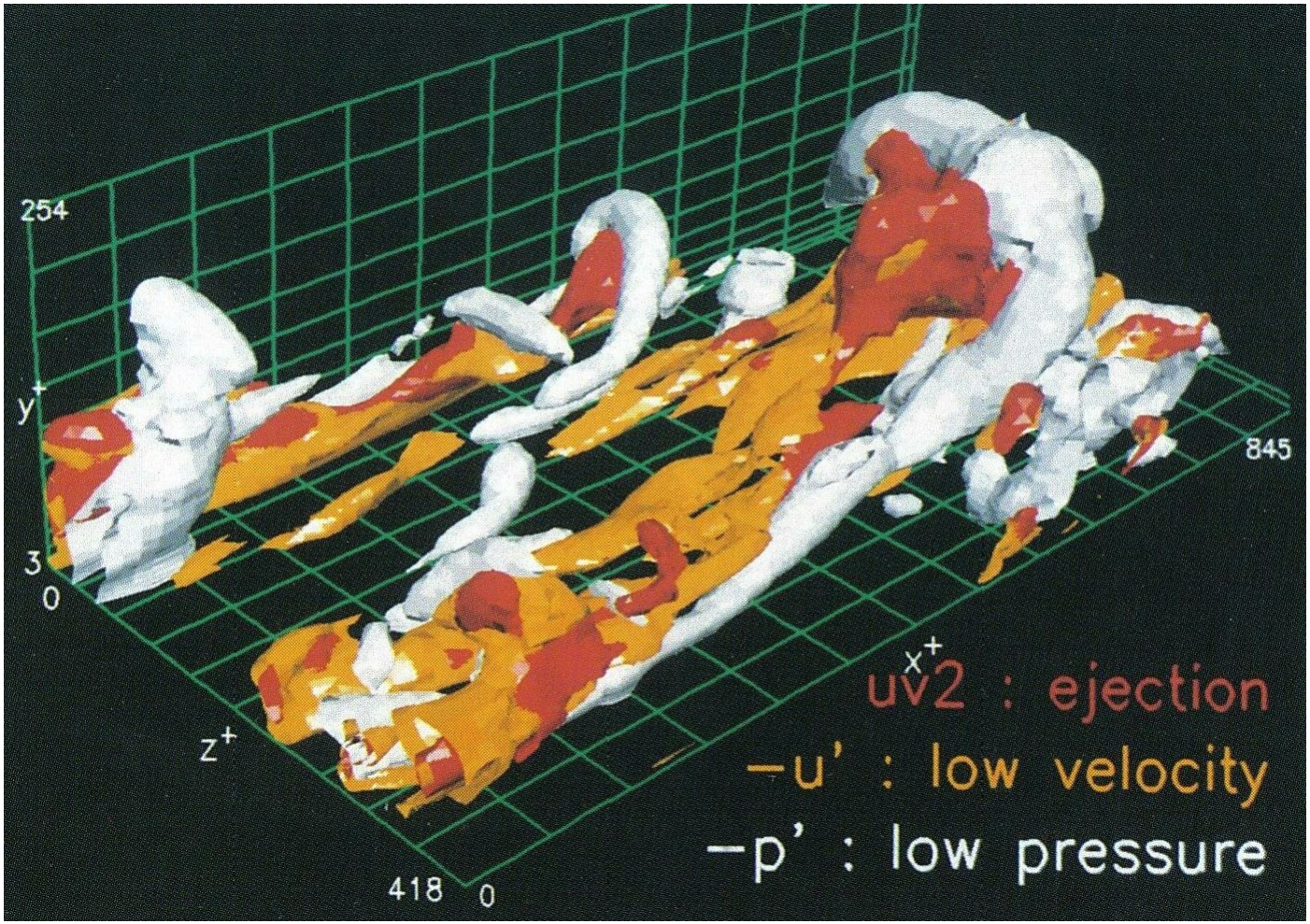

Robinson 1991

Model-based drag reduction

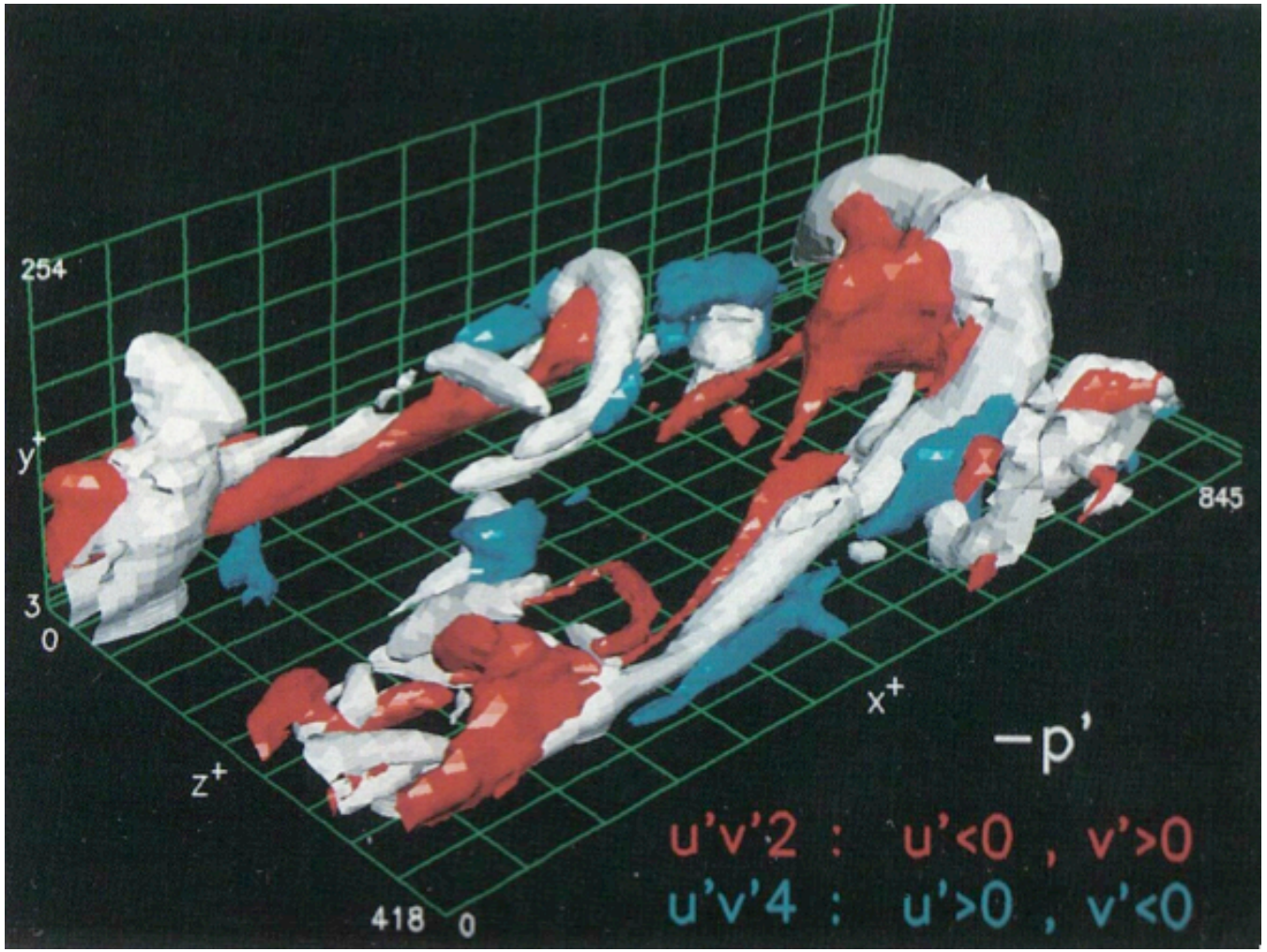

Robinson 1991

High Re: Inner – Outer Interaction

"Bottom-up": Adrian 2007

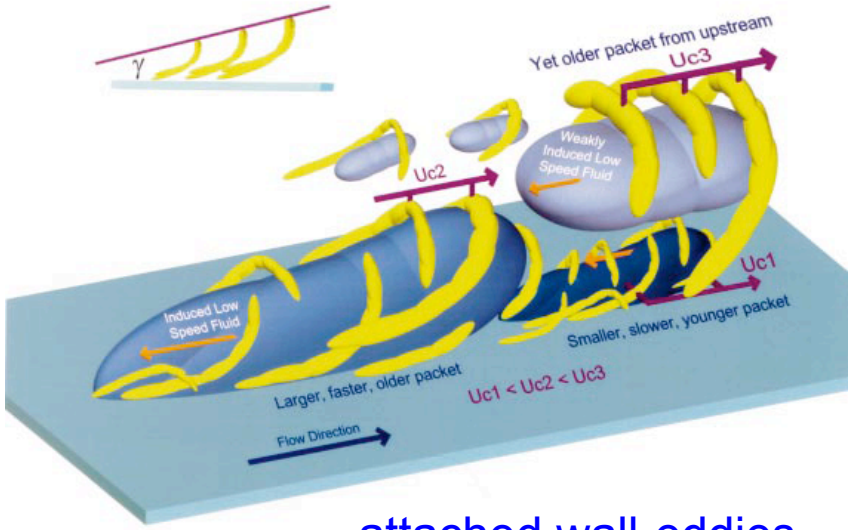

attached wall-eddies

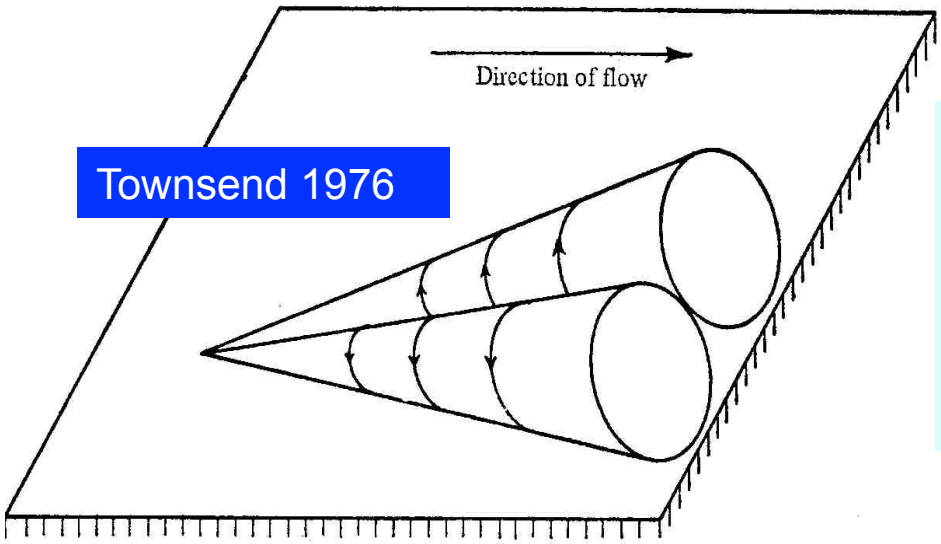

Townsend 1976

"Top-down": Hunt & Morrison 2000

- packets carry roughly half the turbulence kinetic energy and shear stress
- fill most of the boundary layer
- reach to the wall – "splat"
- at least 20δ in length – "meandering"

A useful theory for Inner-Outer Interaction?

- Landahl ('93, '90, '75): initial disturbance scales L, u_0 with timescales: shear interaction $\left\{U_w'\right\}^{-1}$<< viscous $\left\{L^2/(\nu U'^2)\right\}^{1/3}$<< nonlinear L/u_0.
- Large and small-scale decomposition: $u_i = \tilde{u}_i + u_i'$
- Small scale, λ' large scale, $\tilde{\lambda}$ where $\lambda'/\tilde{\lambda} = \varepsilon << 1$
- To first order in ε, large-scale and small-scale fields may be represented separately by the same equations:

$$\left(\frac{\partial}{\partial t} + U\frac{\partial}{\partial x}\right)\nabla^2 v - U''\frac{\partial v}{\partial x} - \frac{\nabla^4 v}{\mathrm{Re}} = q$$

$$\left(\frac{\partial}{\partial t} + U\frac{\partial}{\partial x}\right)\omega_y + U'\frac{\partial v}{\partial z} - \frac{\nabla^2 \omega_y}{\mathrm{Re}} = r$$

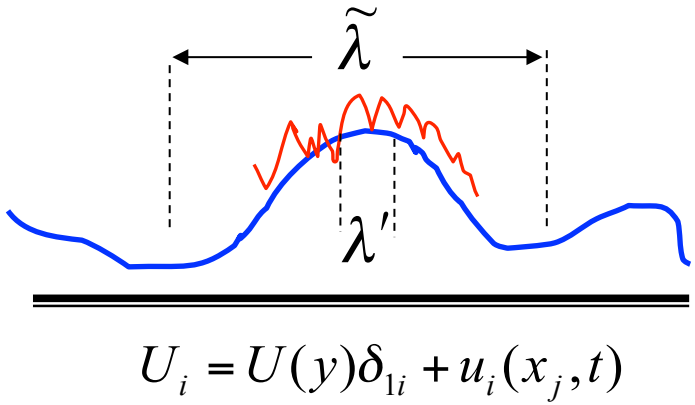

- q, r nonlinear source terms (turbulent stresses) significant only in local regions: "intense small-scale turbulence of an intermittent nature" interspersed with "laminar-like unsteady motion of a larger scale".

Linear theory

- Linear disturbance equations (r=q= 0): $\left(\frac{\partial}{\partial t}+U\frac{\partial}{\partial x}\right)\nabla^2 v - U''\frac{\partial v}{\partial x} - \frac{\nabla^4 v}{\mathrm{Re}} = 0$

  wall-normal velocity, v

  wall-normal vorticity, η

  $$\left(\frac{\partial}{\partial t}+U\frac{\partial}{\partial x}\right)\omega_y - \frac{\nabla^2\omega_y}{\mathrm{Re}} = -U'\frac{\partial v}{\partial z}$$

- v evolves via OS operator, ω_y evolves via Squire operator. L_c, coupling appears through v-forcing of ω_y.
- Streaks and vortices decay if L_c suppressed (Kim & Lim '00), but nonlinearity required to form structures of correct scales (Waleffe & Kim '97)
- Several suggest structure formation requires linear mechanisms only:
  1. RDT (Lee *et al.* '90) and linearised NS + stochastic forcing (Farrell & Ioannou '93) produce vortices & streaks
  2. stability analysis using turbulent velocity profile with variable eddy viscosity – two peaks of maximum amplification (one inner, one outer) del Álamo & Jiménez (2006), Cossu et al. (2009).
  3. Resolvent analysis (McKeon & Sharma 2010, Luhar *et al.* 2014)

Bypass transition

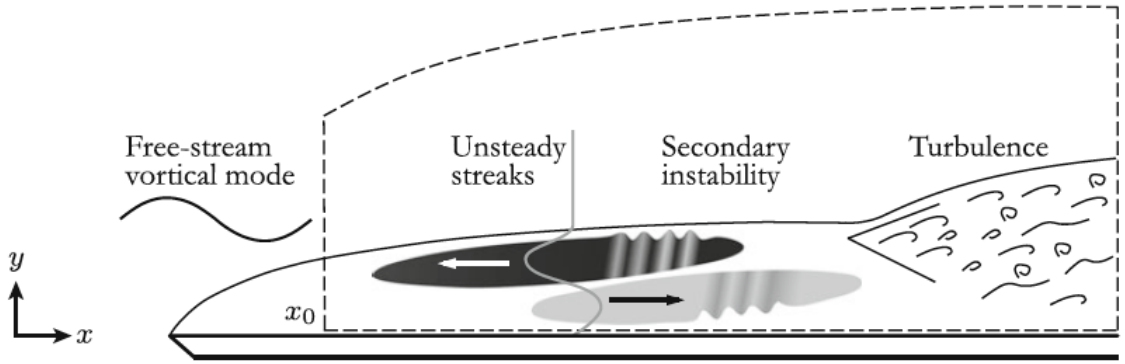

Zaki 2013

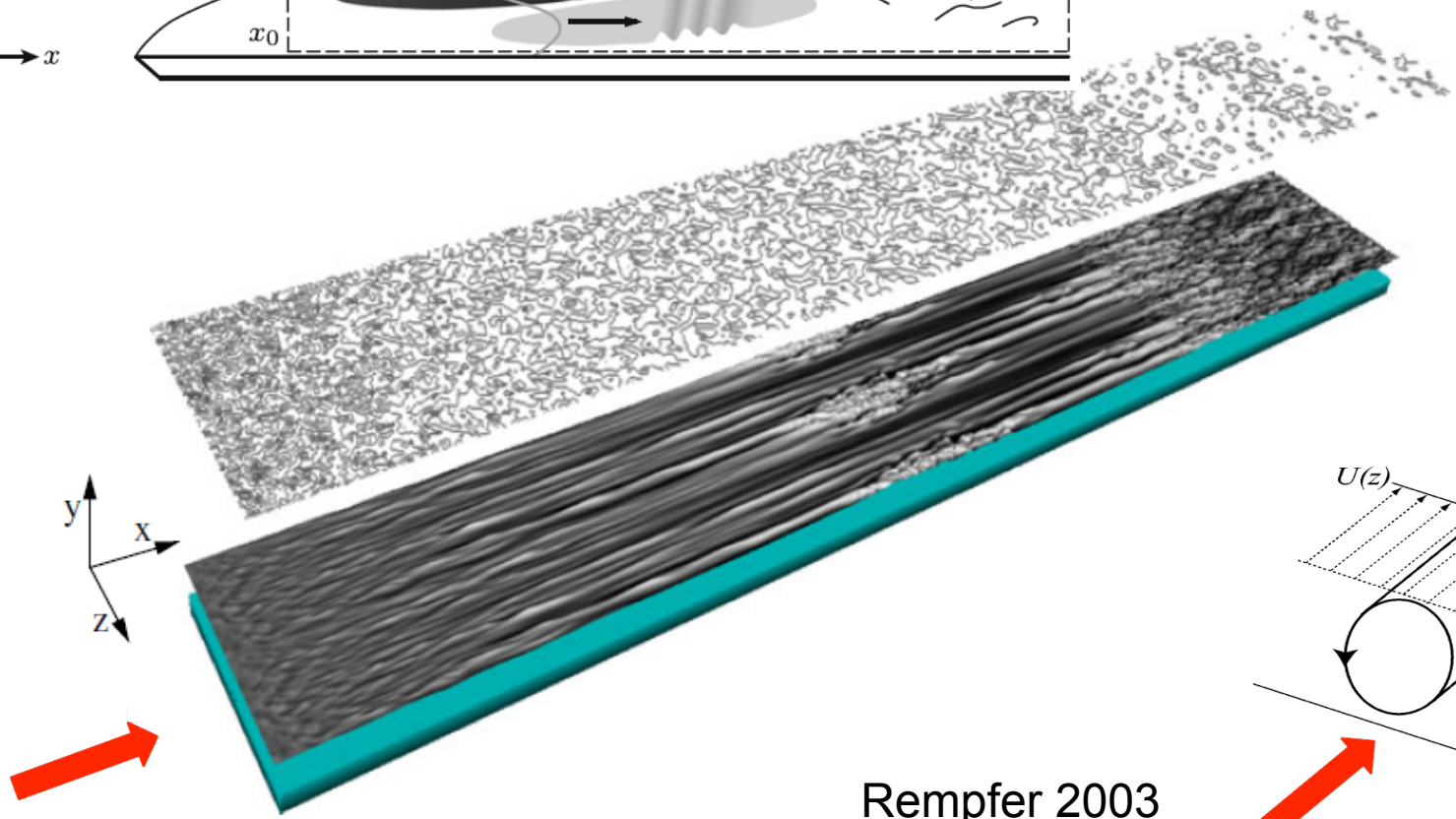

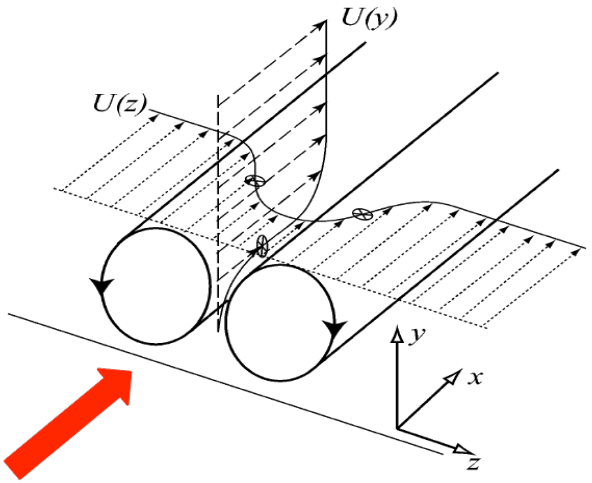

Rempfer 2003

And its control by feedback

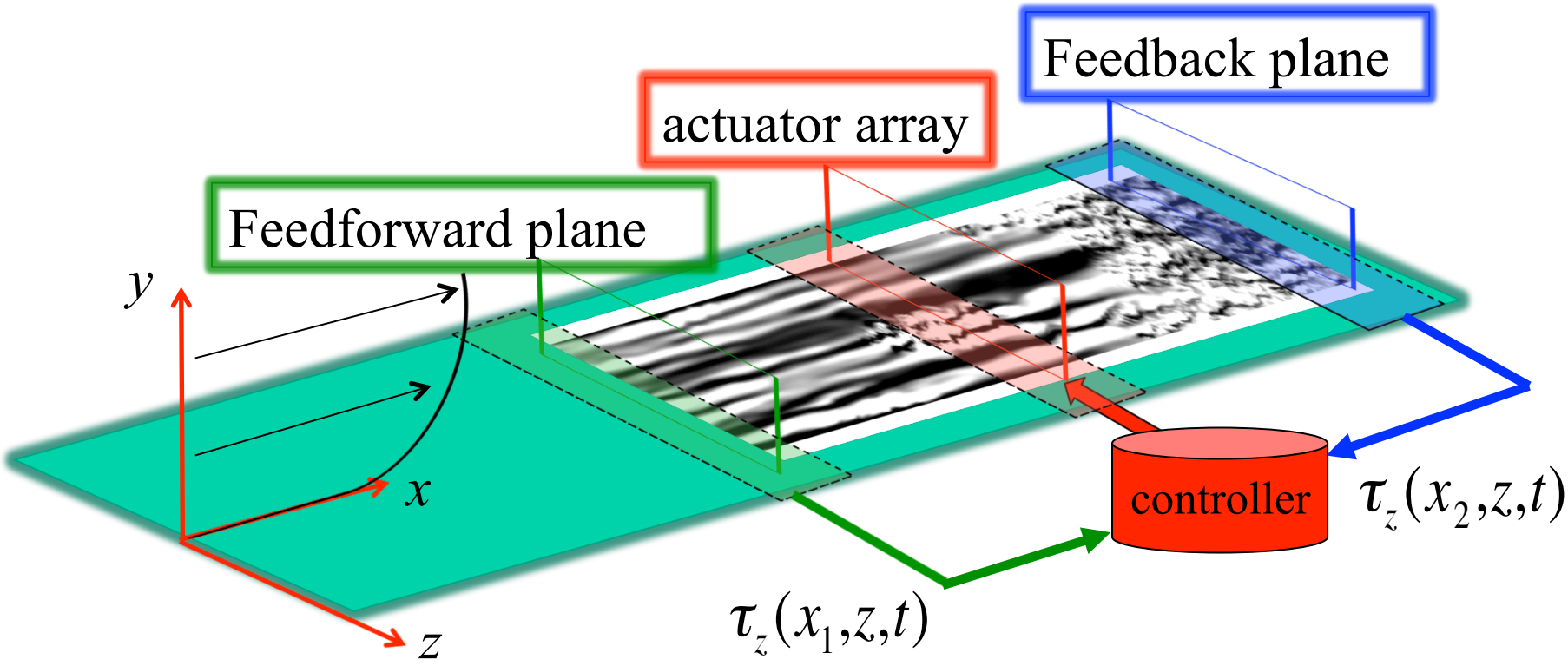

Spanwise component of wall shear stress

Current experiment

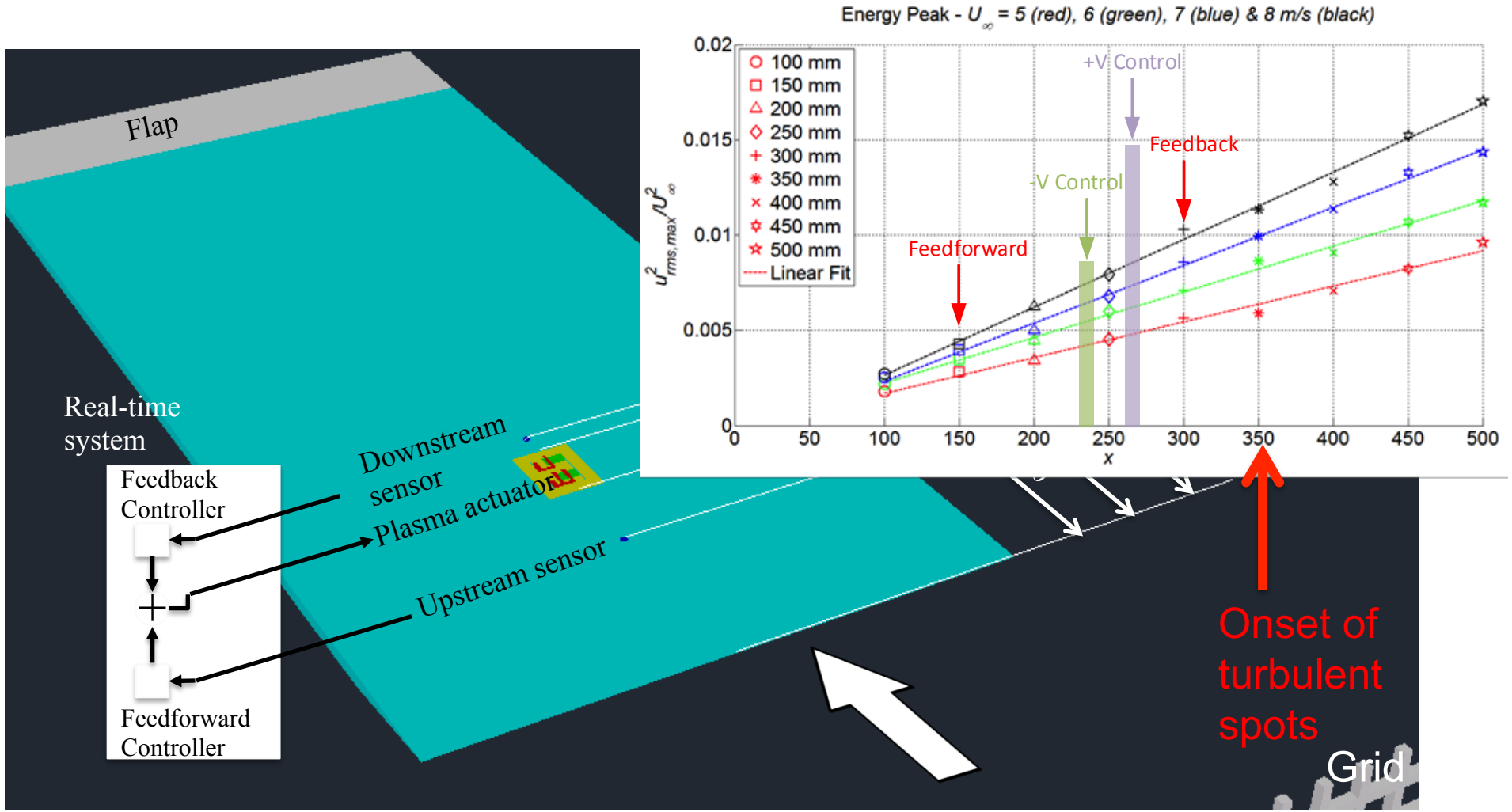

All dimensions in mm

Plasma actuators

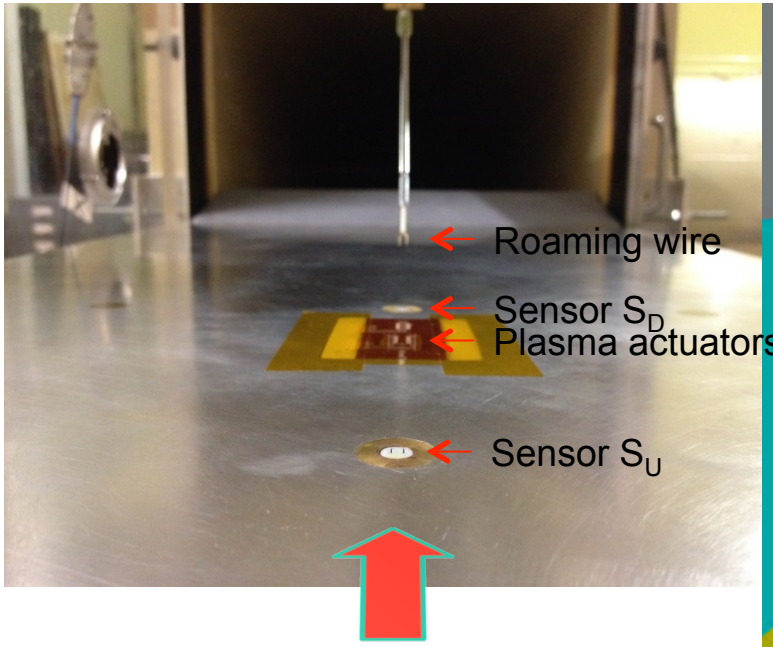

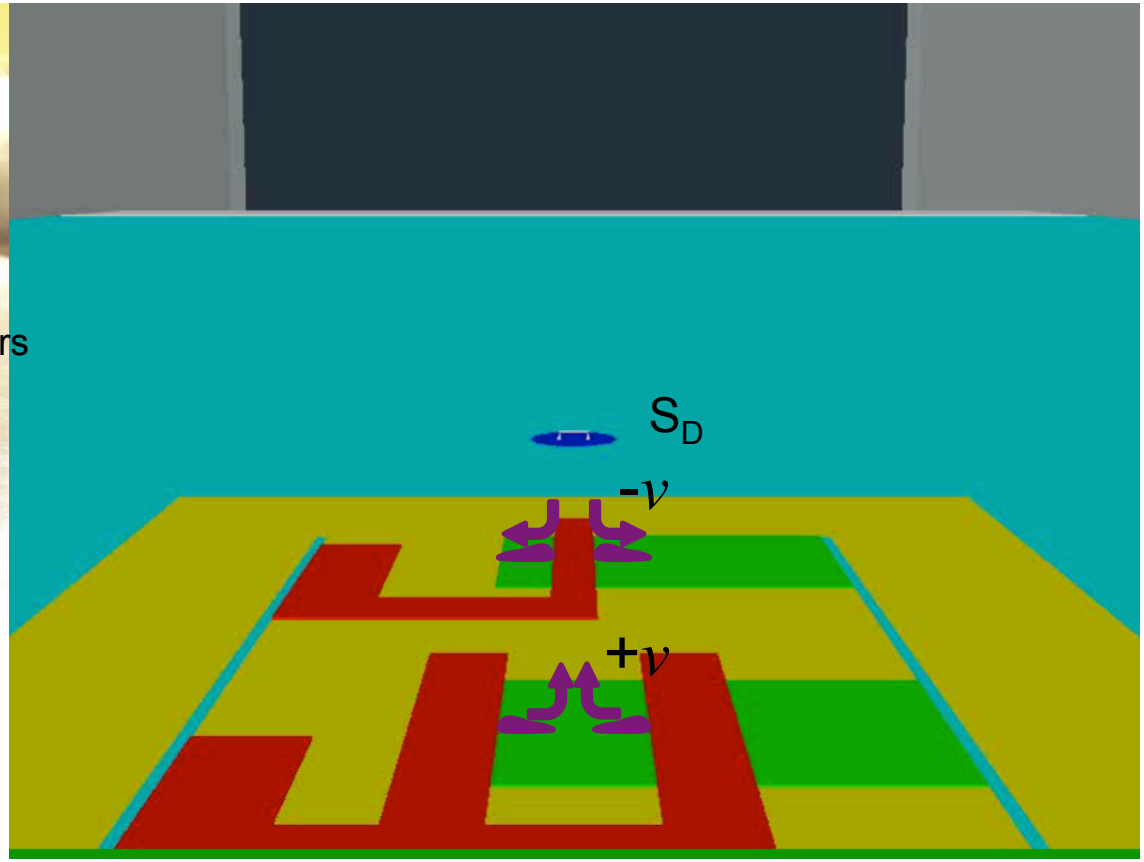

Single-point Linear Stochastic Estimation

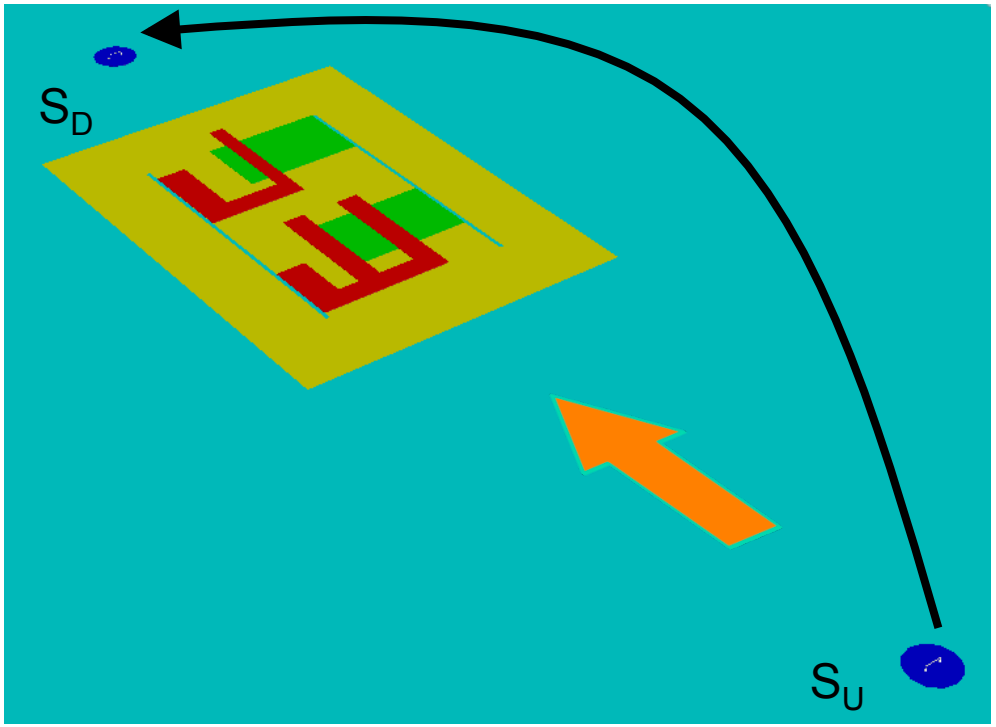

- Model for disturbance at S_D based on measurement S_U and LSE
- Actuator output based on measurement S_U and LSE

- Obtain conditional average $\mathbf{u(x+r)}$ given a condition at $\mathbf{x}$: $\hat{\mathbf{u}}(\mathbf{x};\mathbf{r}) = \left\langle \mathbf{u}(\mathbf{x}+\mathbf{r}) \middle| \mathbf{u}(\mathbf{x}) \right\rangle$
- Estimate for $\hat{\mathbf{u}}(\mathbf{x};\mathbf{r})$:

$$\tilde{u}_i(\mathbf{x};\mathbf{r}) = A_{ij}(\mathbf{r})u_j(\mathbf{x}) + B_{ijk}(\mathbf{r})u_j(\mathbf{x})u_k(\mathbf{x}) + \ldots.$$

- A_{ij} determined by least-squares minimisation: $\left\langle \left[\tilde{u}_i(\mathbf{x};\mathbf{r}) - u_i(\mathbf{x}+\mathbf{r}) \right]^2 \right\rangle_{MIN}$

Actuator response model

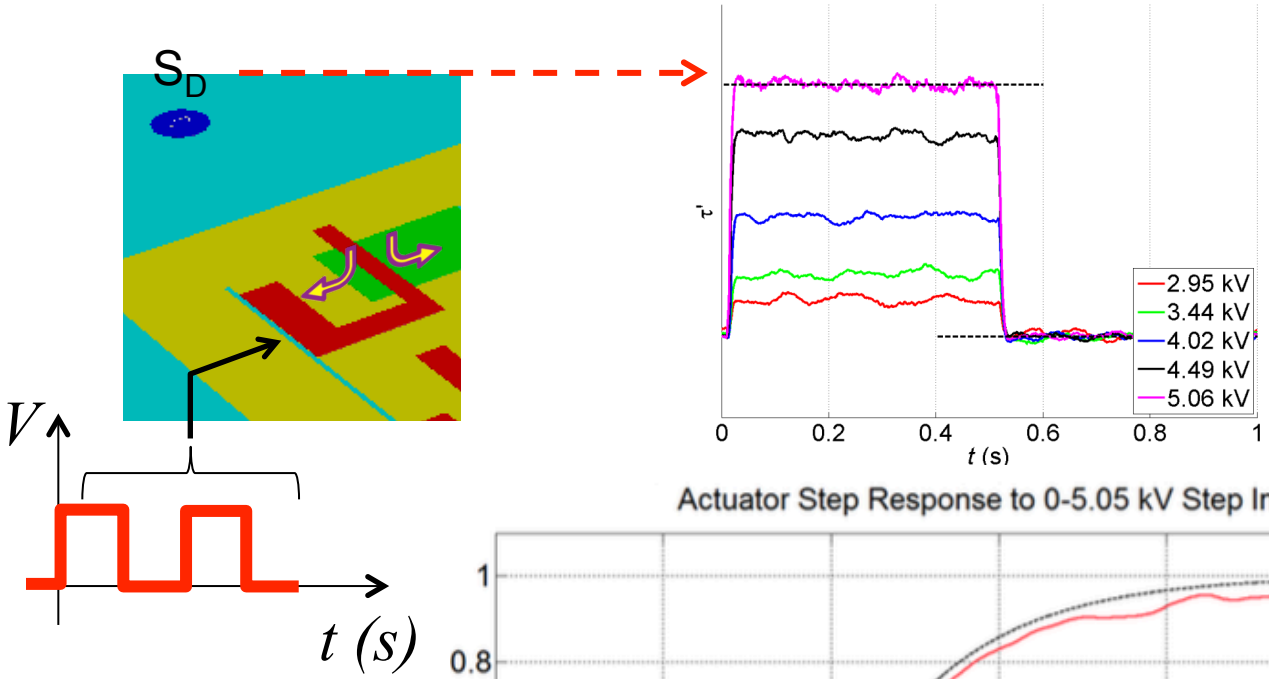

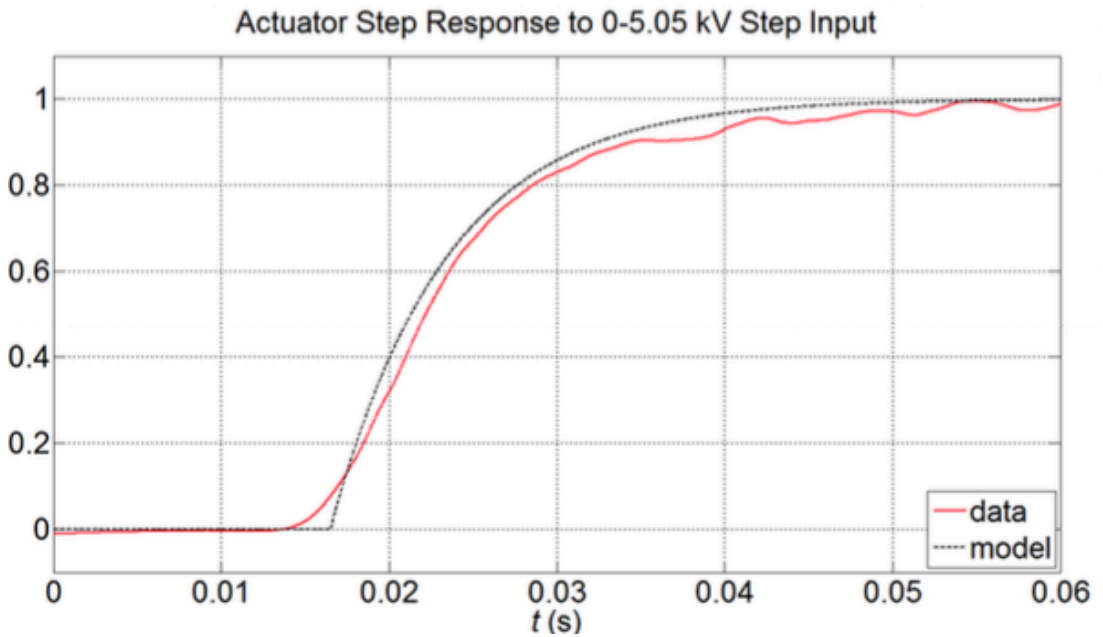

Single-point Linear Stochastic Estimation

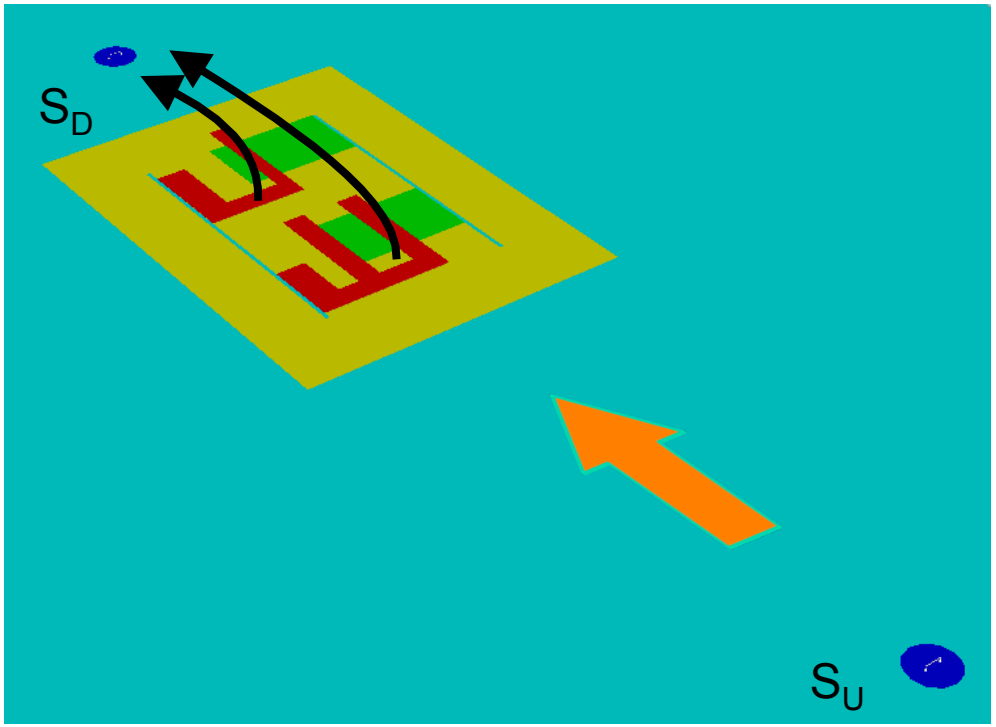

- Generates a counter-disturbance, which at the downstream sensor location, cancels the naturally occurring streak.
- First-order response model for effect of forcing from previous slide

Feedforward + Feedback control

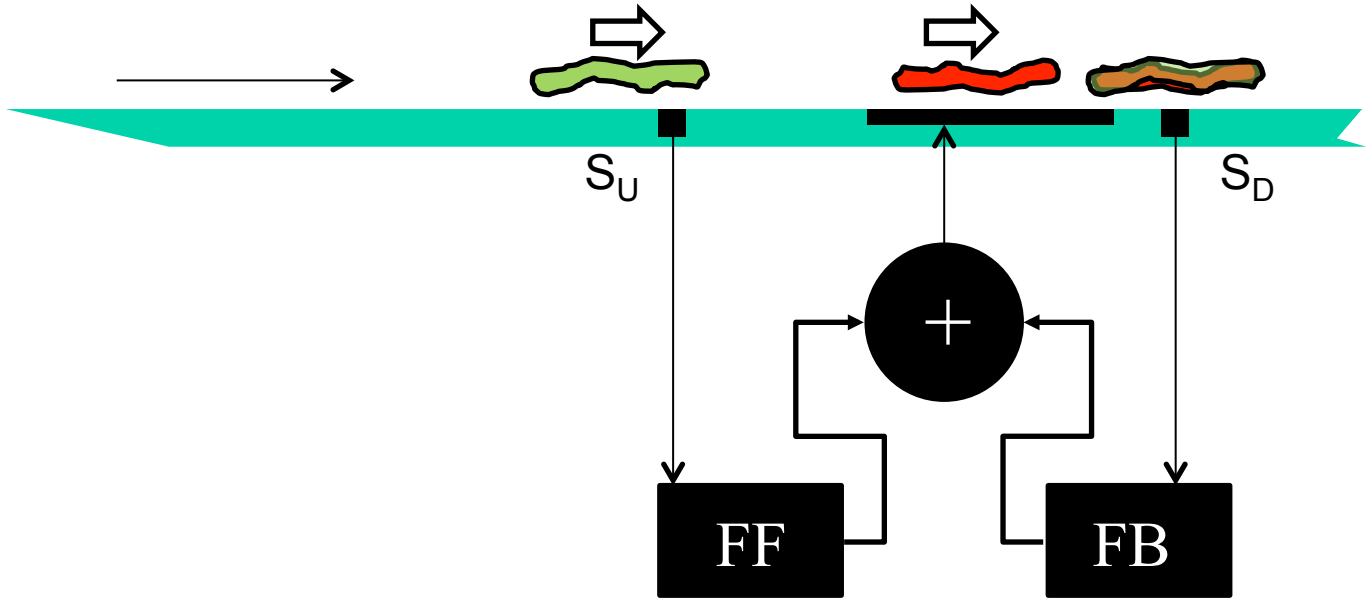

- Streak measured by upstream sensor, S_U
- Counter-disturbance from actuator cancels streak at downstream wall sensor, S_D
- Remaining disturbance measured by the downstream sensor, is fed to a PI controller
- Actuator output adjusted through PI output

Spectrum at feedback sensor

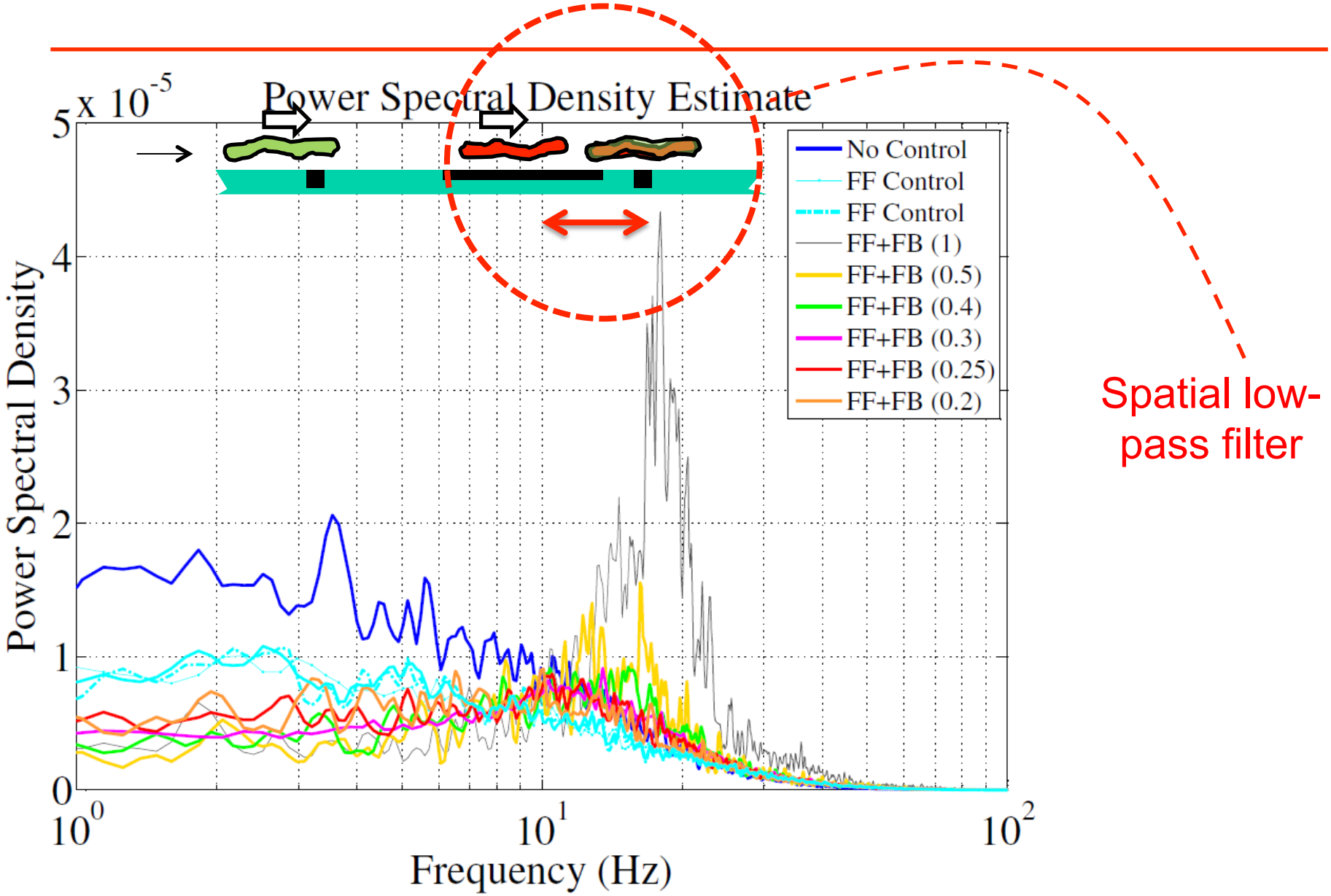

Conclusions

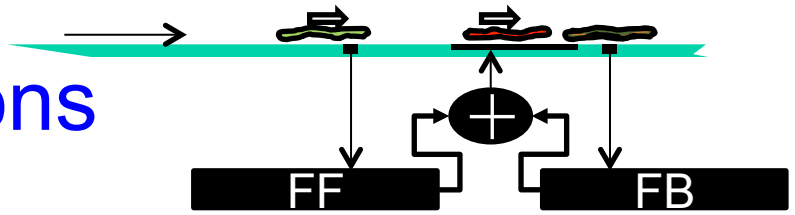

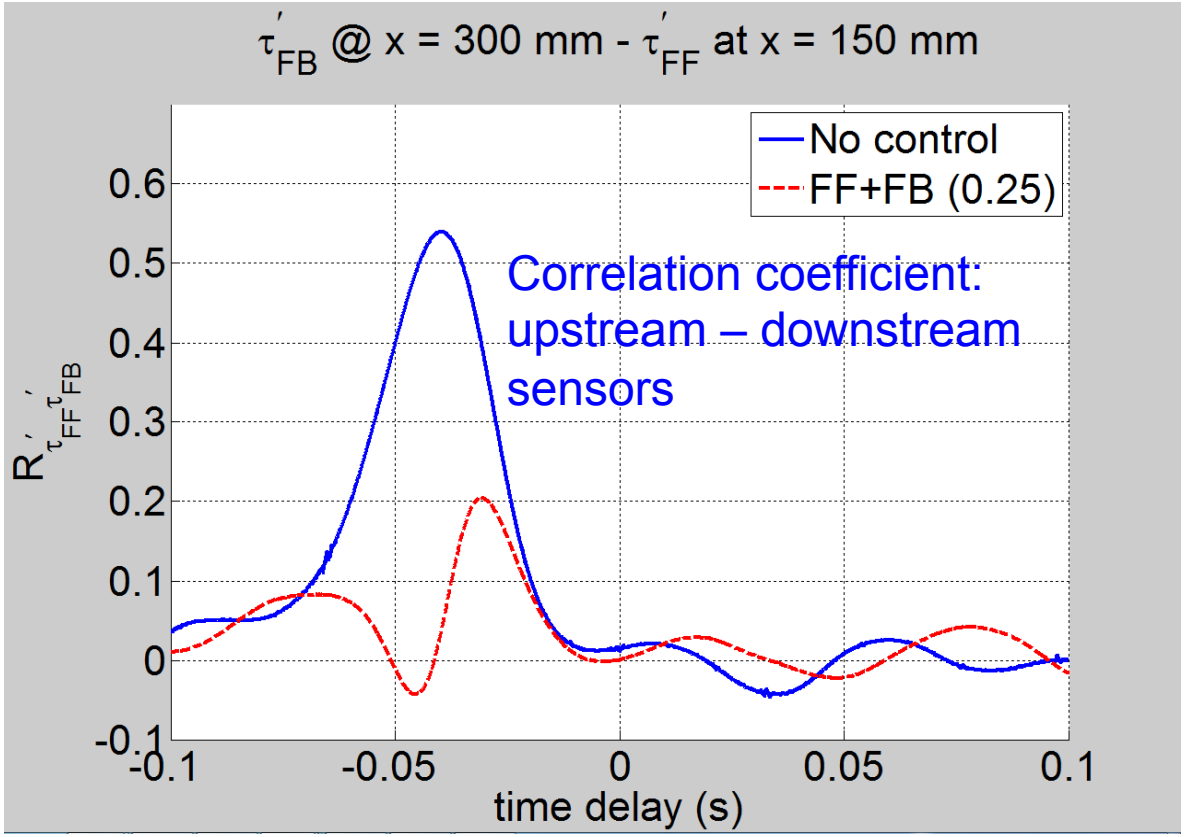

- One-point stochastic estimation is very simple
- Physical reasoning suggests use of $\tau_z(x_1,z,t)$ but not $\boldsymbol{\tau}_x(x_1,z,t)$
- Stochastic environment requires feedback

Outline

- Tollmien-Schlichting (TS) wave cancellation
- Transient growth: a linear paradigm for near-wall turbulence control
- Role of linear feedback in the control of turbulent channel flow
- Open-loop control and travelling surface waves for turbulent skin-friction reduction

Full domain control

- A full-domain linear controller that relaminarises turbulent channel flow $\mathrm{Re}_\tau \leq 400$
- How does this work?
- Temporal evolution – comparison of timescales
- Importance of pressure field: Poisson equation
  - “rapid” and “slow” source terms
  - pressure-*gradient* fluctuations
  - Batchelor, Landahl & Townsend (BLT)

Important points

- Inner – Outer Interaction top-down and bottom-up
- Two imposed lengthscales: $\delta \Big/ \frac{\nu}{u_\tau}$ – how can their effects be separated?
- Single velocity scale, u_τ, but range of convection velocities suggests a range of timescales.
- Shear timescale (linear): $t_s = \left[U'_w \right]^{-1}$, $t_s^+ = 1$
- Blocking timescale (nonlinear): $t_n = \delta / u_\tau$, $t_n^+ \approx 100$
- Impermeability constraint – role of pressure?

Brown Roshko structures

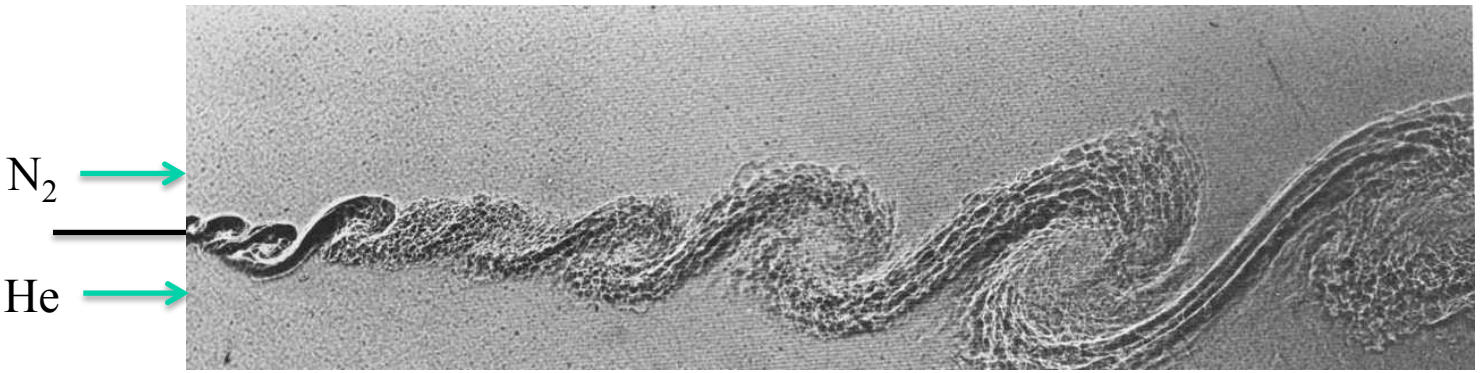

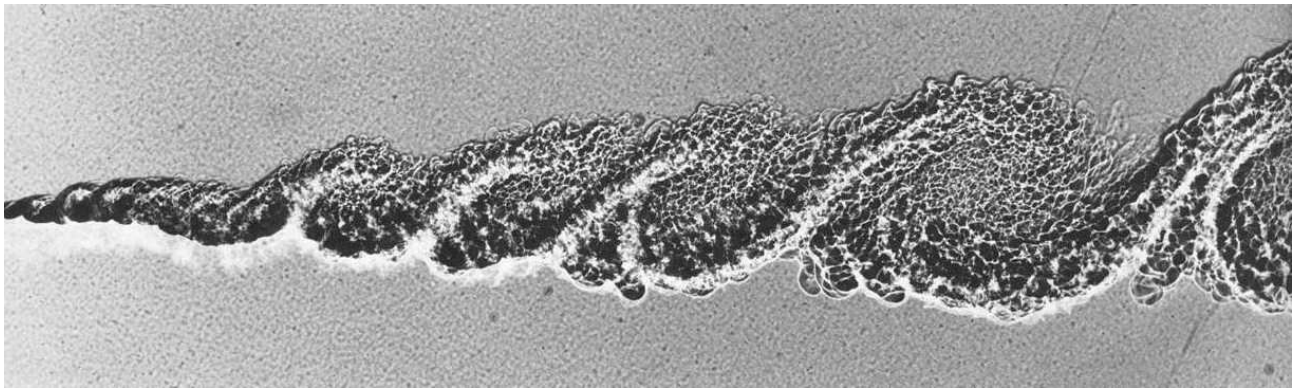

Re x 2

Brown & Roshko 1974

Linear theory

- Linear disturbance equations (r=q= 0): $\left(\frac{\partial}{\partial t}+U\frac{\partial}{\partial x}\right)\nabla^2 v - U''\frac{\partial v}{\partial x} - \frac{\nabla^4 v}{\mathrm{Re}} = 0$

  wall-normal velocity, v

  wall-normal vorticity, η

  $$\left(\frac{\partial}{\partial t}+U\frac{\partial}{\partial x}\right)\omega_y - \frac{\nabla^2\omega_y}{\mathrm{Re}} = -U'\frac{\partial v}{\partial z}$$

- v evolves via OS operator, ω_y evolves via Squire operator. L_c, coupling appears through v-forcing of ω_y.
- Streaks and vortices decay if L_c suppressed (Kim & Lim '00), but nonlinearity required to form structures of correct scales (Waleffe & Kim '97)
- Several suggest structure formation requires linear mechanisms only:
  1. RDT (Lee *et al.* '90) and linearised NS + stochastic forcing (Farrell & Ioannou '93) produce vortices & streaks
  2. stability analysis using turbulent velocity profile with variable eddy viscosity – two peaks of maximum amplification (one inner, one outer) del Álamo & Jiménez (2006), Cossu et al. (2009).
  3. Resolvent analysis (McKeon & Sharma 2010, Luhar *et al.* 2014)

State space description and wall forcing

$$\frac{d}{dt}\begin{bmatrix}\hat{v}\\ \hat{\omega}_y\end{bmatrix}=\begin{bmatrix}L_{os} & 0\\ L_c & L_{sq}\end{bmatrix}\begin{bmatrix}\hat{v}\\ \hat{\omega}_y\end{bmatrix}+\begin{bmatrix}B_v\\ B_\omega\end{bmatrix}\hat{f}$$

$$L_{os}=\left[\nabla^2\right]^{-1}\left\{-ik_xU\nabla^2+ik_xU''+\frac{\nabla^2\nabla^2}{\mathrm{Re}}\right\}$$

$$\nabla^2=\frac{\partial^2}{\partial y^2}-k_x^2-k_z^2$$

$$L_{sq}=-ik_xU+\frac{\nabla^2}{\mathrm{Re}}$$

$$L_c=-ik_zU'$$

- L_c makes the operator A non-normal. It is intrinsic to maintaining turbulence.
- The effects of wall forcing can be included with either B_v finite and $B_\omega = 0$ (blowing, sucking) or $B_v = 0$, and B_ω finite (in-plane motion).

Turbulent channel flow

- Re_τ = 80, 100, 180, 300: Domain $4\pi h$ x $2h$ x $2\pi h$
- Re_τ = 400: Domain $2.5\pi h$ x $2h$ x πh
- Channelflow 0.9.15 (Gibson *et al.* '08)
- Fully-developed: constant mass flux
- Full-domain sensing, actuation on v
- Control focuses on vU'
- Forcing bandwidth progressively increased
- Details for Re_τ = 400, k_x, $k_z \leq 20$
- & at $y^+ \approx 25\big|_{\text{init}}$

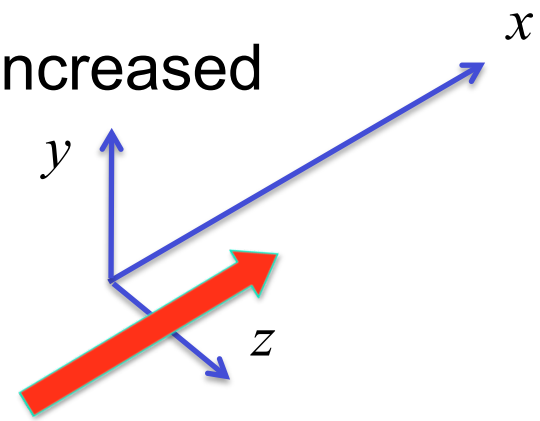

Model formulation

- Navier-Stokes nonlinearity: not stochastic, nor bounded
- In closed or periodic domain, nonlinearity is conservative – Reynolds-Orr equation
- Perturbation equations in which n_i, the nonlinearity is treated as part of the forcing, f_j

$$\frac{\partial u_i}{\partial t} = \Pi\left(U_{0j}\frac{\partial u_i}{\partial x_j} - u_j\frac{\partial U_{0i}}{\partial x_j} - \frac{\partial p}{\partial x_i} + \nu\frac{\partial^2 u_i}{\partial x_j^2} + n_i + B_{ij}f_j + d_i \right)$$

$$n_i = -u_j\frac{\partial u_i}{\partial x_j}$$

- Control counters energy supply via vU'

Linear Globally Stabilising Controller

- Navier-Stokes equations written as a linear system G with control K and nonlinear forcing, f
- Nonlinear term N is conservative w.r.t. disturbance energy
- Turbulent shear stresses treated as part of perturbations we wish to force
- Linear controller works in presence of nonlinearity by characterising it as positive real i.e. passive.
- Stability: choose K such that linear part of closed loop is passive
- The linear terms always dissipate disturbance energy

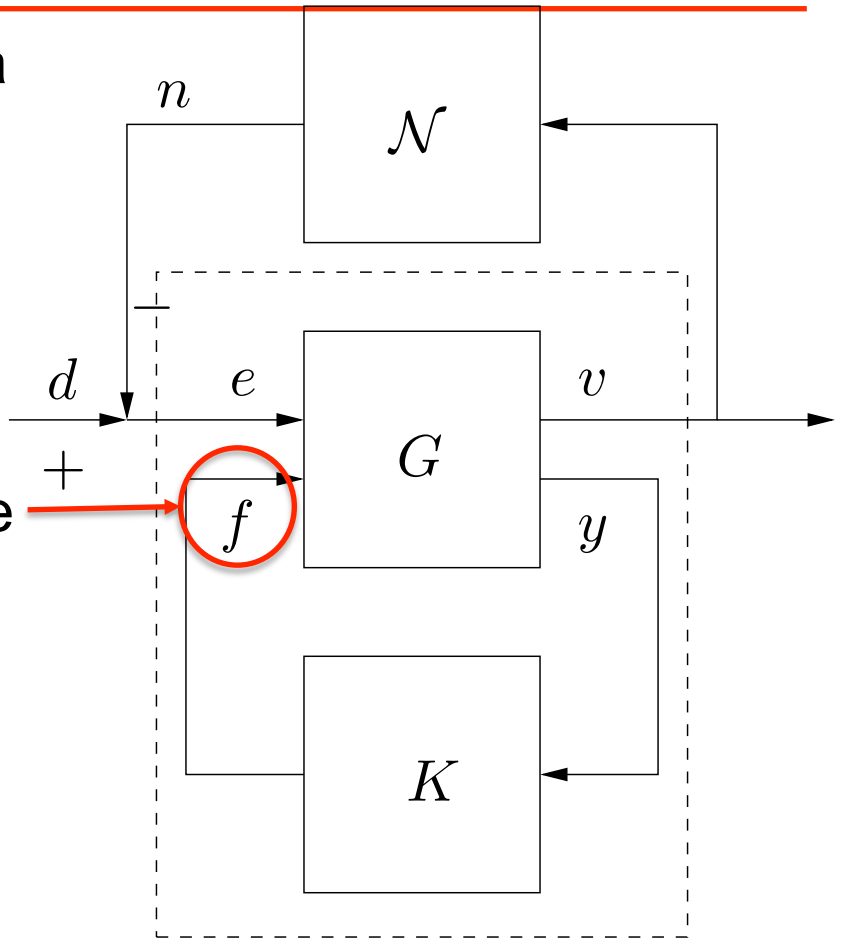

$$\frac{dE}{dt} = \oint_{x\in\Omega} \left(U_L'(y)uv + \frac{\varepsilon}{\mathrm{Re}} \right) \leq 0$$

Sharma *et al.* 2011

$Re_\tau = 180$

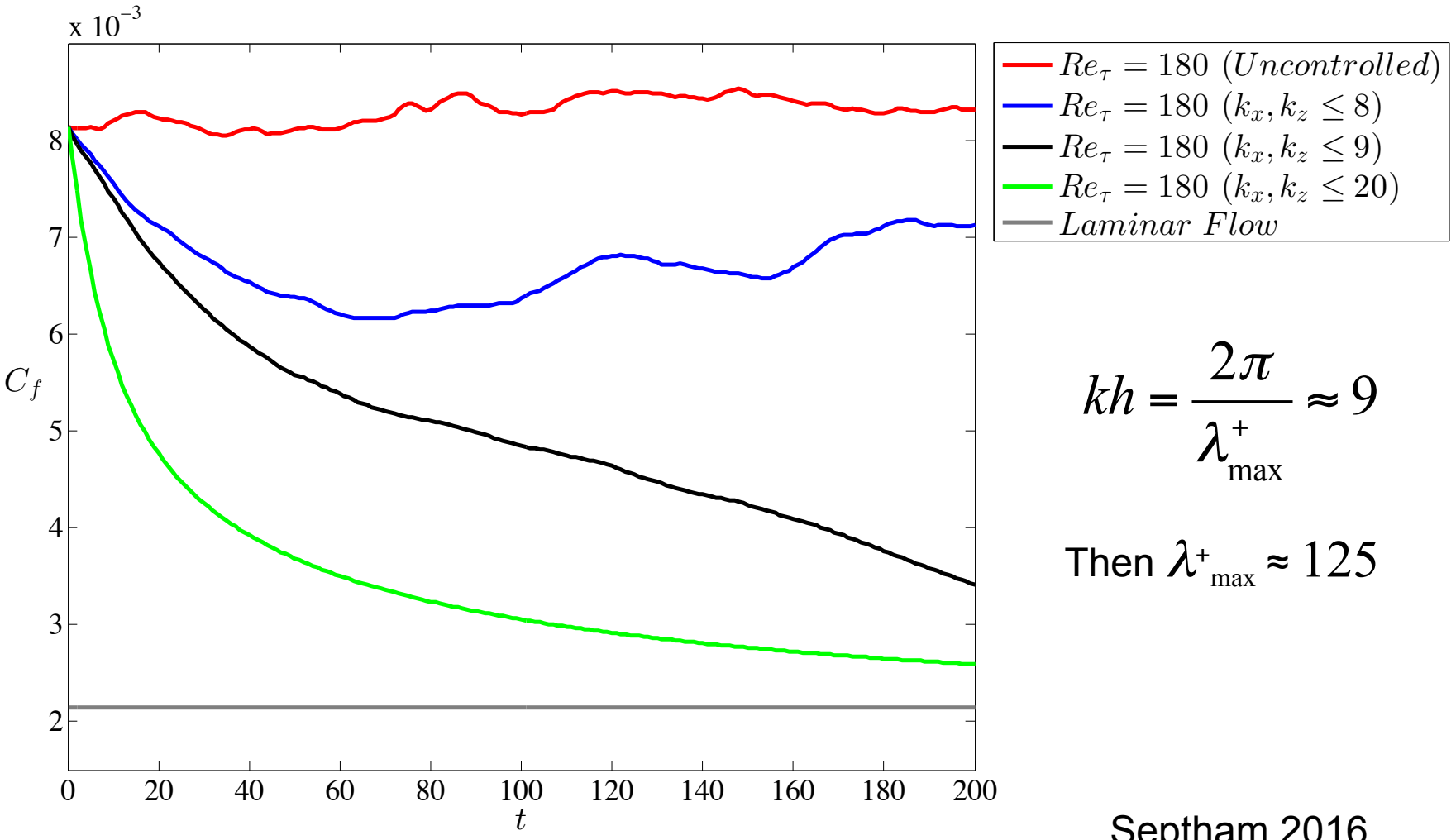

$$kh = \frac{2\pi}{\lambda^+_{\max}} \approx 9$$

Then $\lambda^+_{\max} \approx 125$

Septham 2016

$Re_\tau = 400$

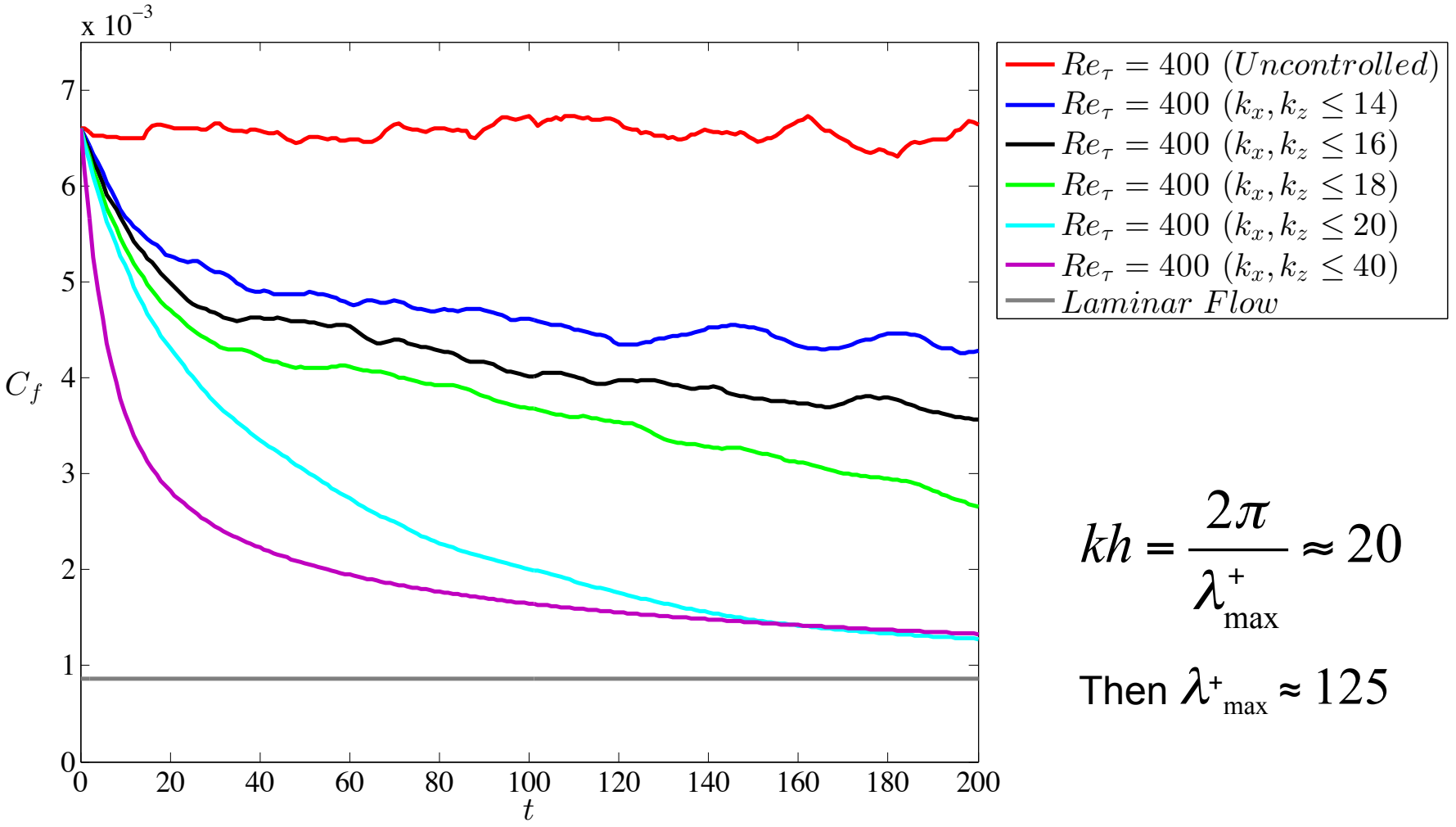

$$kh = \frac{2\pi}{\lambda^+_{\max}} \approx 20$$

Then $\lambda^+_{\max} \approx 125$

Minimum wavenumber for relaminarisation

Re_τ	76.40	97.92	180.70	301.46	397.09
$(k_x, k_z)_{min}$	4	5	9	15	20

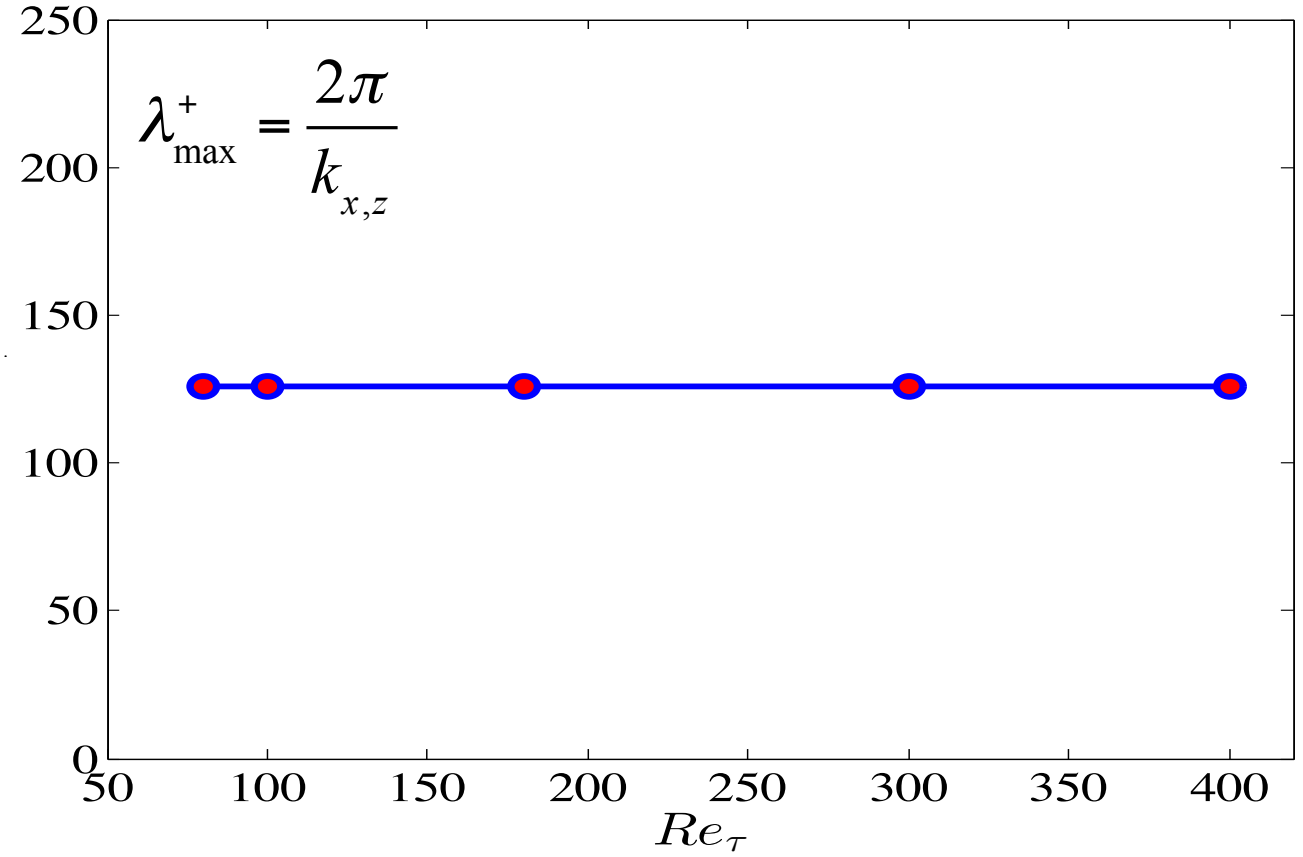

Mean square forcing: $\overline{f^2}(y)$

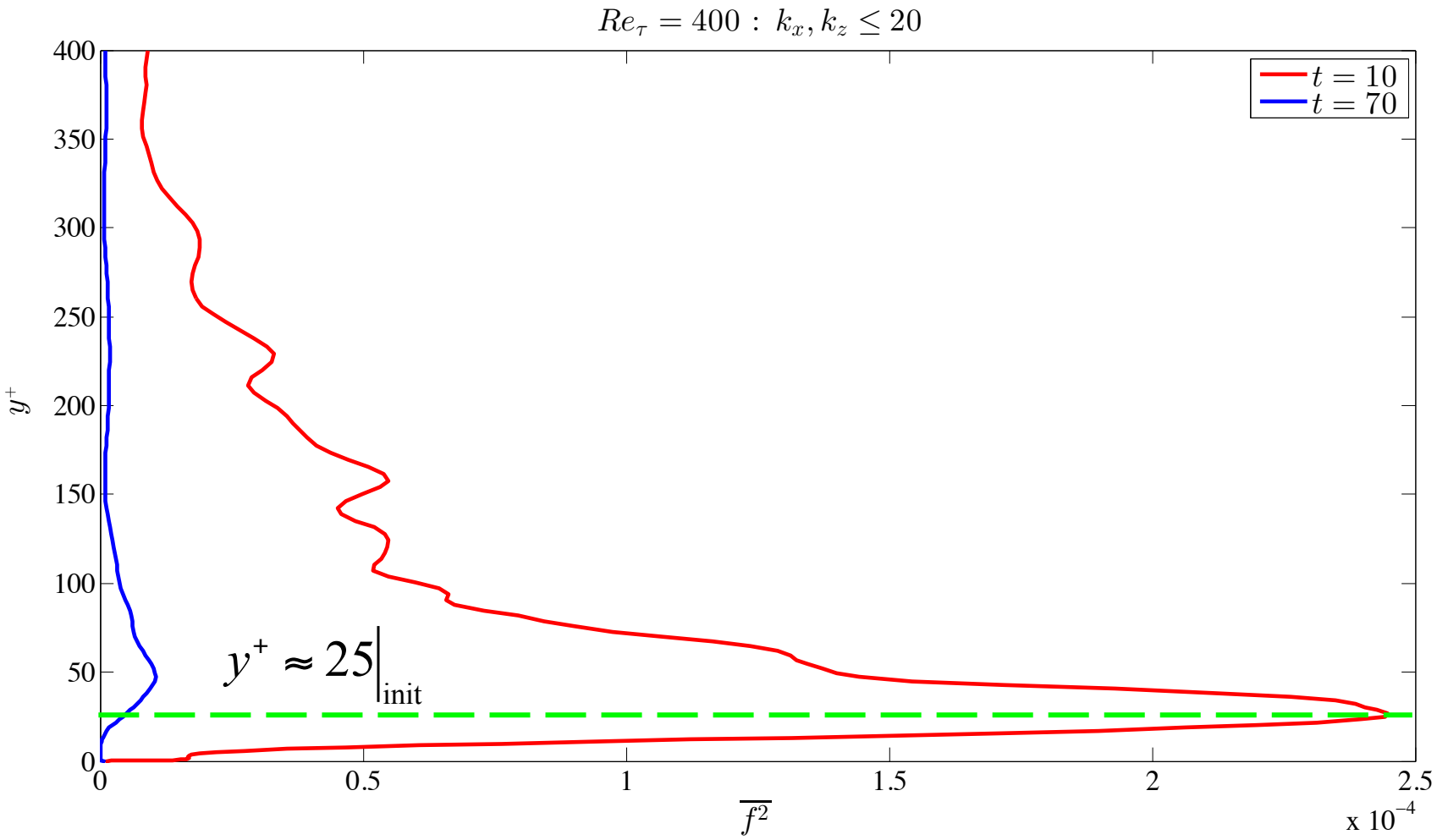

Mean velocity profile

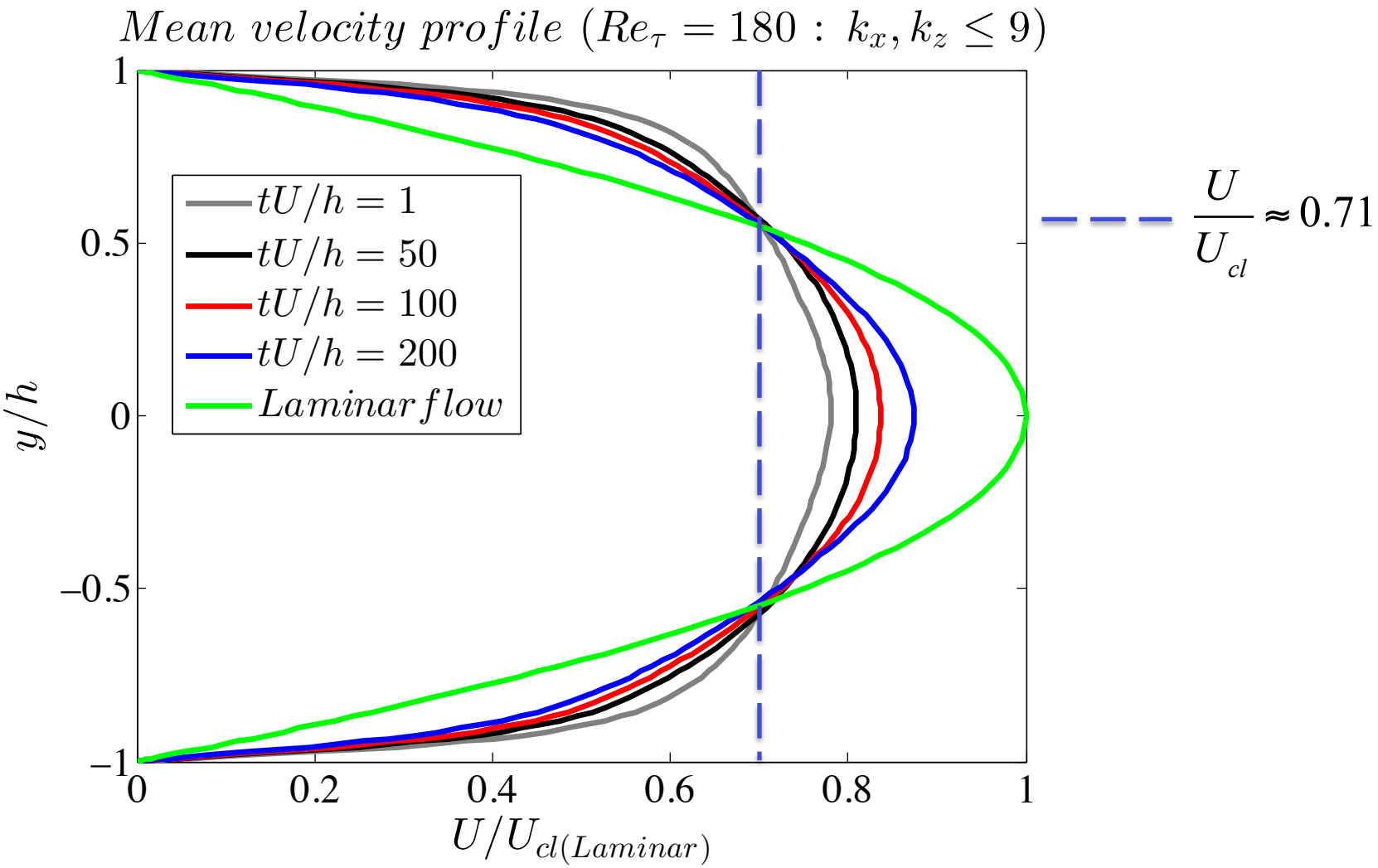

Temporal evolution

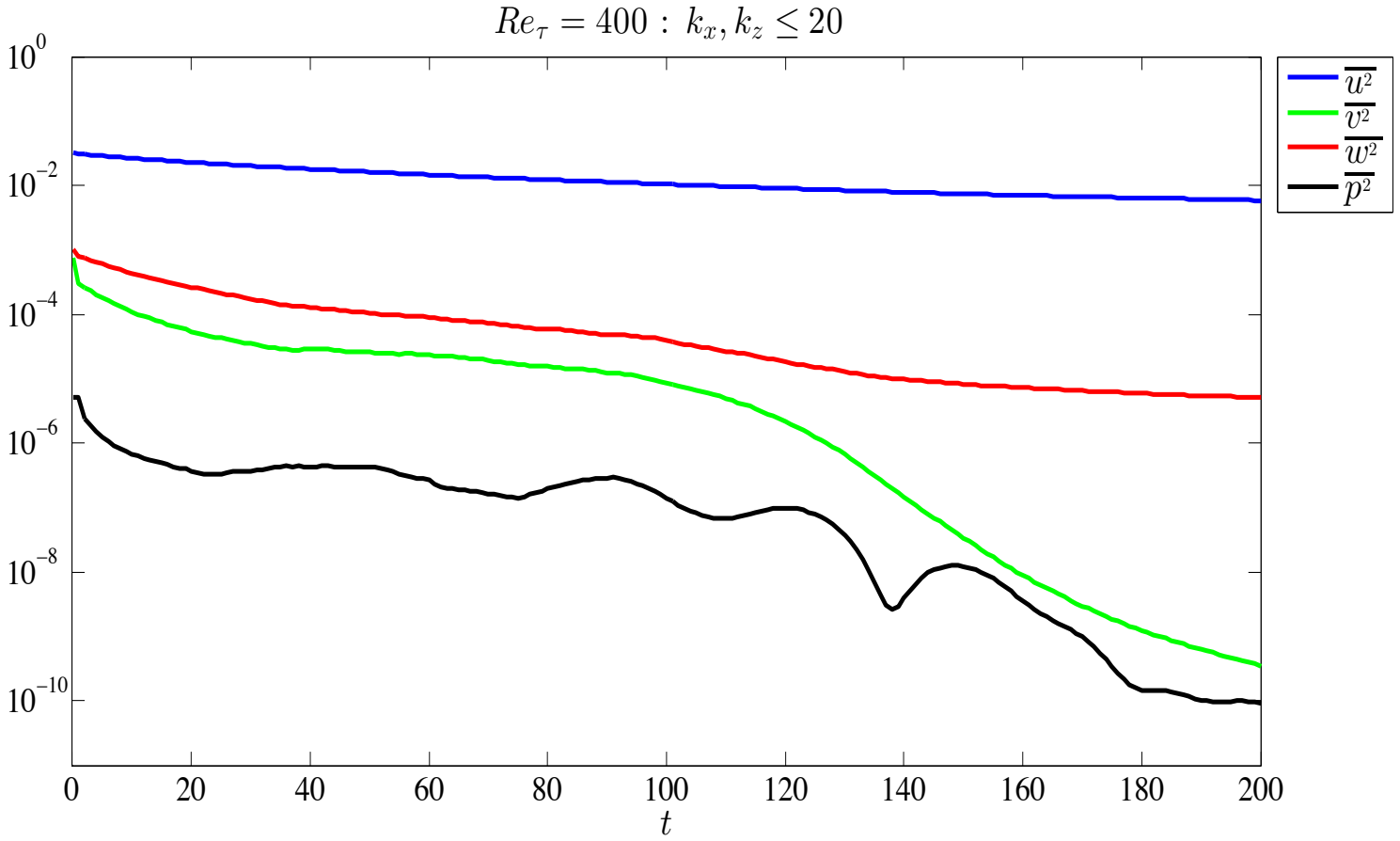

$$\overline{u_i^2}(t) = \frac{1}{\Omega} \oint_{x \in \Omega} u_i^2(x, y, z, t) dx dy dz$$

Quasi-streamwise vortices and relaminarisation

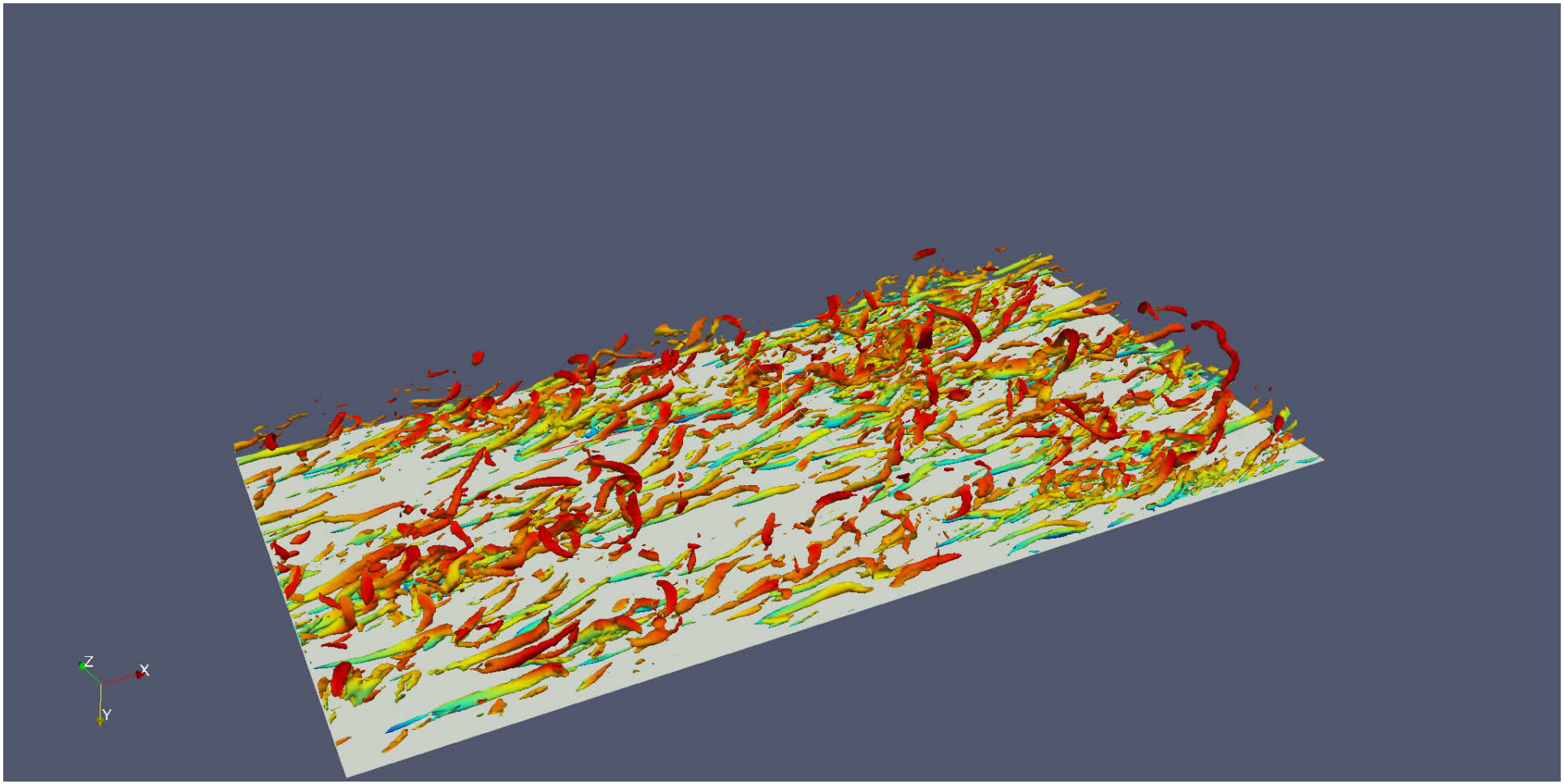

Temporal evolution: Re_τ=100; y^+=15

u

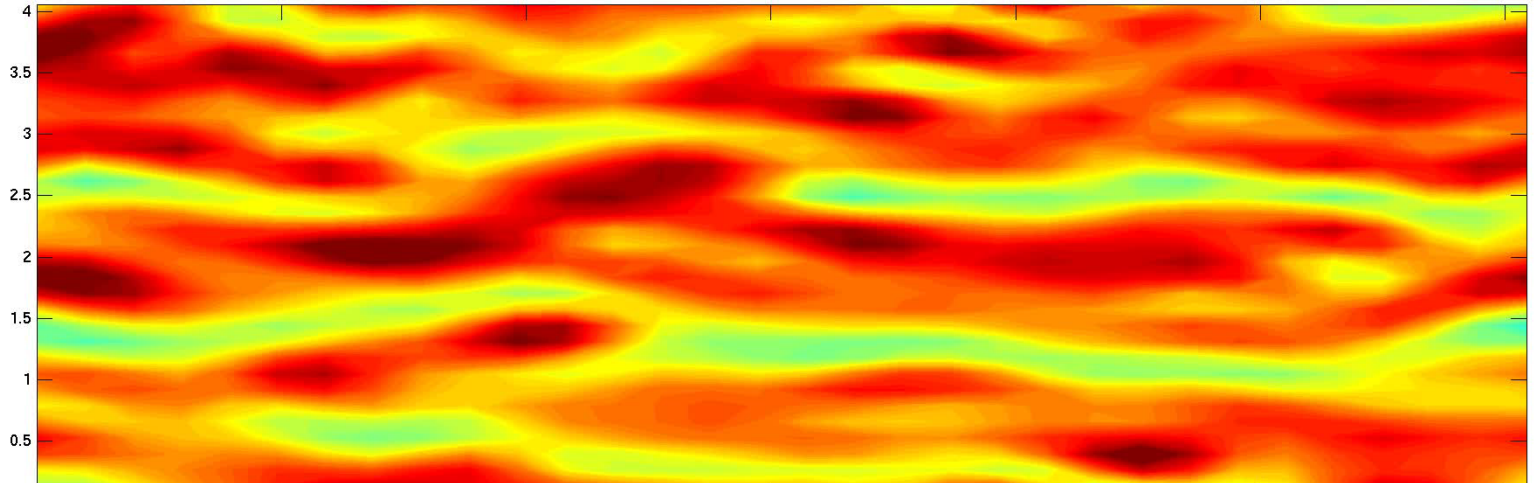

v

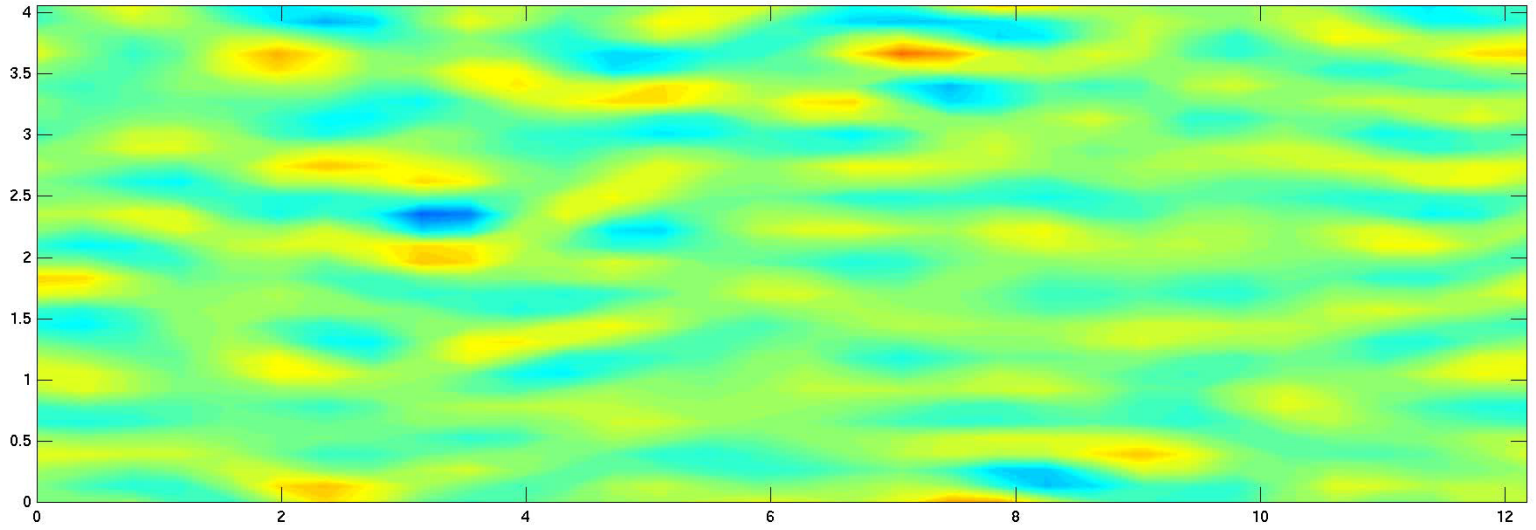

Controlled u: $y^+ = 15|_{\text{init}}$

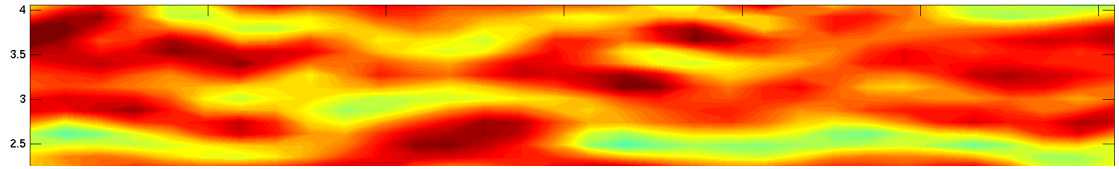

$t = 2$

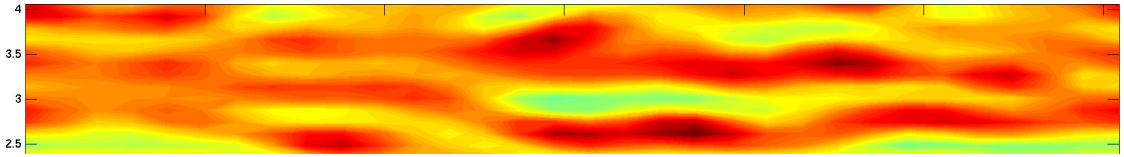

$t = 10$

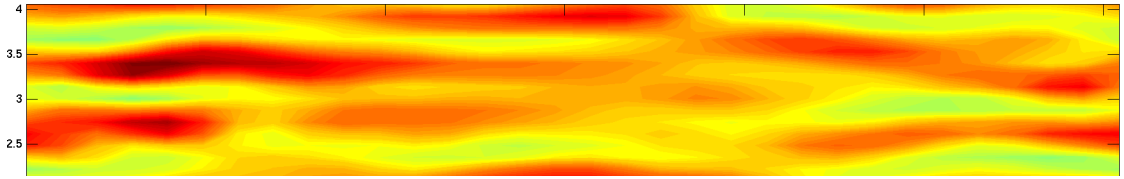

$t = 20$

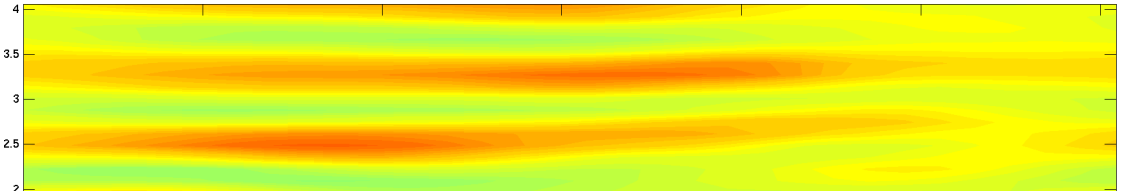

$t = 50$

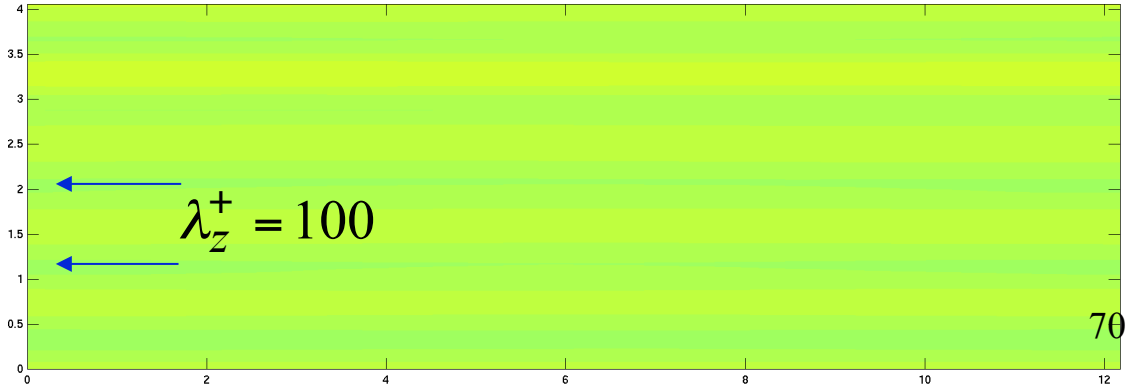

$t = 100$

Controlled p: $y^+ = 15|_{\text{init}}$

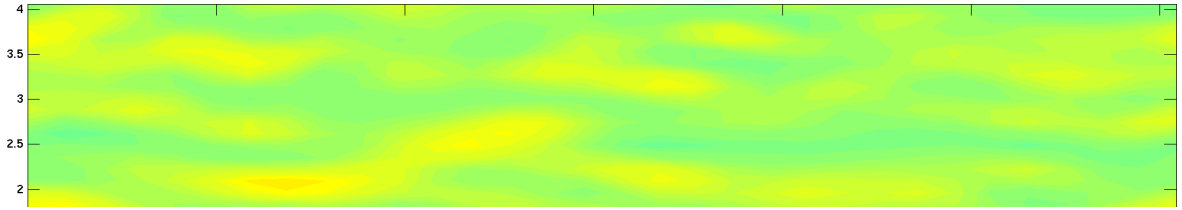

$t = 2$

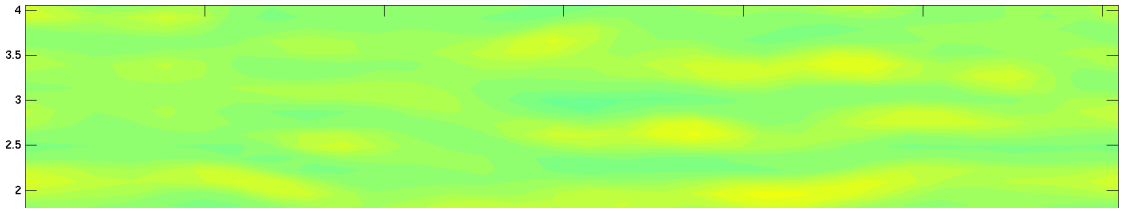

$t = 10$

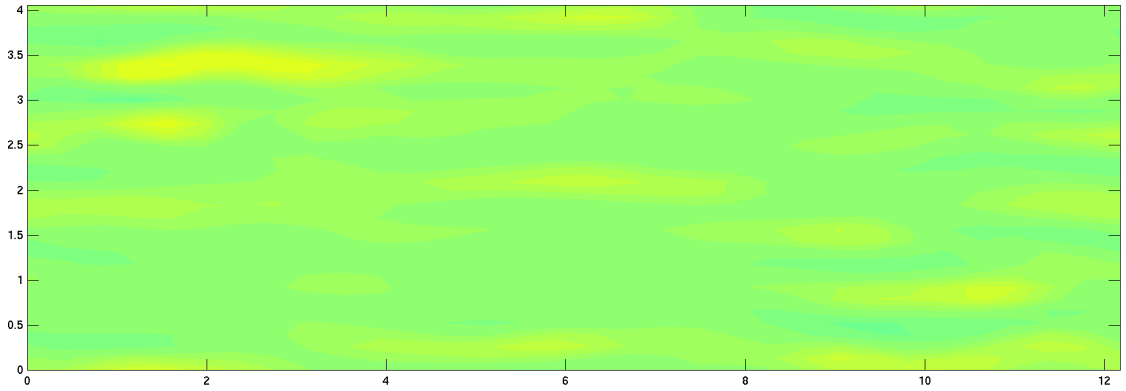

$t = 20$

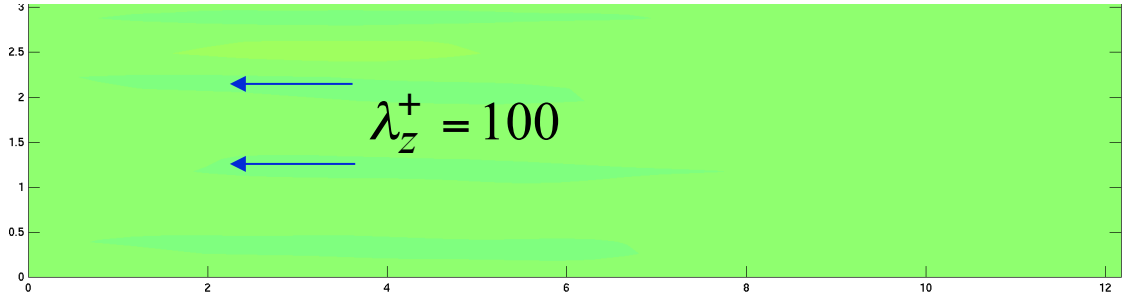

$t = 50$

Controlled u,v and p: $y^+ = 15|_{\text{init}}$ t = 20

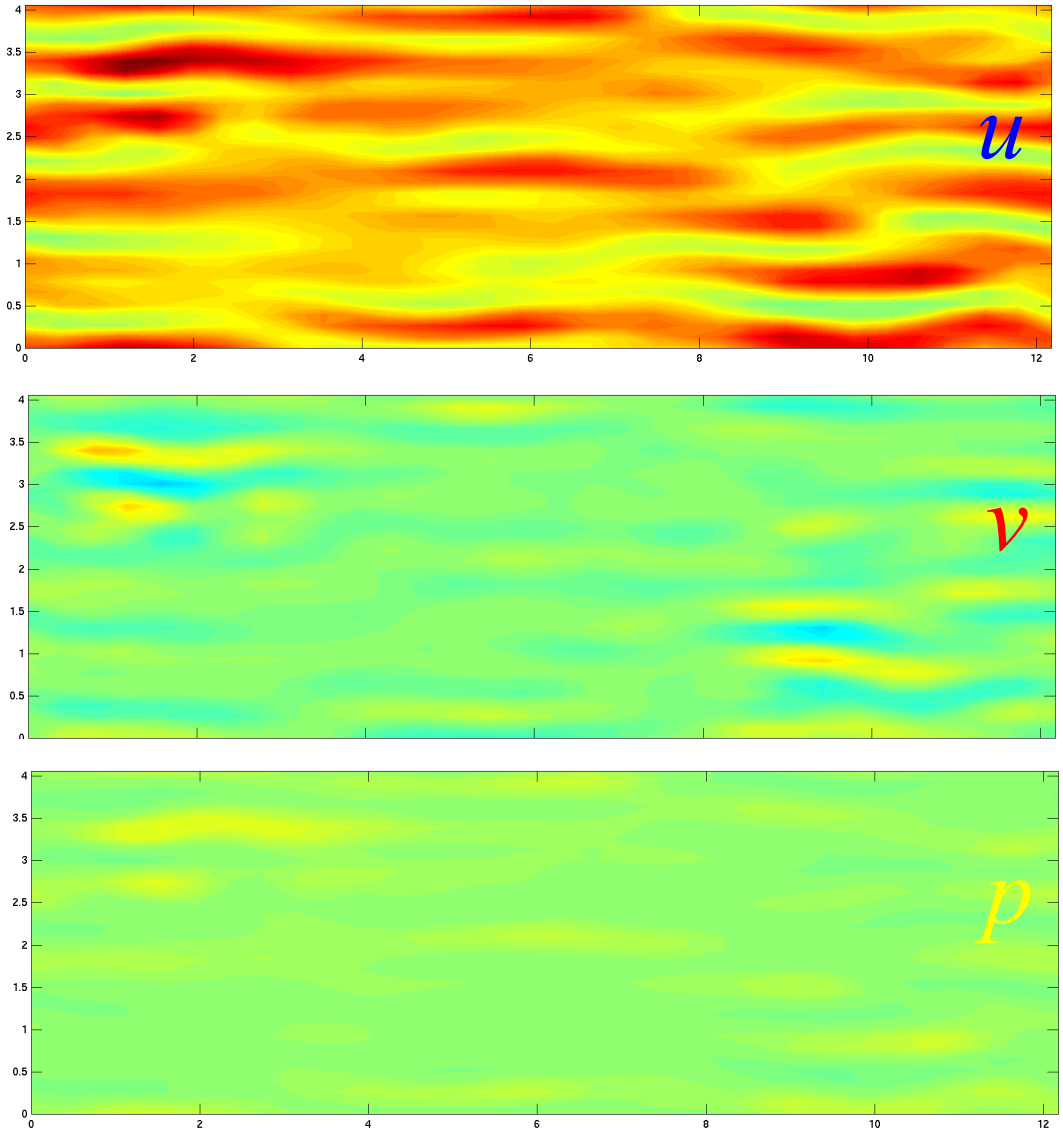

Controlled u,v and p: $y^+ = 15|_{\text{init}}$ t = 50

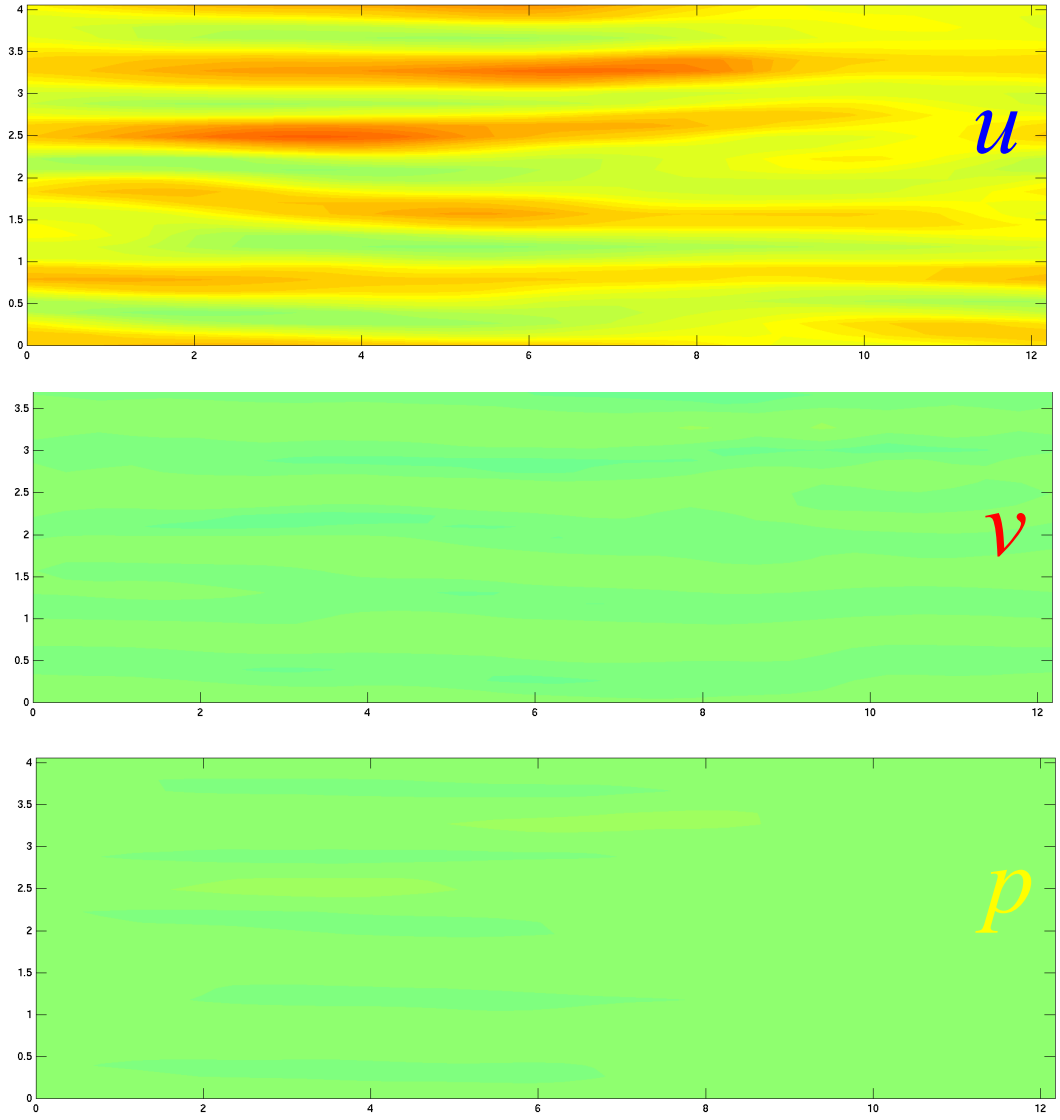

Production and dissipation

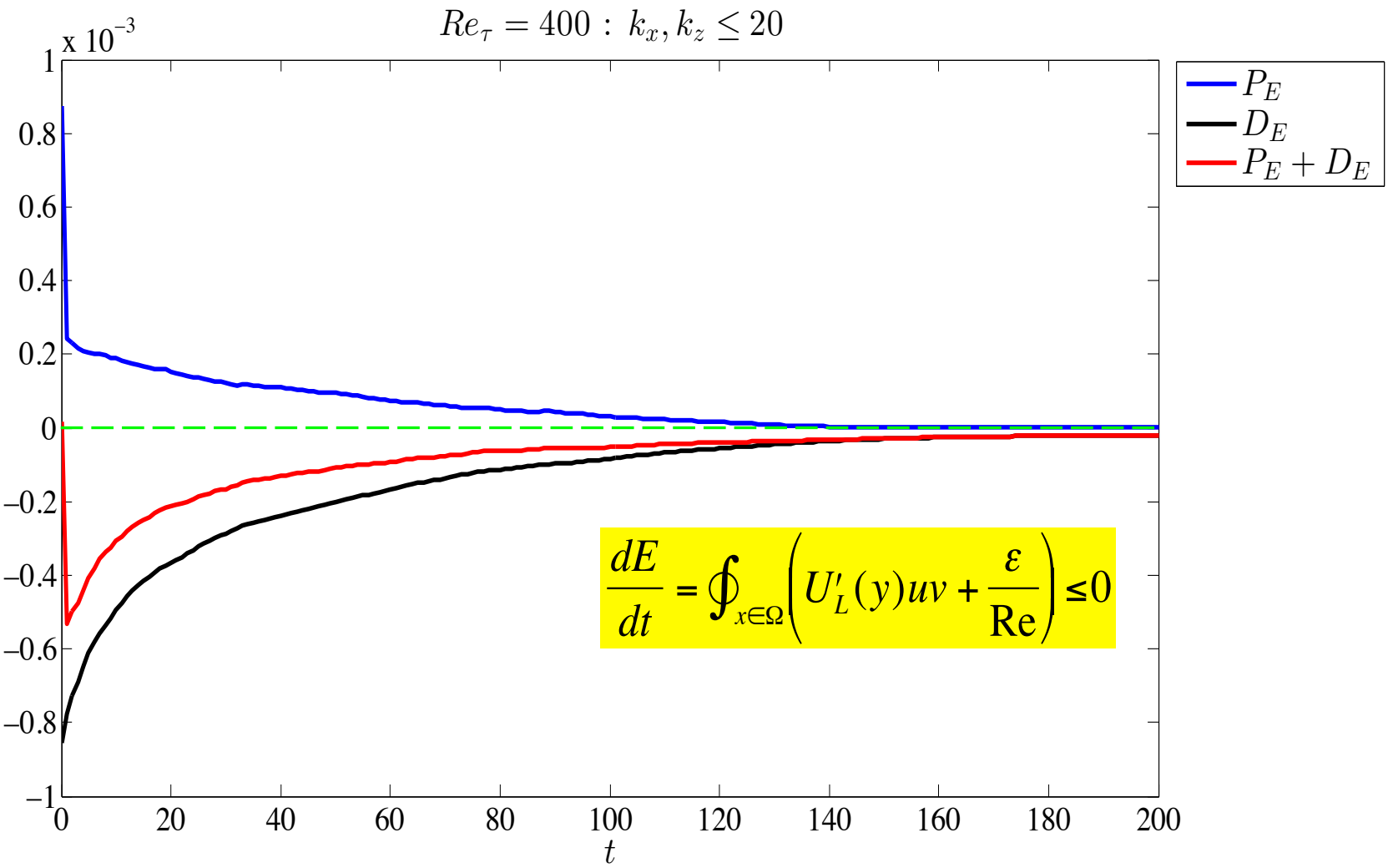

Green's function decomposition of pressure field

- Poisson equation for pressure fluctuations:

$$-\nabla^2 p = 2U'\frac{\partial v}{\partial x} - \frac{\partial^2}{\partial x \partial y}\left[uv - \overline{uv}\right]$$

$$-\left(\nabla^2 p_{rapid} + \nabla^2 p_{slow} + \nabla^2 p_{Stokes}\right)$$

$$-\nabla^2 p_{Stokes} = 0, \quad \frac{\partial p}{\partial y}(\pm h) = \frac{1}{\mathrm{Re}}\frac{\partial^2 v}{\partial y^2}$$

Kim 1989

Instantaneous wall pressure $\mathrm{Re}_\tau = 400$

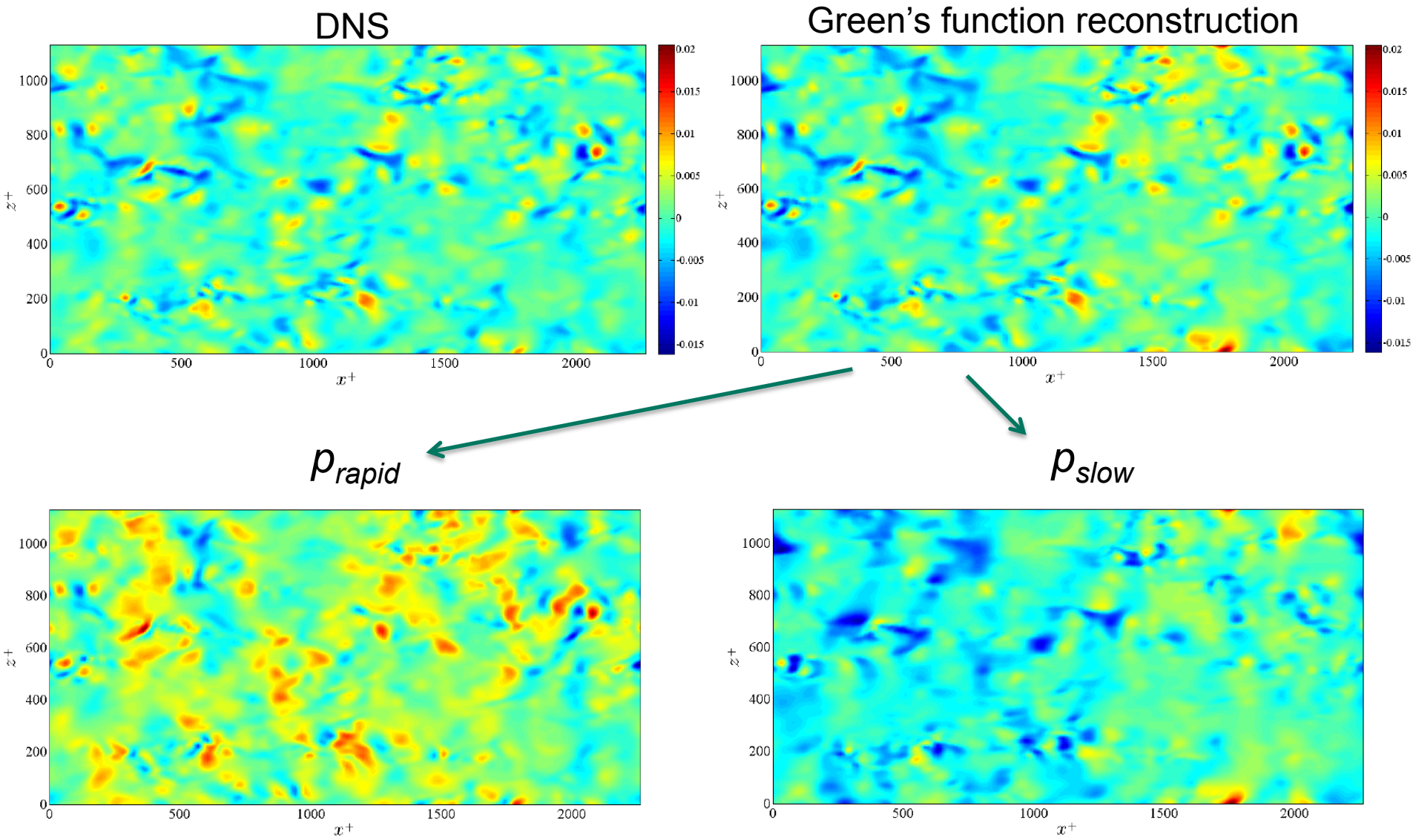

Temporal evolution of p'_{rapid} and p'_{slow}

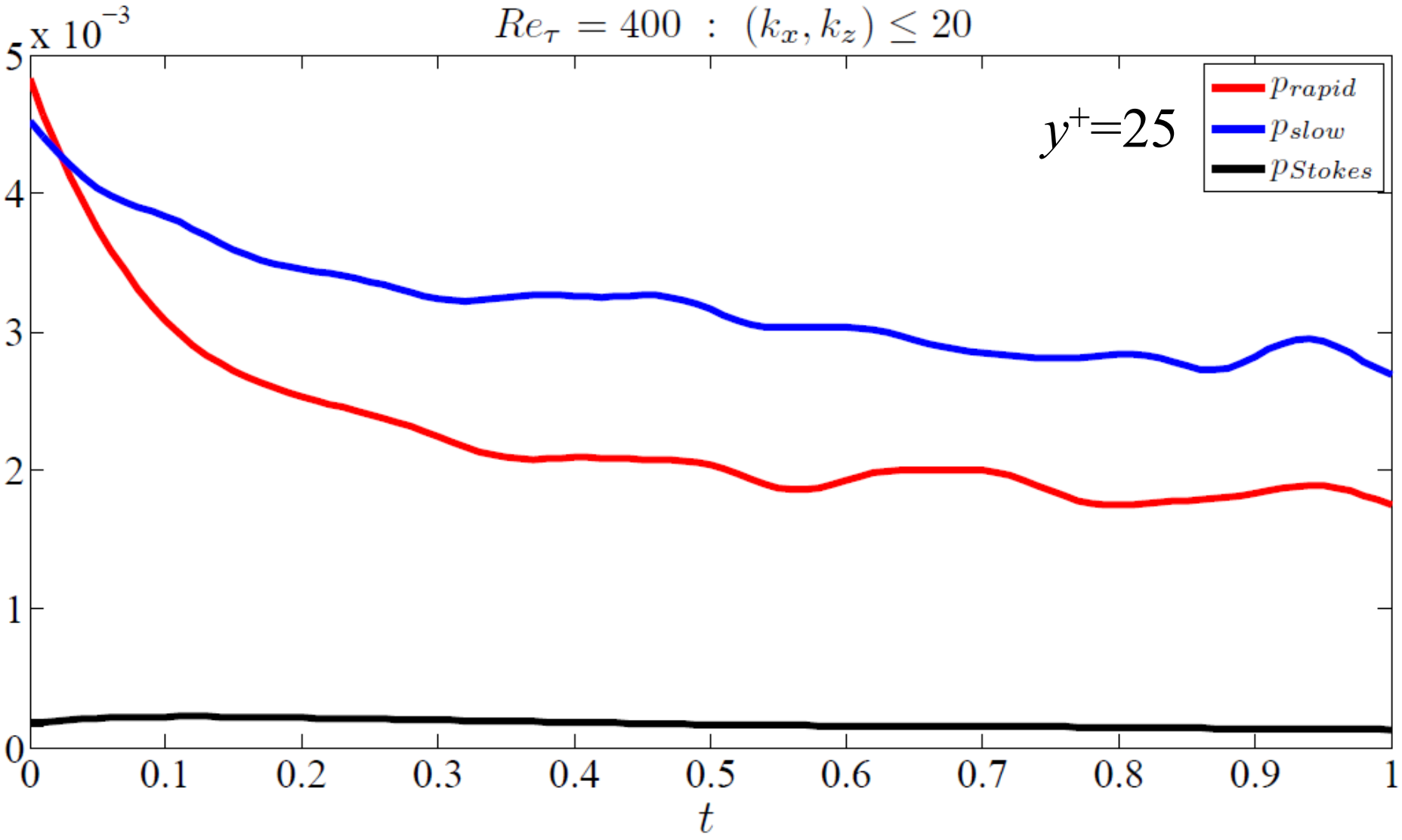

Source terms for mean-square pressure

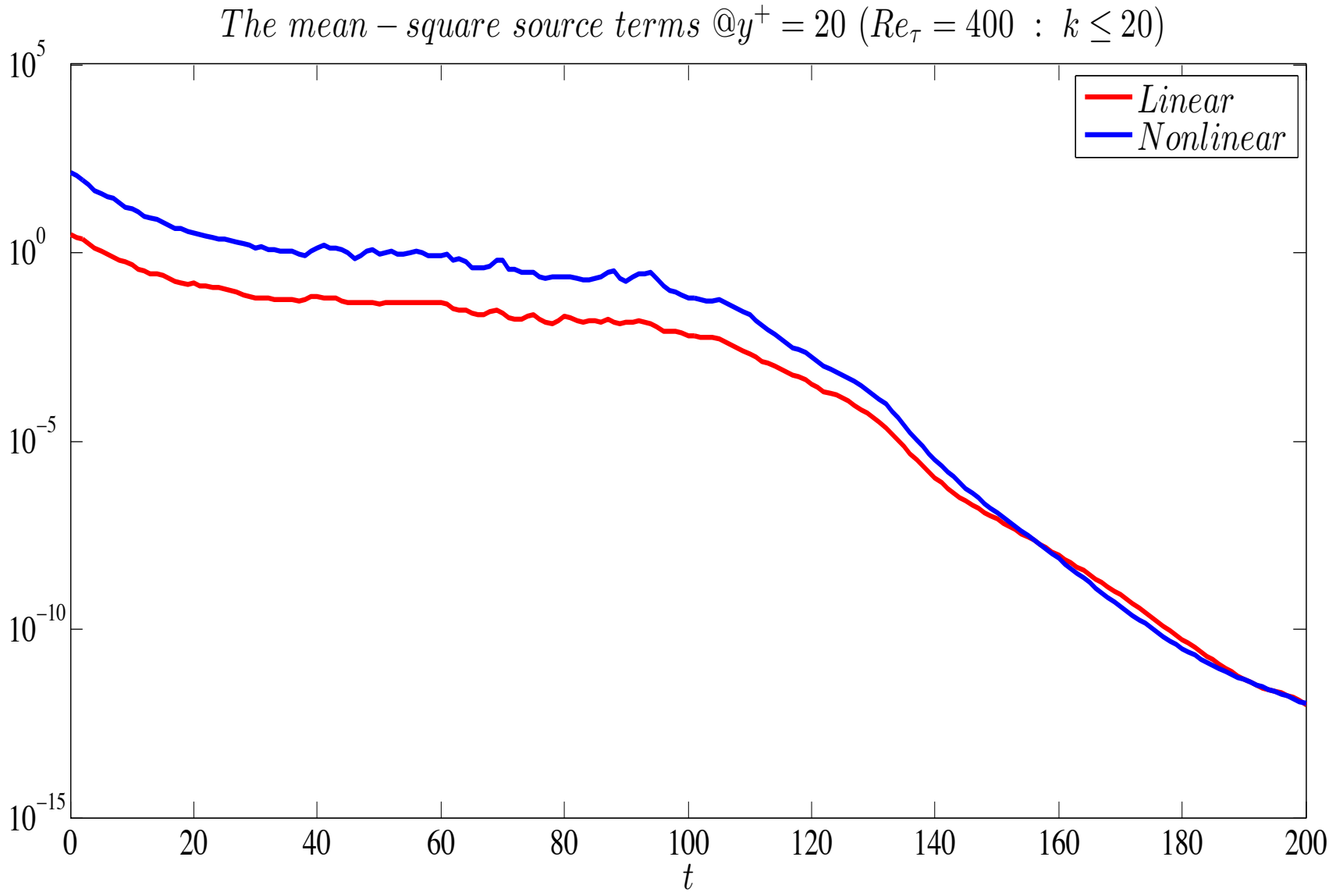

Pressure gradient fluctuations

- High Reynolds numbers: local isotropy and negligible viscous diffusion
- Mean-square acceleration becomes

$$\overline{\left(\frac{Du_i}{Dt}\right)^2} \approx \overline{\left(\frac{\partial p}{\partial x_i}\right)^2} + \nu^2 \overline{\left(\frac{\partial^2 u_i}{\partial x_j^2}\right)^2} - 2\nu \frac{\partial}{\partial x_i}\left(\overline{p \frac{\partial^2 u_i}{\partial x_j^2}}\right)$$

- where

$$\overline{\left(\frac{\partial p}{\partial x_i}\right)^2} \approx 20\nu^2 \overline{\left(\frac{\partial^2 u_i}{\partial x_j^2}\right)^2}$$

- Therefore, even the smallest scale motion is driven by pressure gradients and not by viscous forces.

Batchelor & Townsend 1956

Fully developed turbulent channel flow
no control

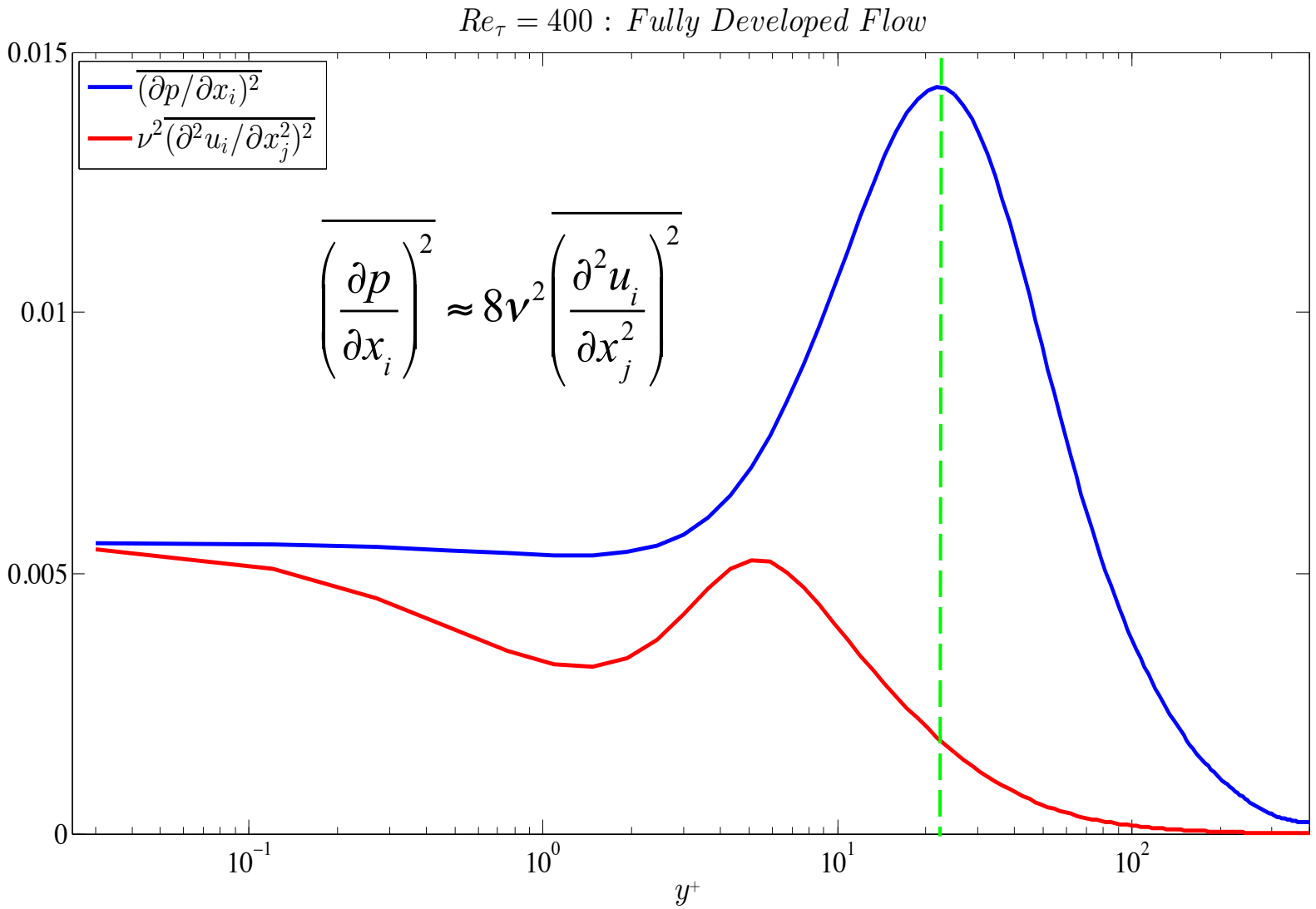

$$\overline{\left(\frac{\partial p}{\partial x_i}\right)^2} \Big/ \nu^2 \overline{\left(\frac{\partial^2 u_i}{\partial x_j^2}\right)^2} \quad : t = 50$$

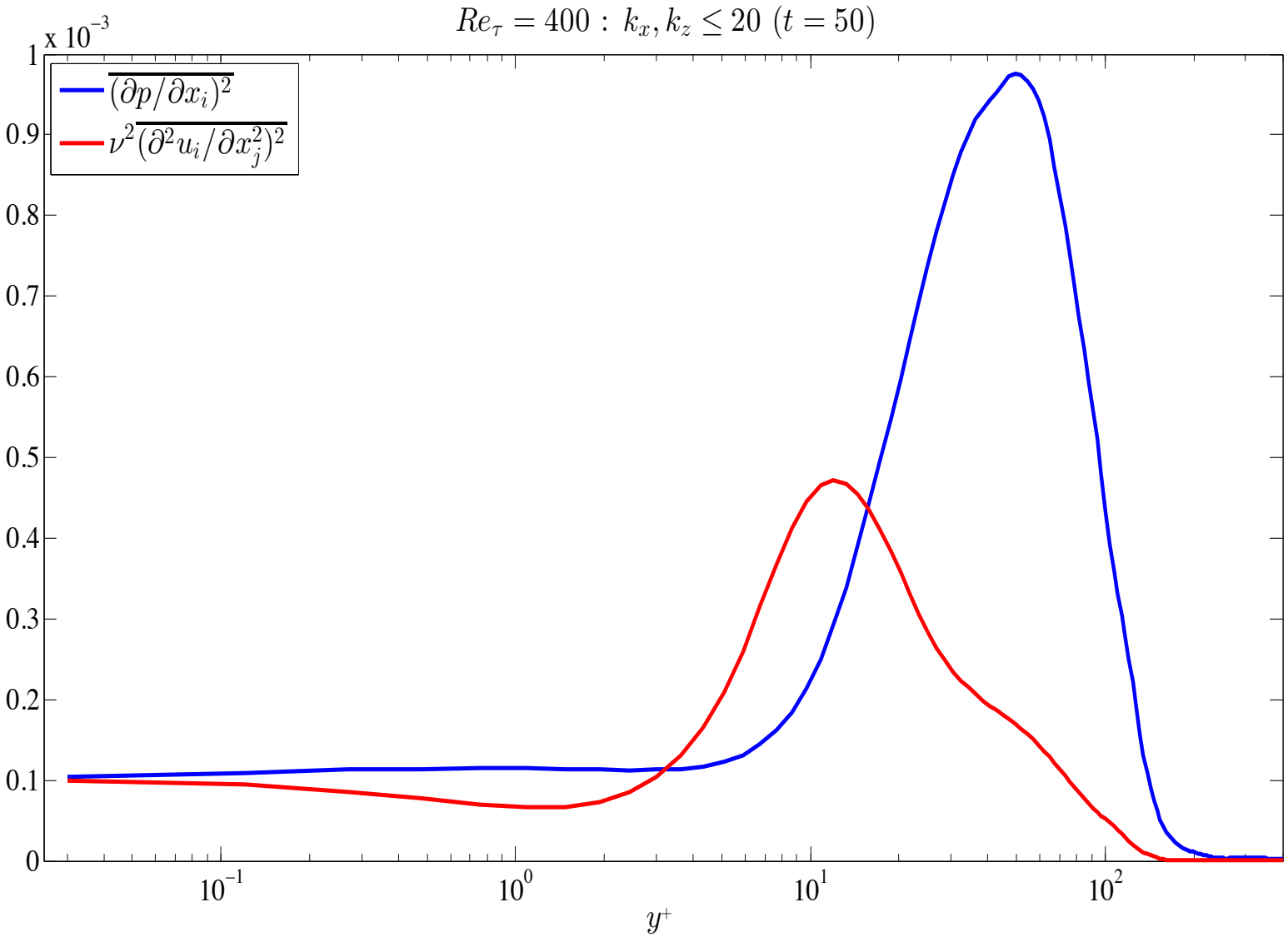

$$\overline{\left(\frac{\partial p}{\partial x_i}\right)^2} \Big/ \nu^2 \overline{\left(\frac{\partial^2 u_i}{\partial x_j^2}\right)^2}$$

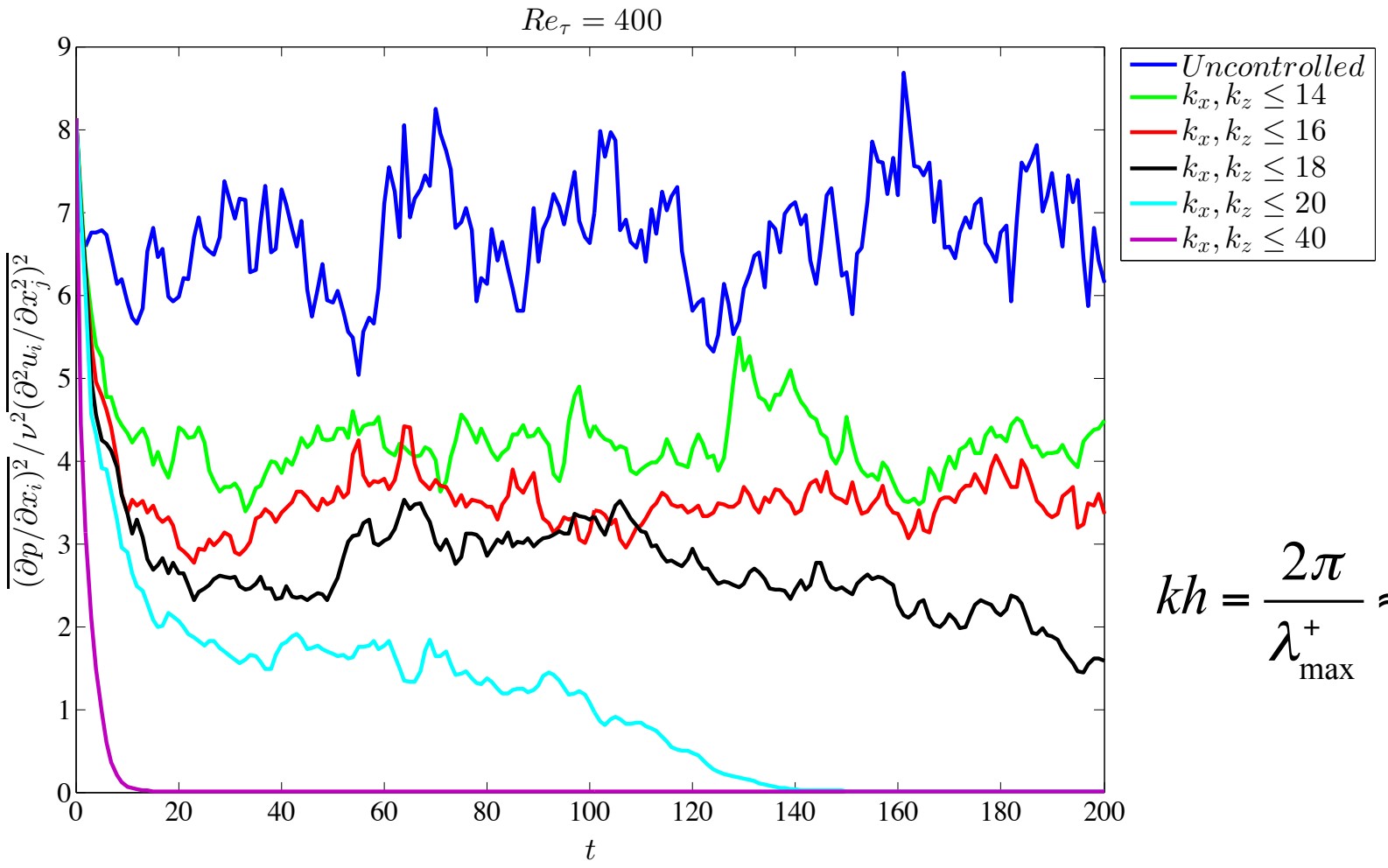

$$kh = \frac{2\pi}{\lambda^+_{\max}} \approx 20$$

Turbulent channel flow pressure statistics

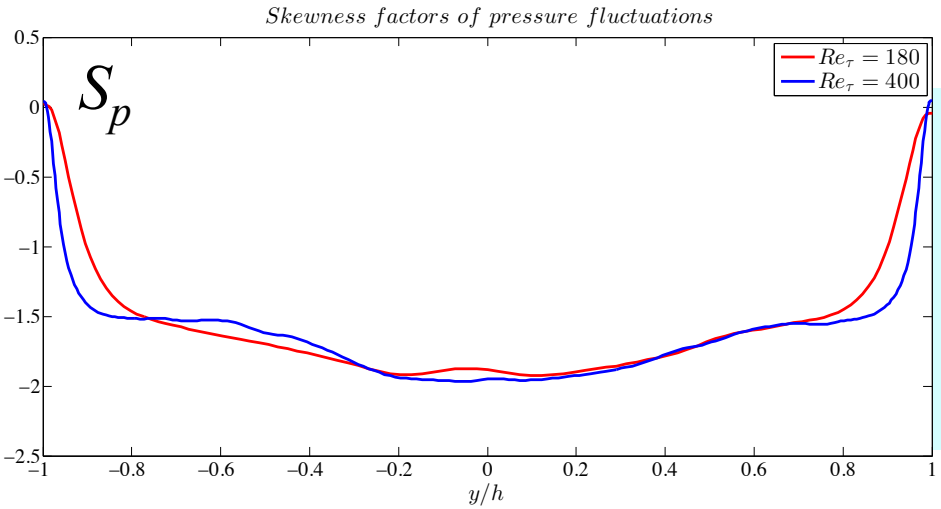

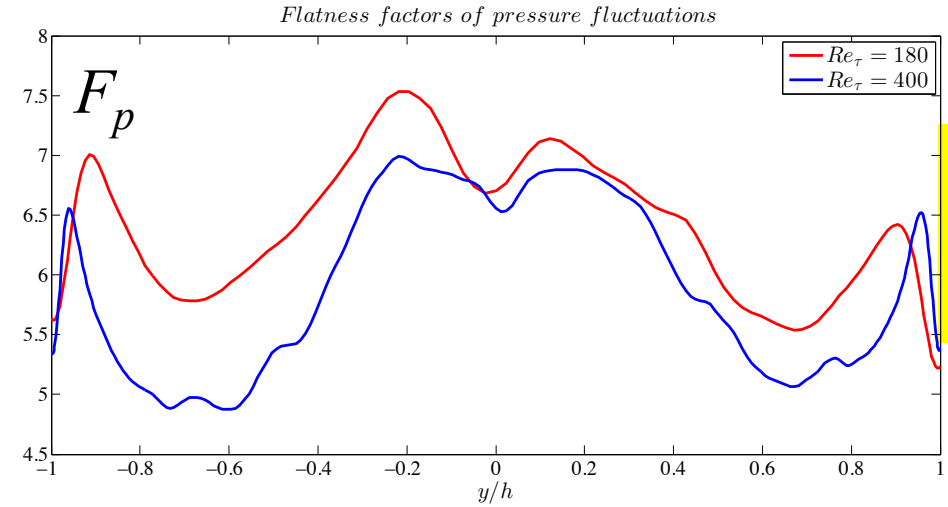

- Spatial intermittency: $S_p \approx 0$, $F_p \approx 6$
- Green's function integral shows that contribution to wall pressure comes mostly from near-wall velocity field, both rapid and slow

$$-\nabla^2 p = 2U' \frac{\partial v}{\partial x} - \frac{\partial^2}{\partial x \partial y}\left[uv - \overline{uv}\right]$$

BLT theory

- Sublayer as a waveguide: primarily for p and v
- u and w also wave-like but including convected eddy behaviour
- Description of both large & small scales – Inner-outer interaction?
- Pressure sources can ‘trigger’ bursts near wall = short shear – interaction timescale

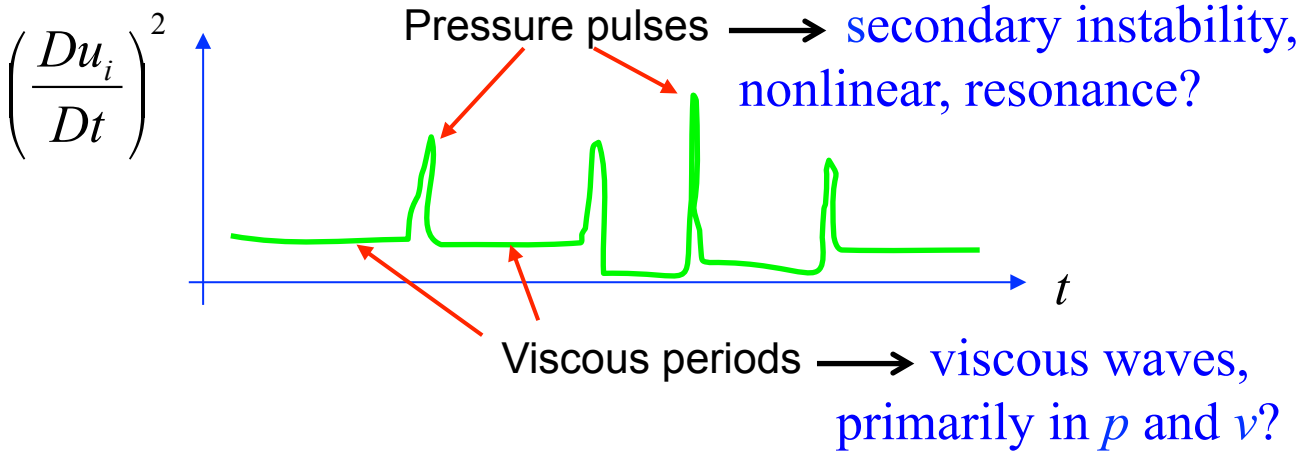

Conclusions

- Linear full-domain forcing via vU' attenuates turbulent channel flow – must resolve streak spacing
- Control acts on v–component field and hence pressure field via rapid source term of Poisson equation
- Inhibiting the propagation of sublayer viscous waves precludes the occurrence of nonlinear secondary instabilities
- Relevance of Landahl's theory for linear control lies in the fact that, over the short time for which the controller is effective, the longer turbulence time scale is not significant
- Shear timescale effective because of pressure – linear source term – an RDT approximation

Outline

- Tollmien-Schlichting (TS) wave cancellation
- Transient growth: a linear paradigm for near-wall turbulence control
- Role of linear feedback in the control of turbulent channel flow
- Open-loop control and travelling surface waves for turbulent skin-friction reduction

Kagome lattices for friction drag reduction

- The design of a wind tunnel experiment to generate in-plane travelling waves $0<u_p<0$ of spanwise forcing.
- Use Kagome lattice to generate the waves (actuated compliant structure).
- Explore the effects of this forcing on a turbulent boundary layer.
- Measure changes in skin friction.

$$u_p = \omega / k_x = f \lambda_x$$

$$W(x,t) = A \sin\left(k_x x - \omega t\right)$$

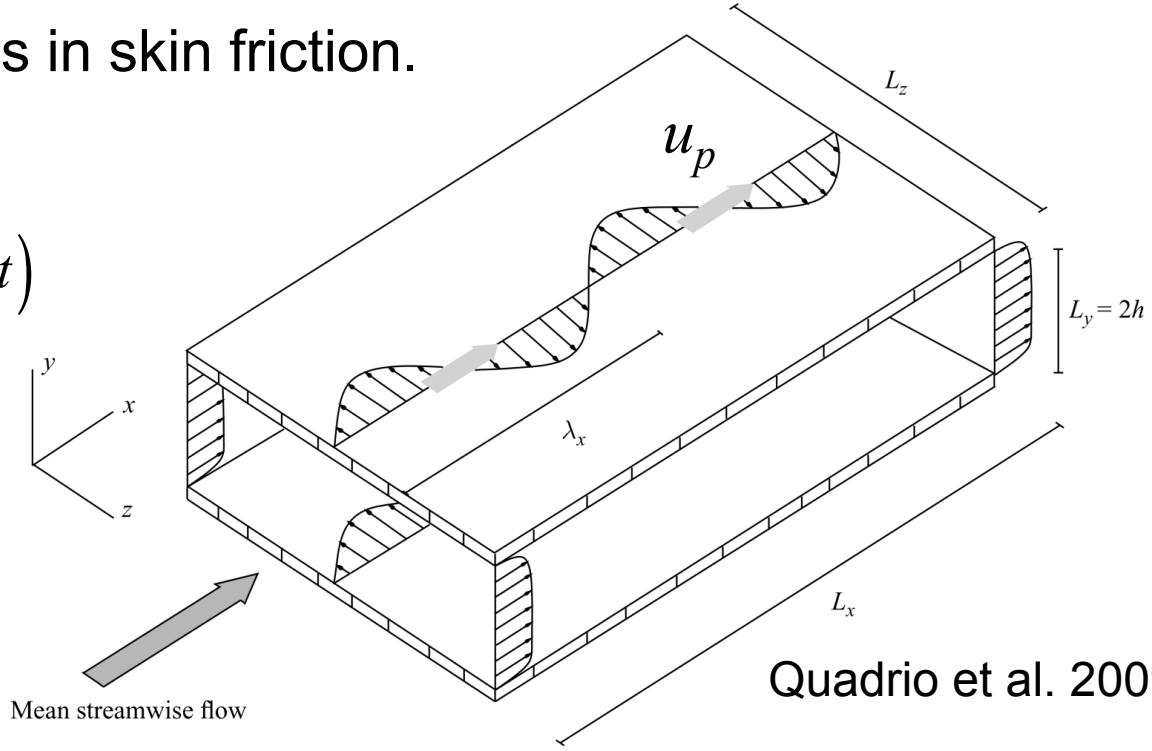

Quadrio et al. 2009

The kagome lattice

- The Kagome lattice is a structure which propagates displacements along discrete “corridors”.
- These corridors can then be driven independently to discretise waveforms.
- By varying the phase between adjacent corridors, a travelling or standing wave can be created.

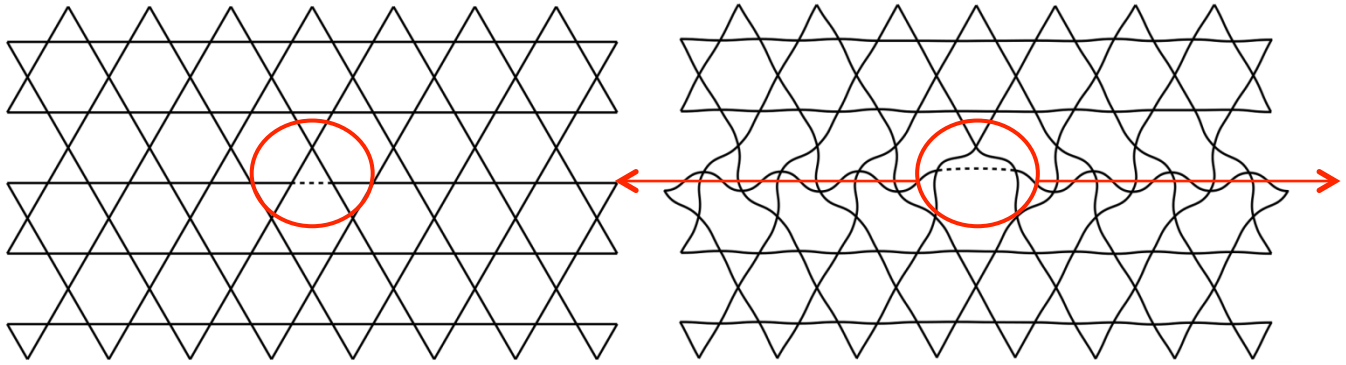

Requirements of an experimental surface: skin friction drag

- Always aim to maximise wave velocity, W^+ .
- Try and achieve the largest wavenumber, k^+, as possible.
- Match suitable frequency to map, but use T^+ = 100 as a good starting point.
- Practical application (higher Re, U_∞ ⟶ higher frequencies.

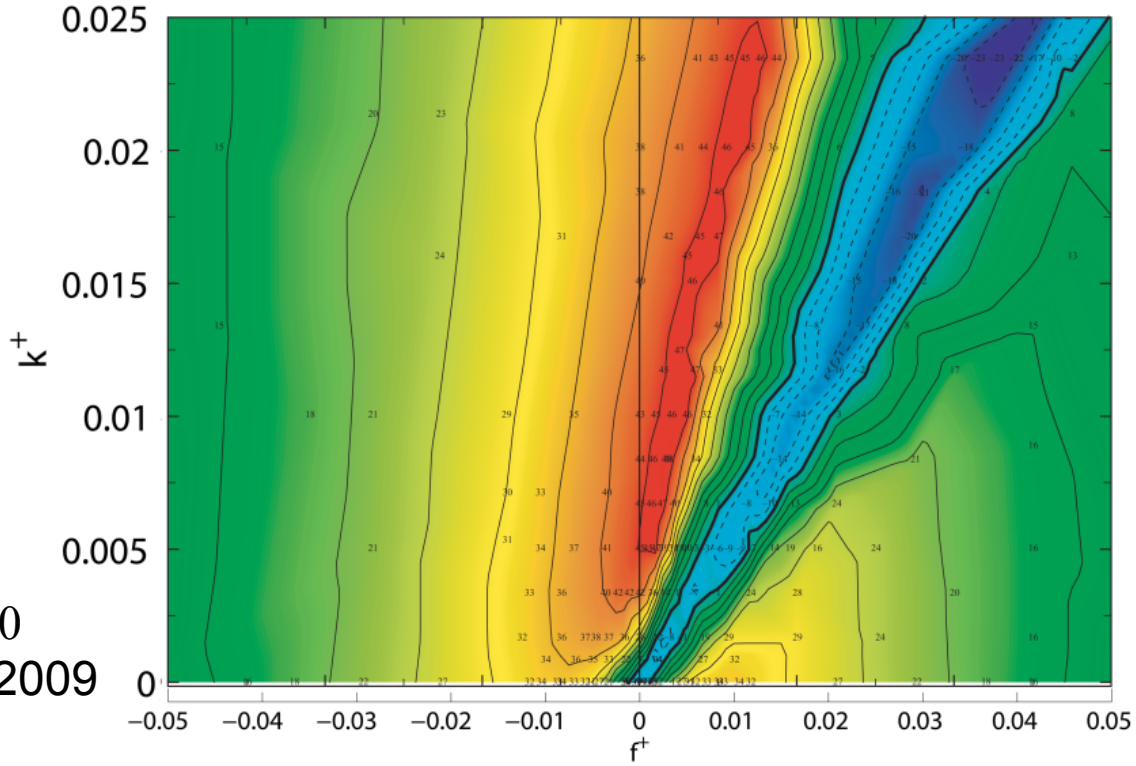

: decrease 46%

: increase 20%

DNS at Re_τ=200
Quadrio et al. 2009

The kagome lattice

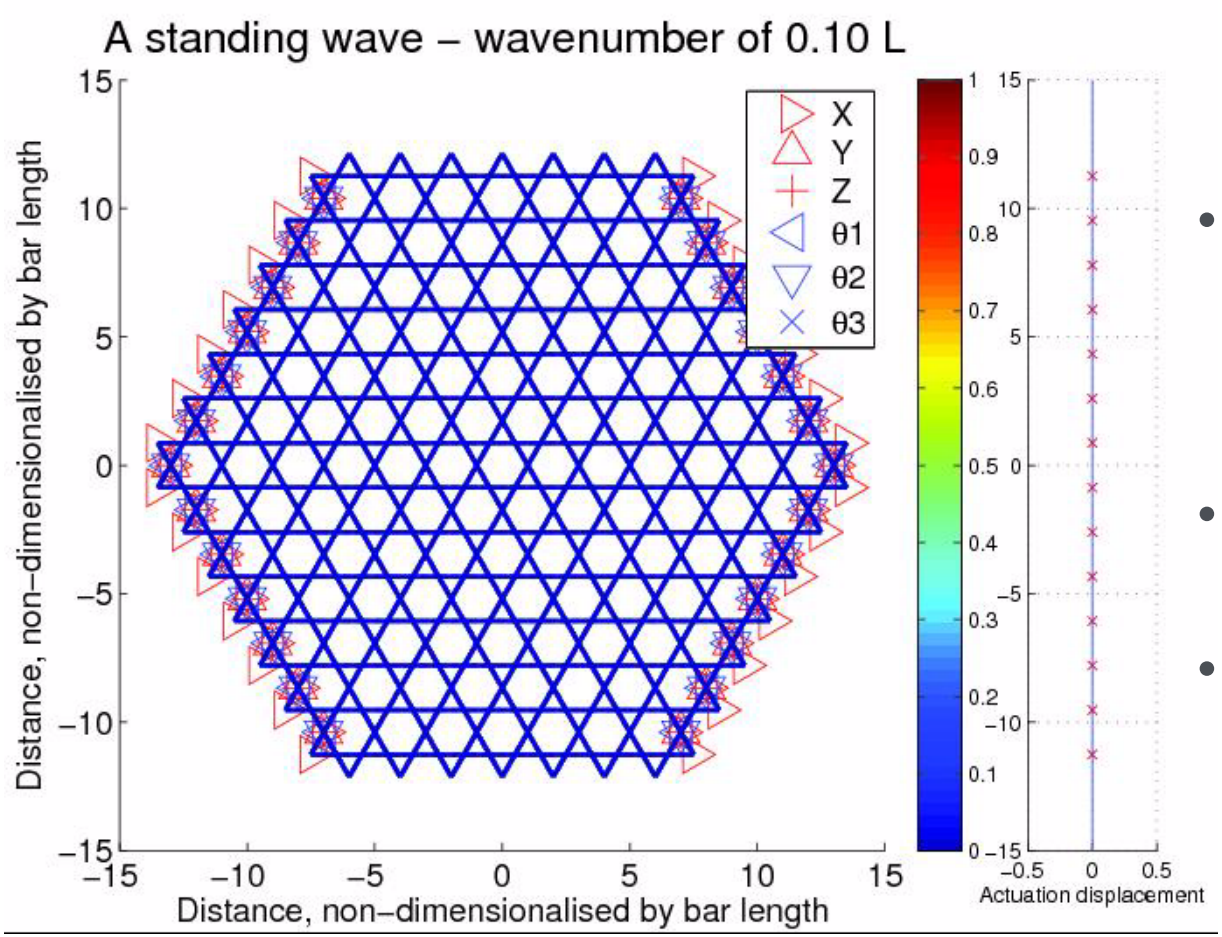

- Finite element model implemented in MATLAB
- Shear deformable beam elements
- Time marched Newmark scheme

The kagome lattice

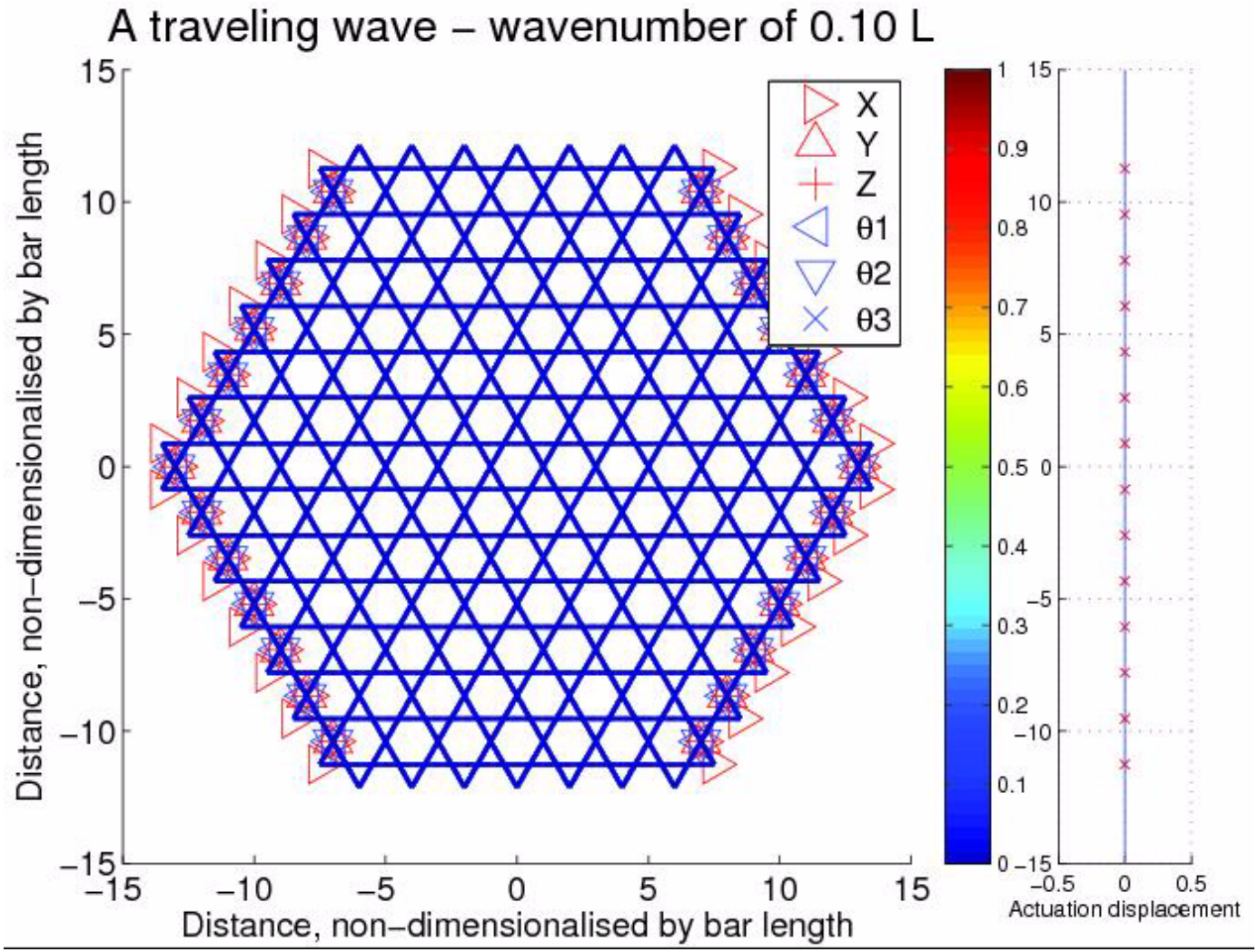

The kagome lattice

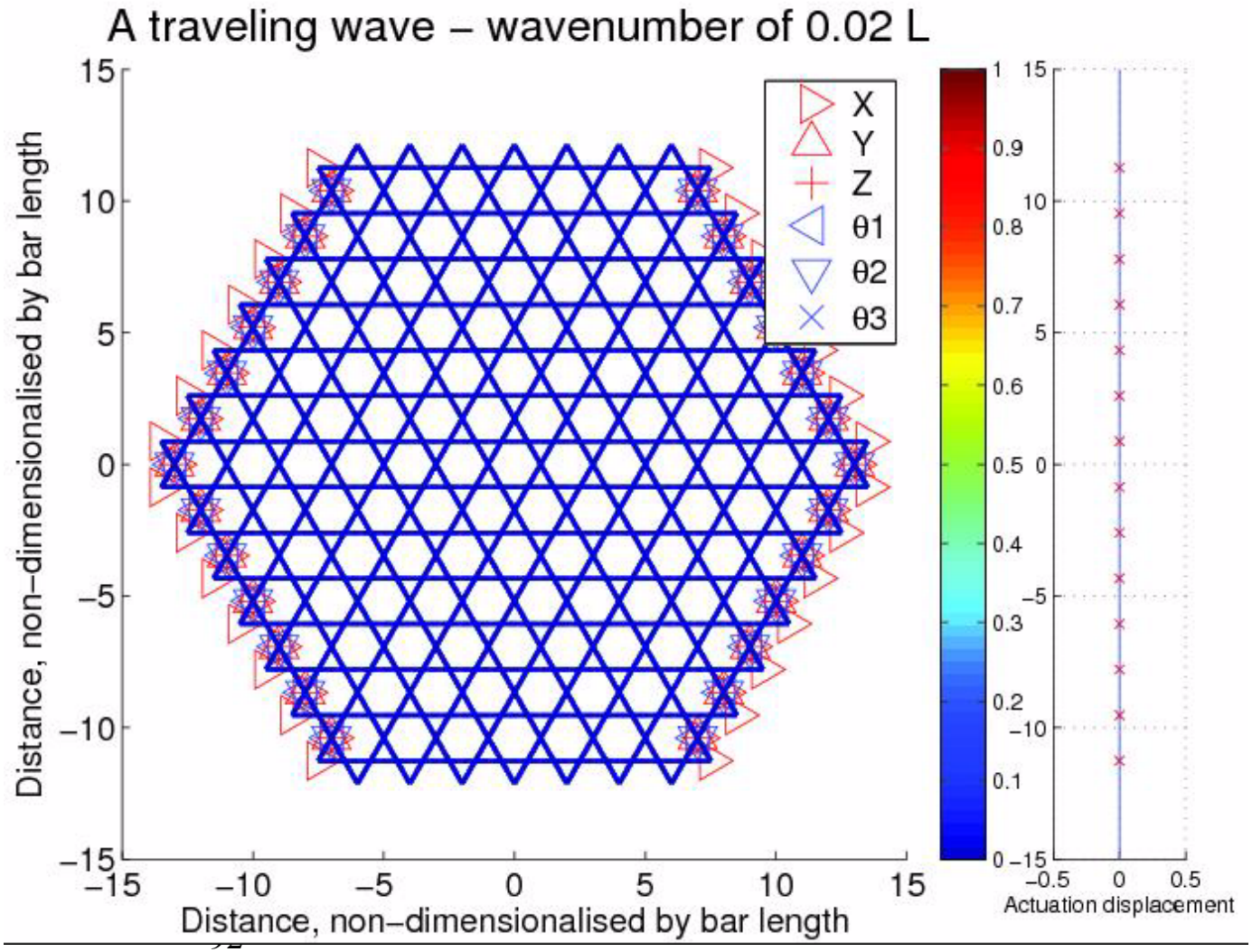

Experimental scope

- Based on the structural limitations of the lattice, a fluids experiment can be carried out with:
- $5 < U_\infty$ < 8 ms^{-1}
- $Re_\tau < 1000$
- $0 < k^+ < 0.0069$
- f_{max}=70 Hz

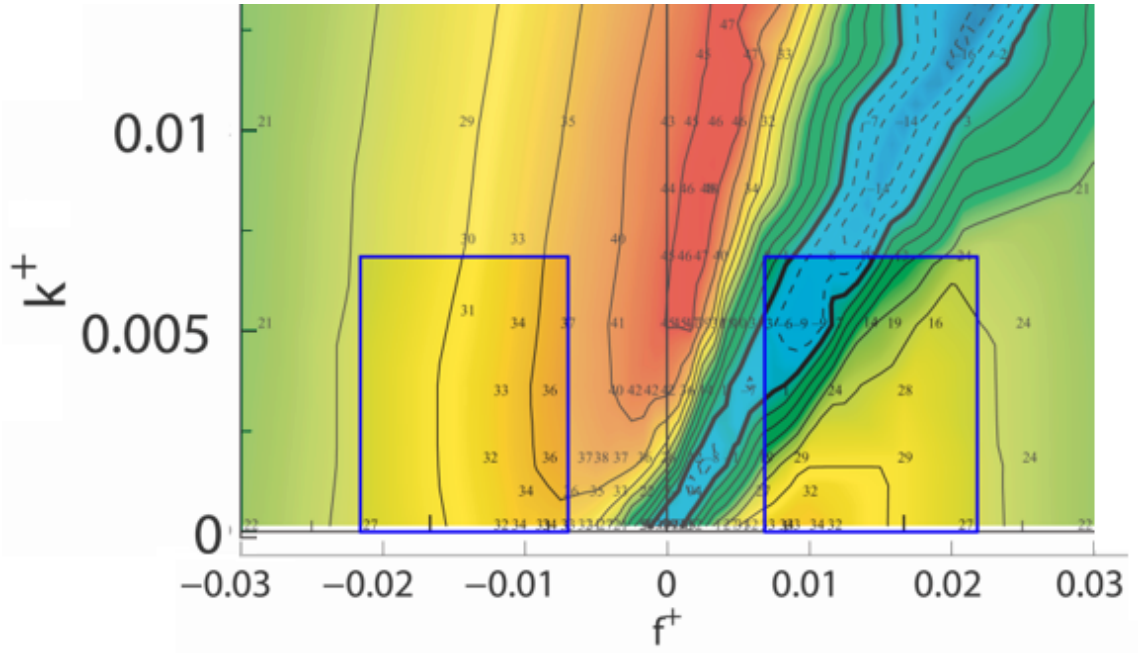

(Assuming W^+ is always greater than 5)

Initial module

Latest module built

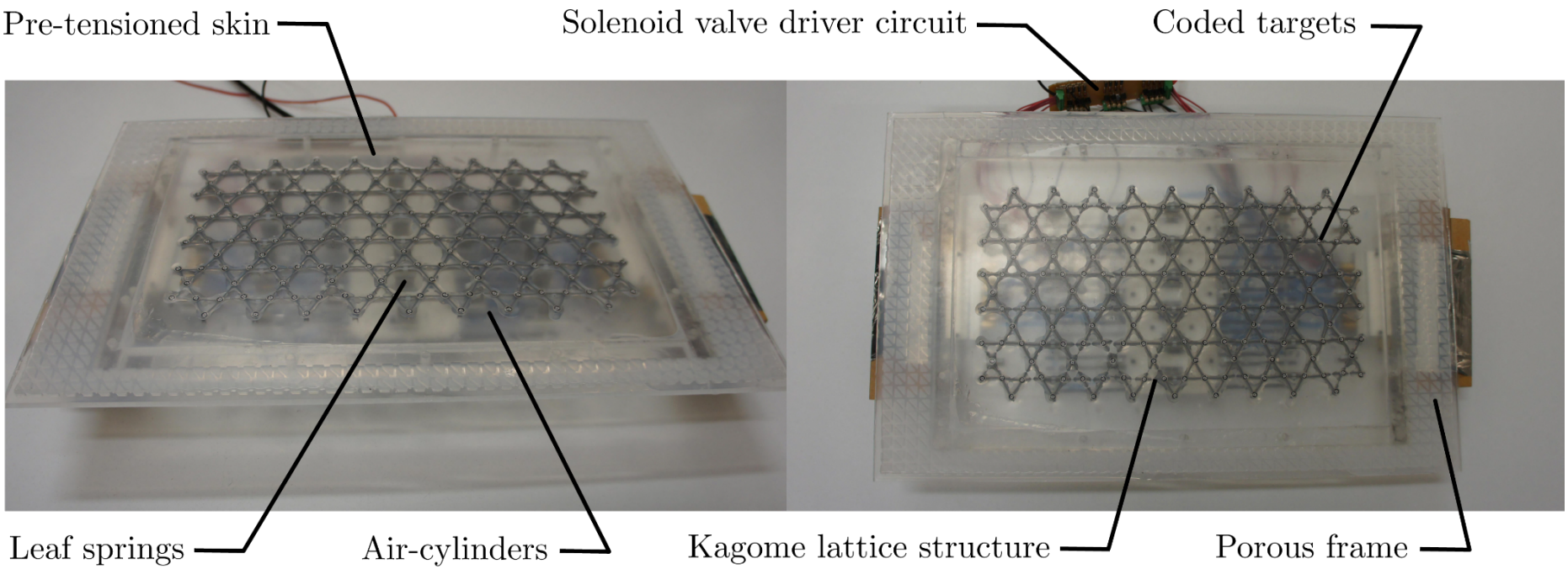

Actuator in situ

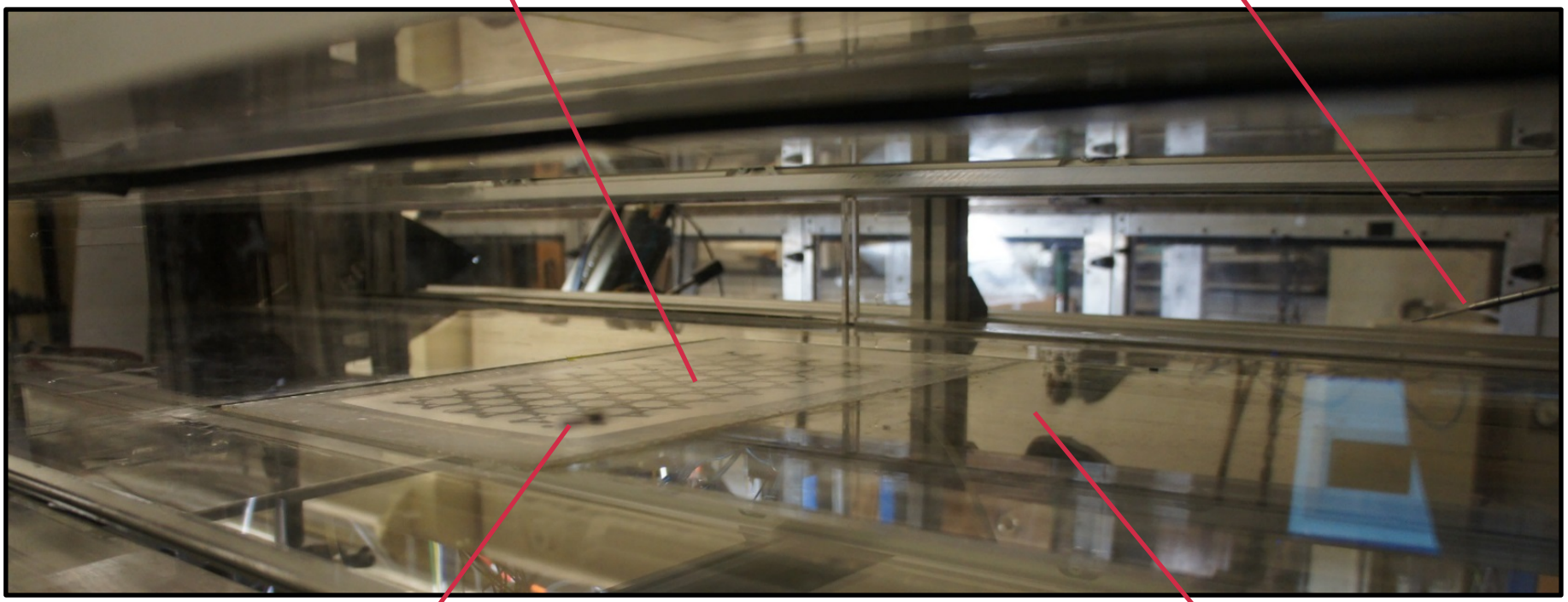

Actuator in situ

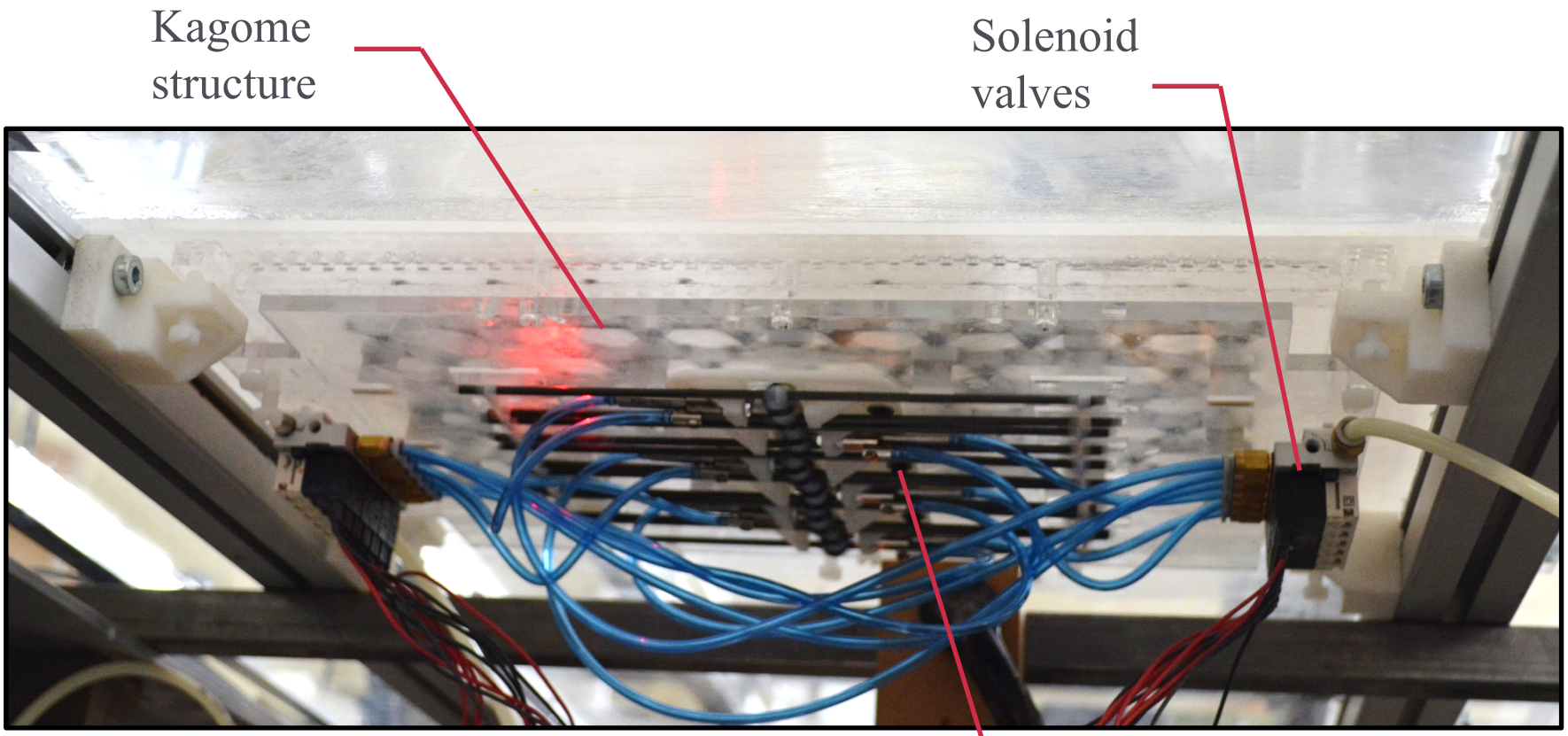

Experimental layout

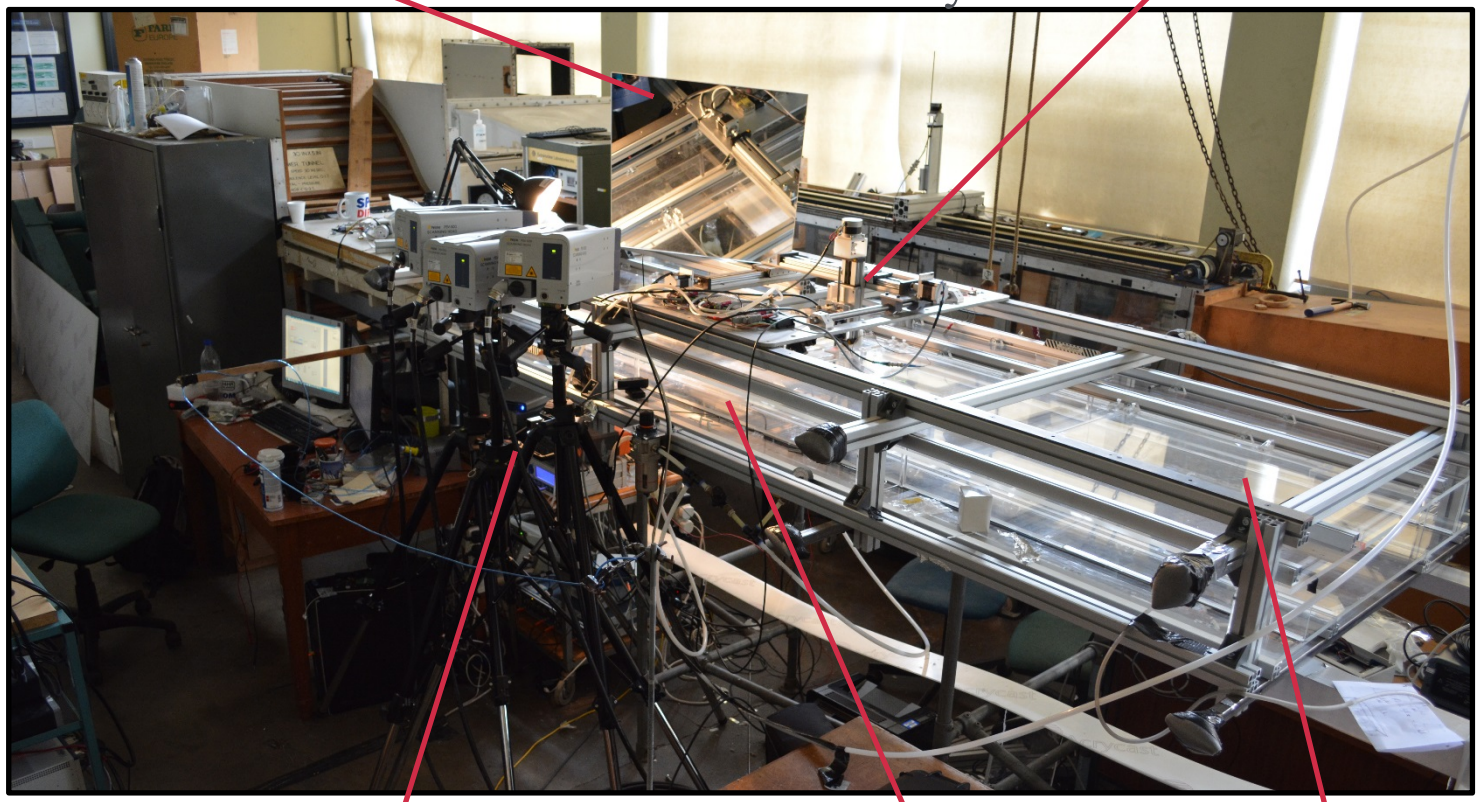

Scanning vibrometer (laser Doppler)

Measurements of surface velocity

- Simultaneous surface velocity and hot-wire measurements
- Measures velocities at a point in 3 dimensions.
- Measurements phased-locked with forcing give a representation of displacements/velocities over a surface.

Standing wave - surface

Travelling wave - surface

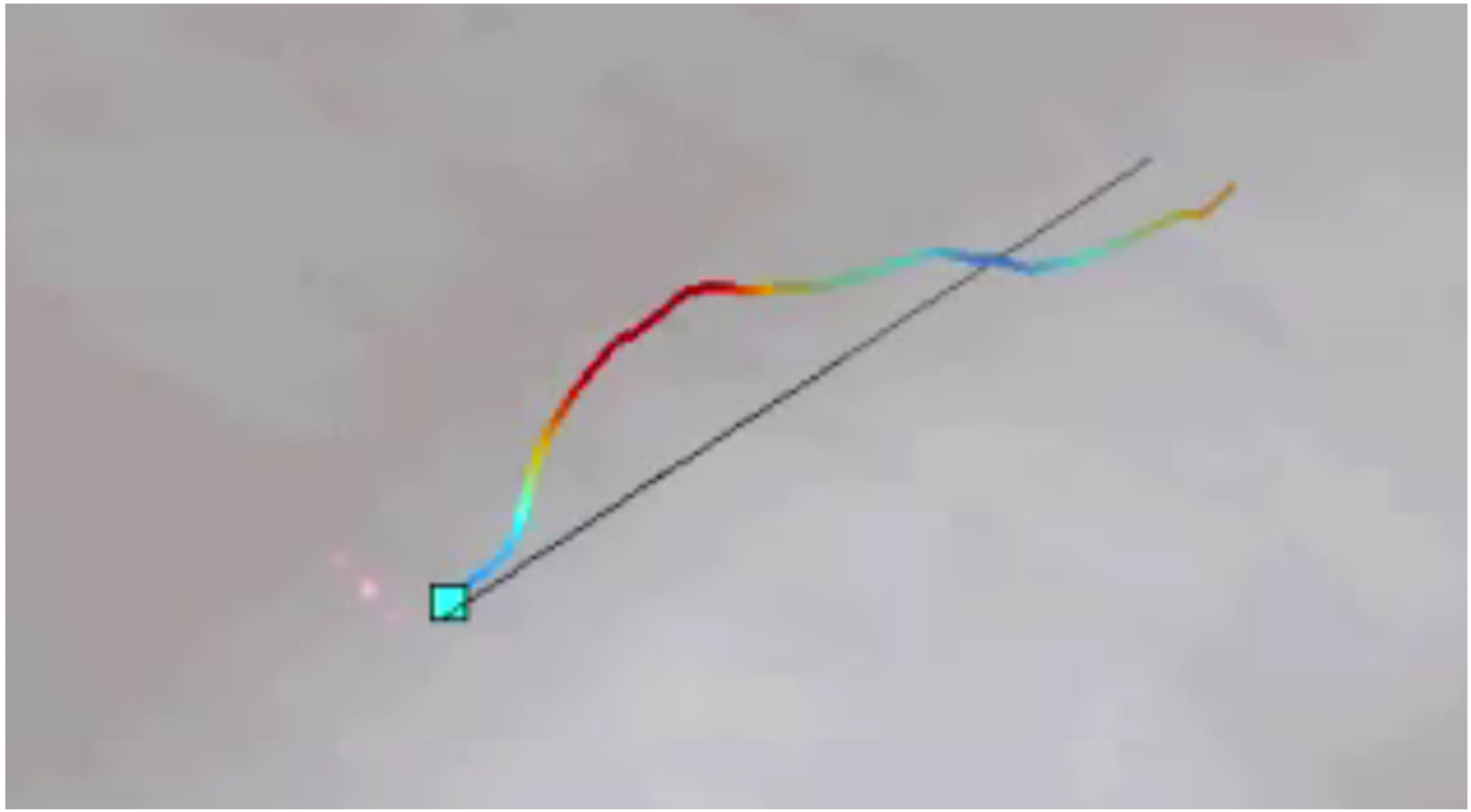

Travelling wave – short wavelength

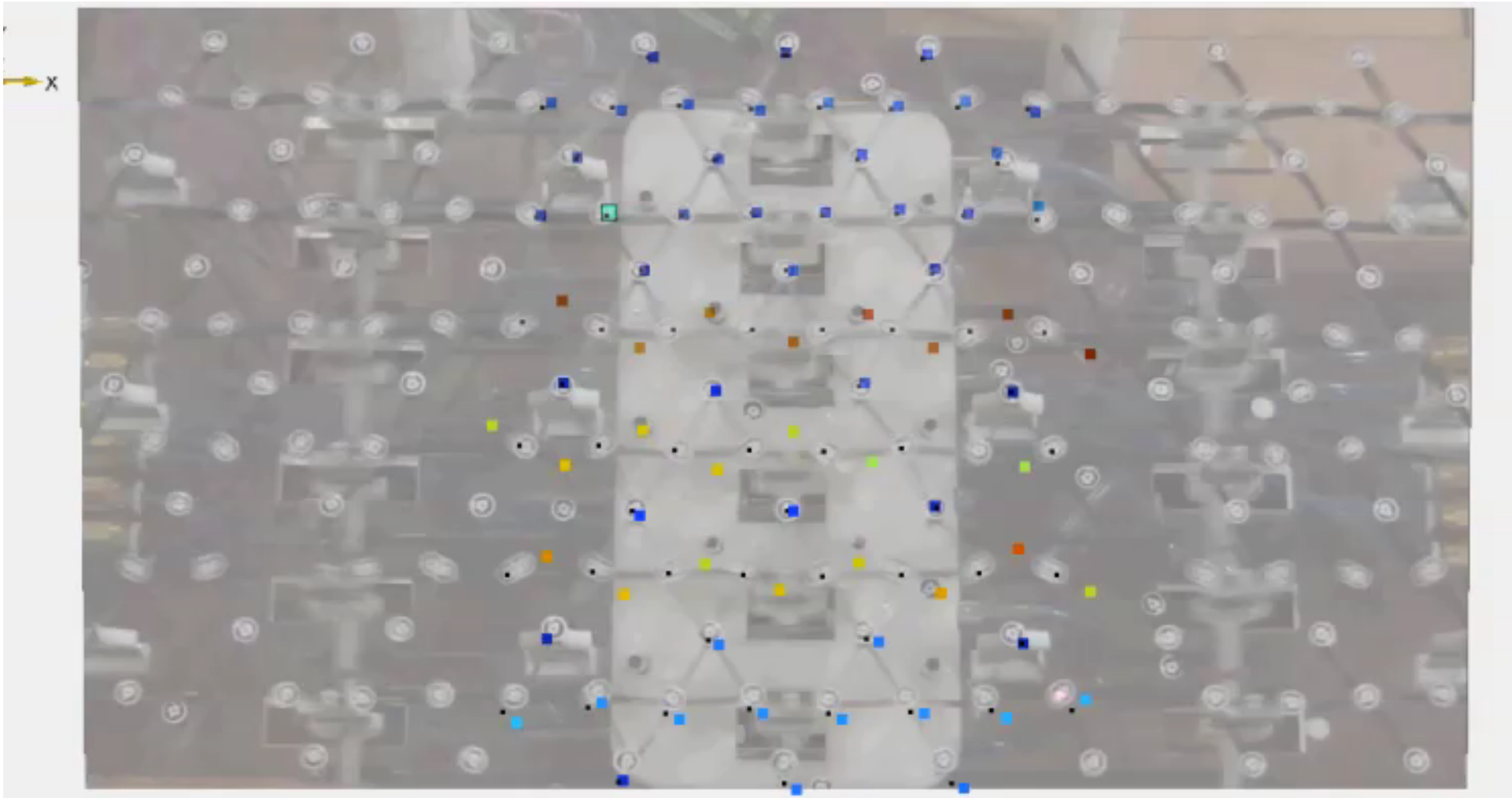

Travelling wave – long wavelength

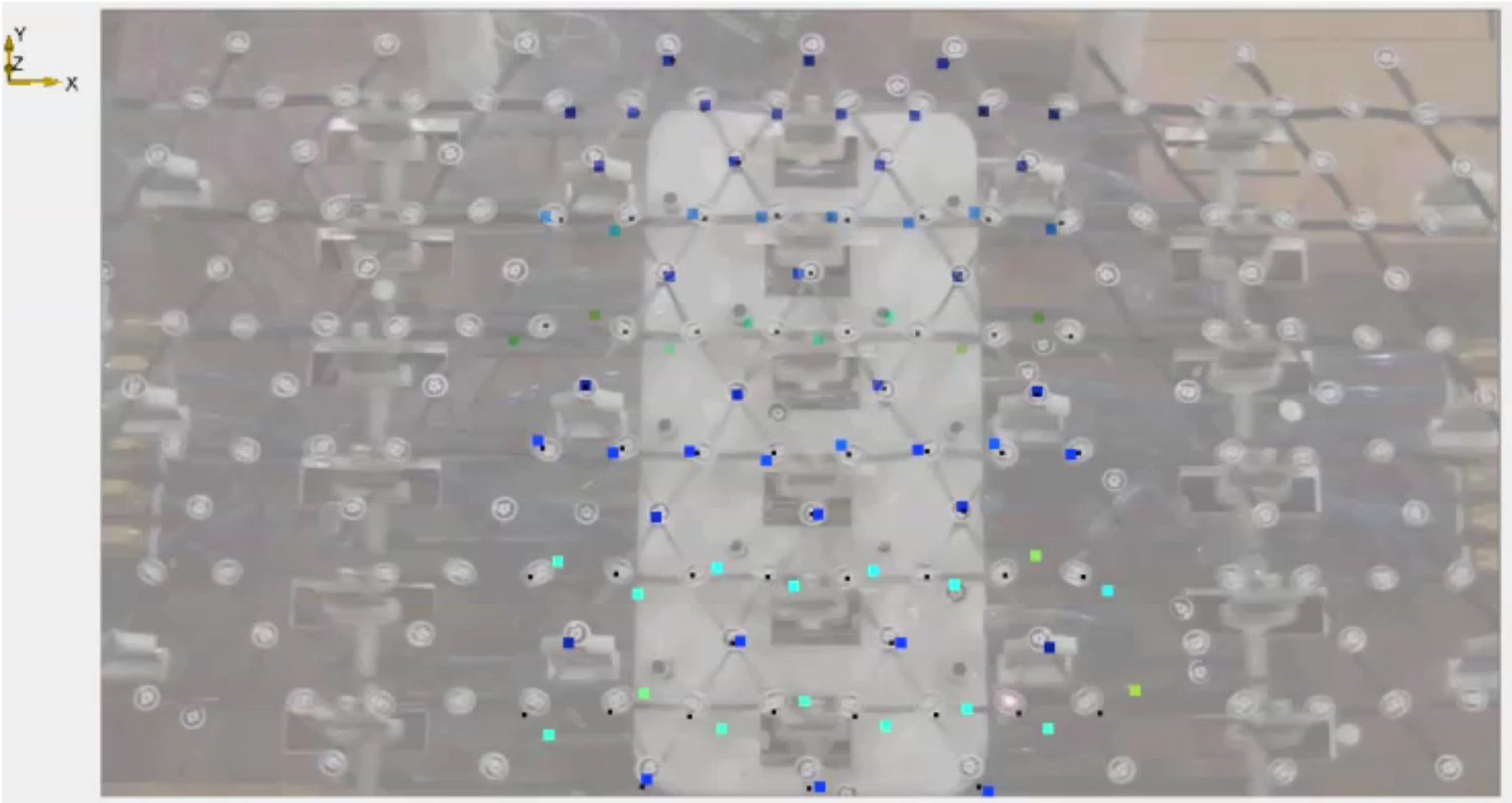

Photogrammetric measurements

Measurements of surface displacement

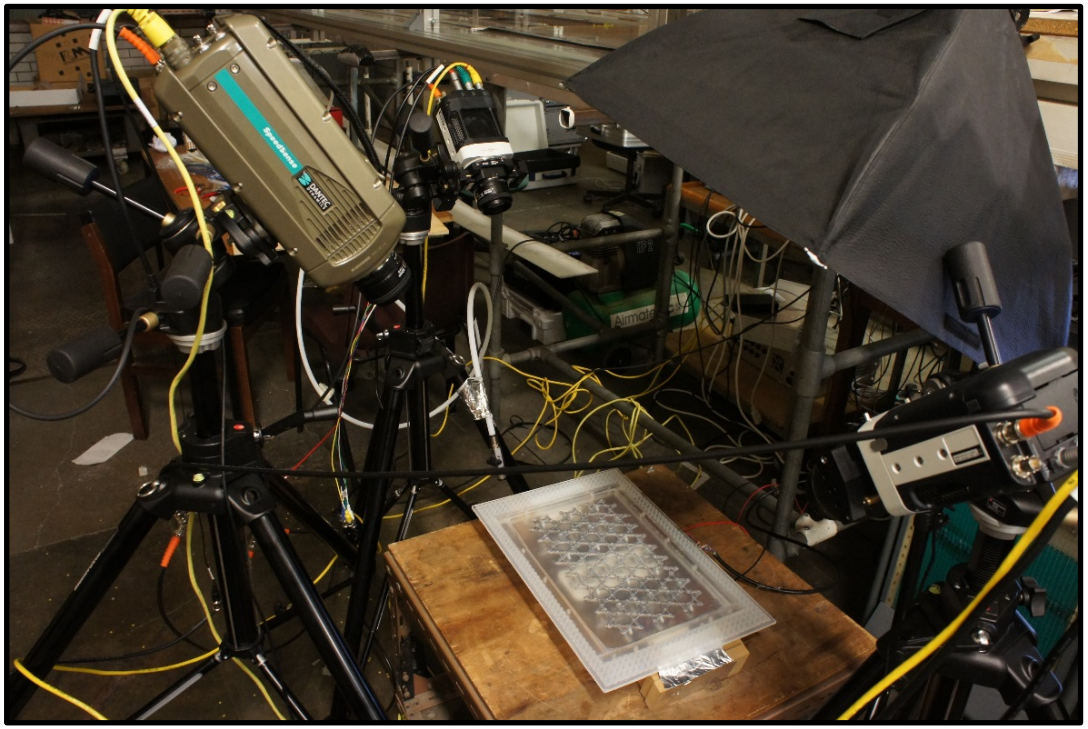

- 3 cameras (1MP 1000 fps)
- Tracked coded targets to get displacement data in 3 dimensions.
- Actuators controlled with a National Instruments FPGA PCIe card.

Actuated at 50 Hz – standing wave

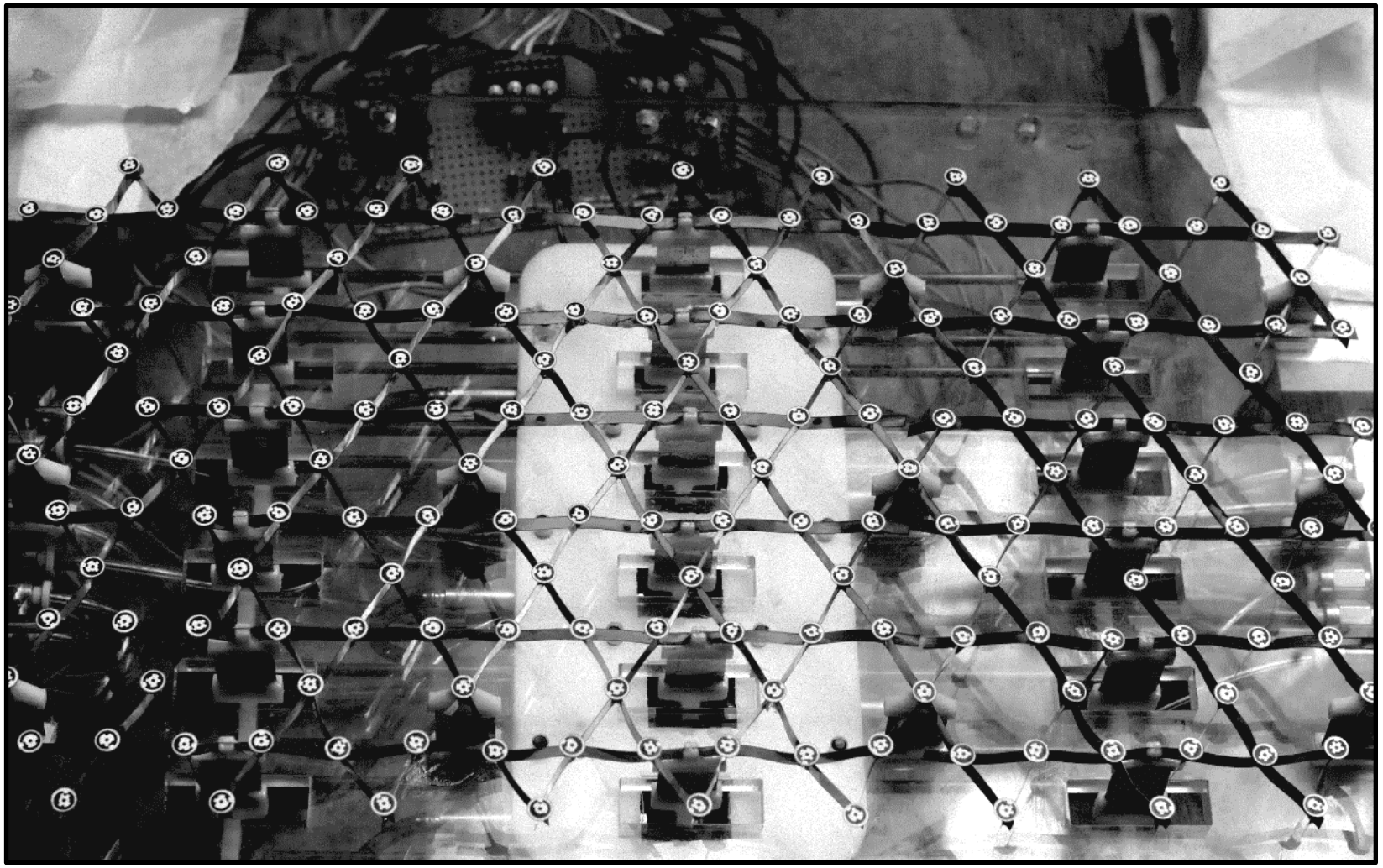

Actuated at 50 Hz – travelling wave

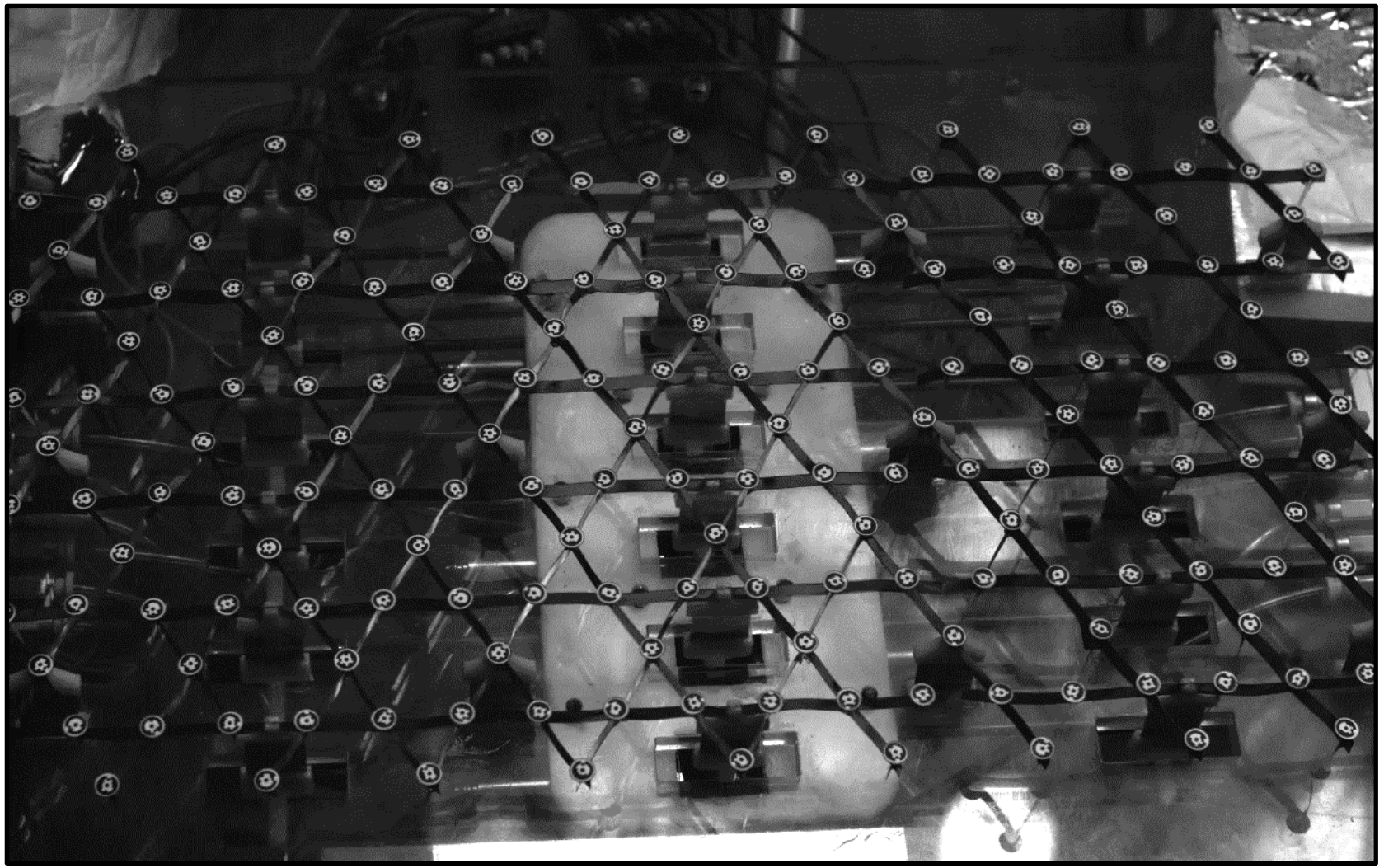

Drag reduction– log law

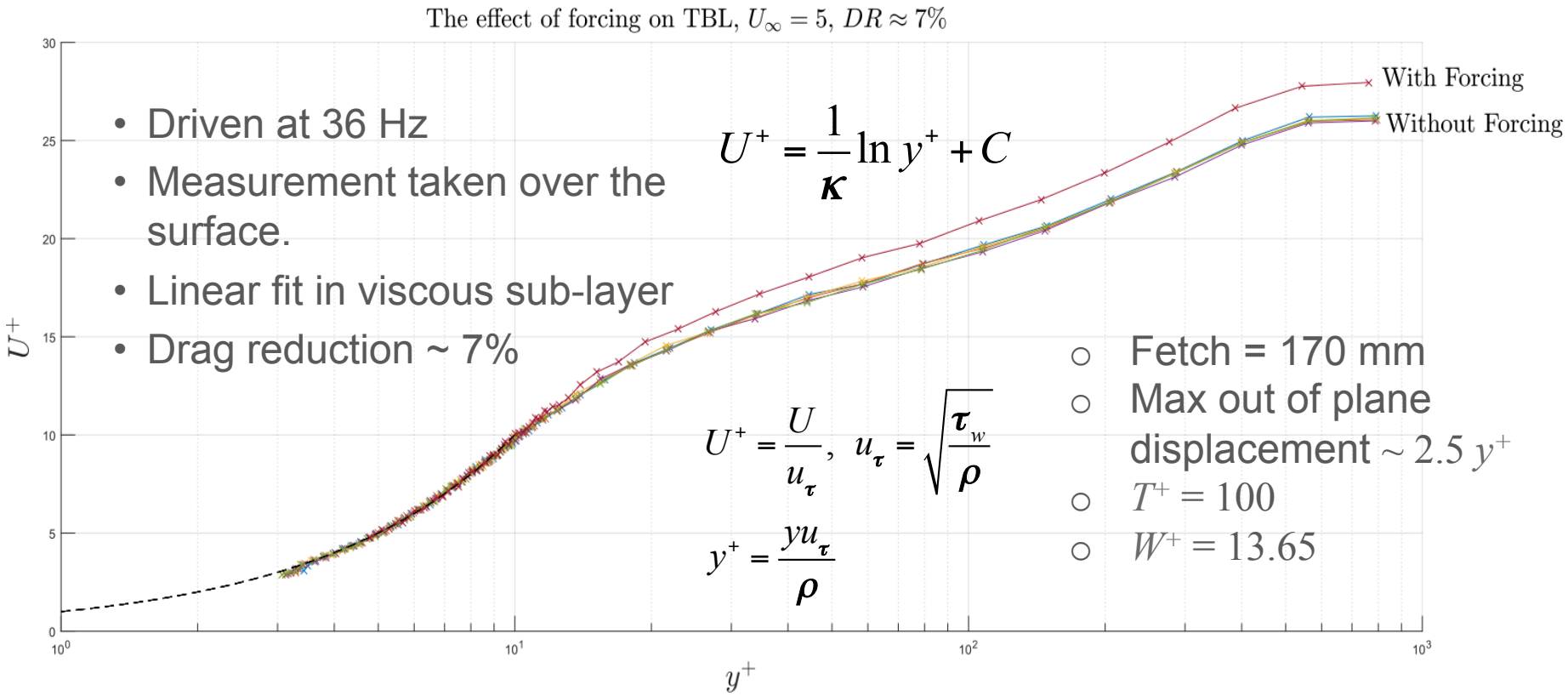

- Driven at 36 Hz
- Measurement taken over the surface.
- Linear fit in viscous sub-layer
- Drag reduction ~ 7%

$$U^+ = \frac{1}{\kappa}\ln y^+ + C$$

$$U^+ = \frac{U}{u_\tau}, \quad u_\tau = \sqrt{\frac{\tau_w}{\rho}}$$

$$y^+ = \frac{y u_\tau}{\rho}$$

- Fetch = 170 mm
- Max out of plane displacement ~ 2.5 y^+
- $T^+ = 100$
- $W^+ = 13.65$

Summary

- Developed an optimised compliant structure.
- Can withstand frequency, displacement and forcing required.
- Structure drives a surface to create discretised waveforms of (almost) arbitrary wavenumber.
- Low Reynolds number experiment – measured 7% drag reduction.
- But not quite the right experiment!

New internal layer generated from leading edge of active surface

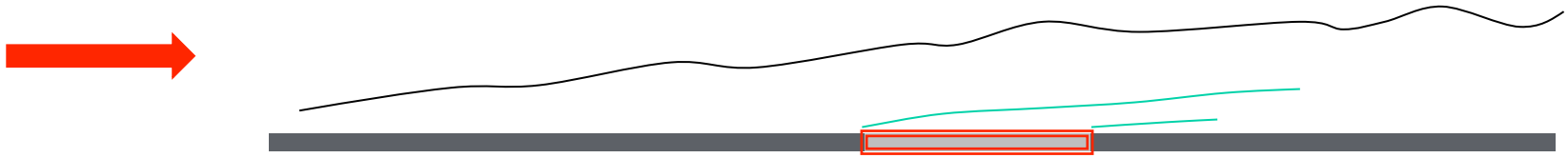

- Further experiments with fully actuated surface $Re_\tau \rightarrow 20{,}000$

References

Adrian R 2007 Hairpin vortex organisation in wall turbulence. *Phys Fluids* **19**, 041301.

Batchelor G K and Townsend A A 1956 Turbulent diffusion. In: *Surveys in Mechanics*, ed. G K Batchelor and R M Davies CUP pp. 352-399.

Bird J W, Santer M and Morrison J F 2015 Adaptive kagome lattices for near wall turbulence suppression. AIAA2015 – 0270.

Bird J W, Santer M and Morrison, J F 2016 The determination of compliant modes for actuation in rigid assemblies. Submitted to *Int. J. Solids and Struct.*

Choi H, Moin P and Kim J 1994 Active turbulence control for drag reduction in wall-bounded flows. *J. Fluid Mech*. **262**, 75.

Cossu C, Pujals G and Depardon S 2009 Optimal transient growth and very large-scale structures in turbulent boundary layers. *J. Fluid Mech*. **619**, 79-94.

del Álamo J C and Jimenéz J 2006 Linear energy amplification in turbulent channels. *J. Fluid Mech.* **559**, 205-213.

Dietz A J 1999 Local boundary-layer receptivity to a convected free-stream disturbance. *J. Fluid Mech.* **378**, 291-317.

Duck P and Ruban A 1996 The generation of Tollmien-Schlichting waves by free-stream disturbance. *J. Fluid Mech*. **312**, 341-371.

Farrell B F and Ioannu P J 1993 Stochastic forcing of the linearized Navier-Stokes equations. *Phys Fluids* **A5**, 2600-2609.

Gibson J F, Halcrow J and P. Cvitanović P 2008 Visualizing the geometry of state space in plane Couette flow. *J. Fluid Mech*. **611**, 107-130. http://www.channelfow.org/

Ho, Y C and Pepyne, D L 2002 Simple Explanation of the No-Free-Lunch Theorem and Its Implications. *J. Optimization Theo. and Applications*. **115**, 549–570.

Hunt J C R and Morrison J F 2000 Eddy structure in turbulent boundary layers. *Eur. J. Mech. B- Fluids* **19**, 673–694.

Jacobson S A and Reynolds W C 1998 Active control of streamwise vortices and streaks in boundary layers. *J. Fluid Mech*. **360**, 179.

Kim J 1989 On the structure of pressure fluctuations in simulated channel flow. *J. Fluid Mech*. **205**, 421-451.

Kim J and Lim J 2000 A linear process in wall-bounded turbulent shear flows. *Phys. Fluids* **12** 1885-1889.

References

Kline S J, Reynolds W C, Schraub F A and Runstadler P W 1967 The structure of turbulent boundary layers. *J. Fluid Mechs.* **30**, 741-773.

Landahl M T 1975 Wave breakdown and turbulence. *SIAM J. Appl. Math.* **28**, 735-756.

Landahl M T 1990 On sublayer streaks. *J. Fluid Mech.* **212**, 593-614.

Landahl M T 1993 Model for the wall-layer structure of a turbulent shear flow. *Eur. J. Mech. B- Fluids* **12**, 85-96.

Lee M J, Kim J and Moin P 1990 Structure of turbulence at high shear rates. *J. Fluid Mech.* **216**, 561-583.

Luhar M, Sharma A S and McKeon B J 2014 On the structure and origin of pressure fluctuations in wall turbulence: predictions based on the resolvent analysis. *J. Fluid Mech.* **751**, 38-70.

McKeon B J and Sharma A S 2010 A critical layer framework for turbulent pipe flow. *J. Fluid Mech.* **658**, 336-382.

Orlandi P and Jiménez J 1994 On the generation of wall friction. *Phys Fluids* **A6**, 634.

Quadrio M, Ricco P and Viotti C 2009 Streamwise-travelling waves of spanwise wall velocity for turbulent drag reduction. *J. Fluid Mech.* **627**, 161-178.

Rempfer 2003 Low dimensional modeling and numerical simulaiton of transition in simple shear flows. *Ann. Rev. Fluid Mech.* **35**, 229-265

Robinson S K 1991 Coherent motions in the turbulent boundary layer. *Ann. Rev. Fluid Mech*. **23**, 601.

Septham K 2016 *Linear mechanisms and pressure fluctuations in wall turbulence*. PhD Thesis, Imperial College.

Sharma A, Morrison J F, McKeon B J, Limebeer D J N, Koberg W H and Sherwin S J 2011 Relaminarisation of turbulent channel flow with a globally stabilising linear control. *Phys. Fluids* **23**, 125105.

Wu X 2001 On local boundary-layer receptivity to vortical disturbances in the free stream. *J. Fluid Mech.* **449**, 373-393.

Zaki T A 2013 From streaks to spots and on to turbulence: exploring the dynamics of boundary layer transition, *Flow Turbulence & Combustion* **91**, 451-473.

Backup

- General

CO_2: Importance to Society

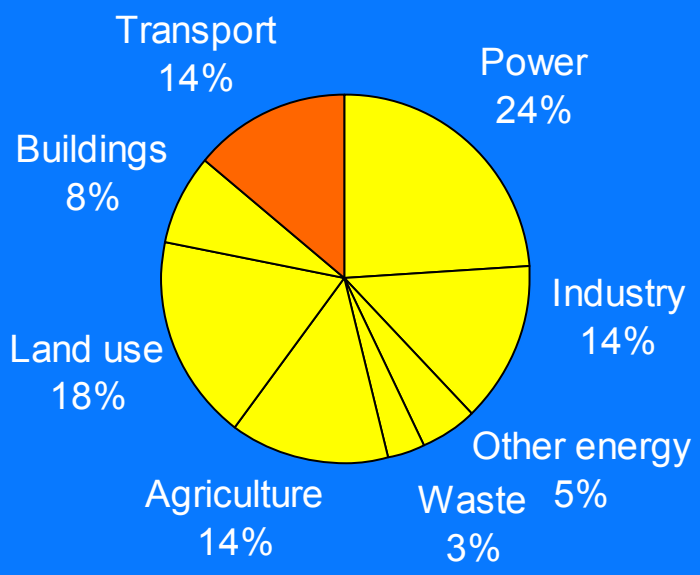

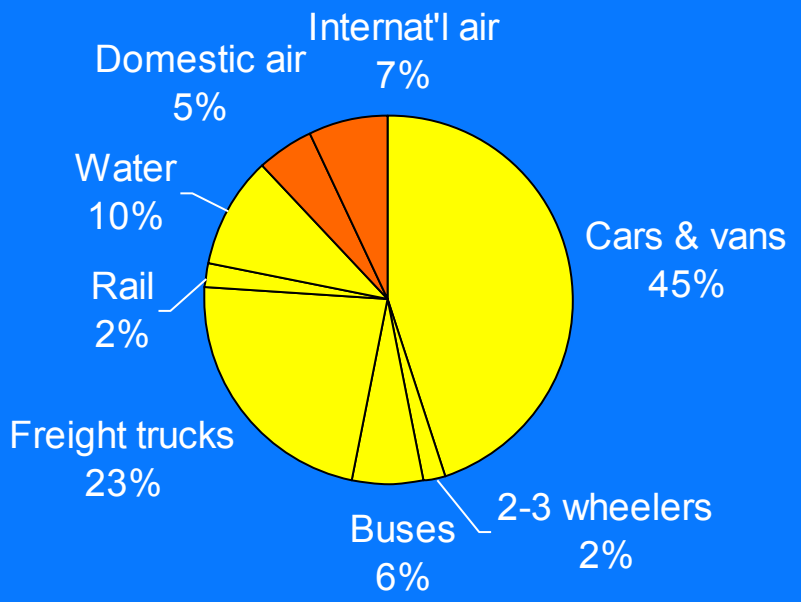

Aviation is a significant growing source of GHG emissions at 2% of global total

Stern Review: The Economics of Climate Change 2006

Motivation

OECD sources of CO_2 emissions

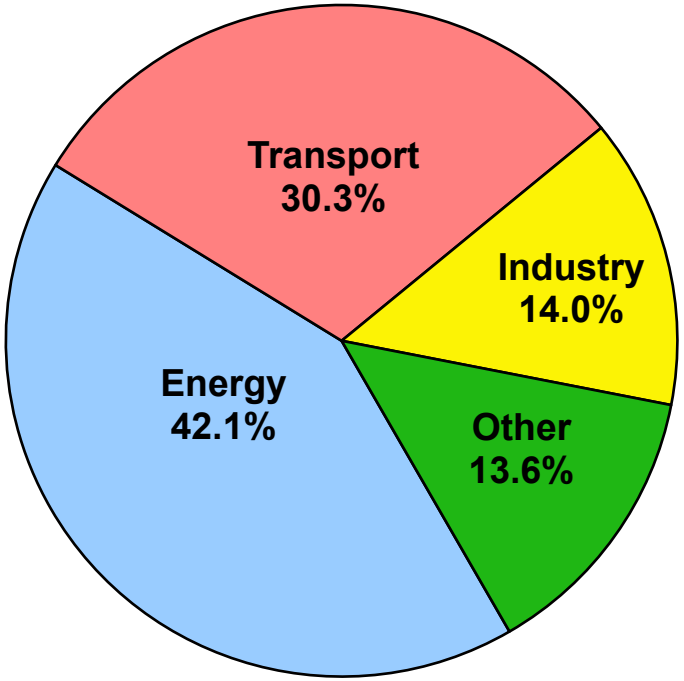

OECD transport sector CO_2 emissions

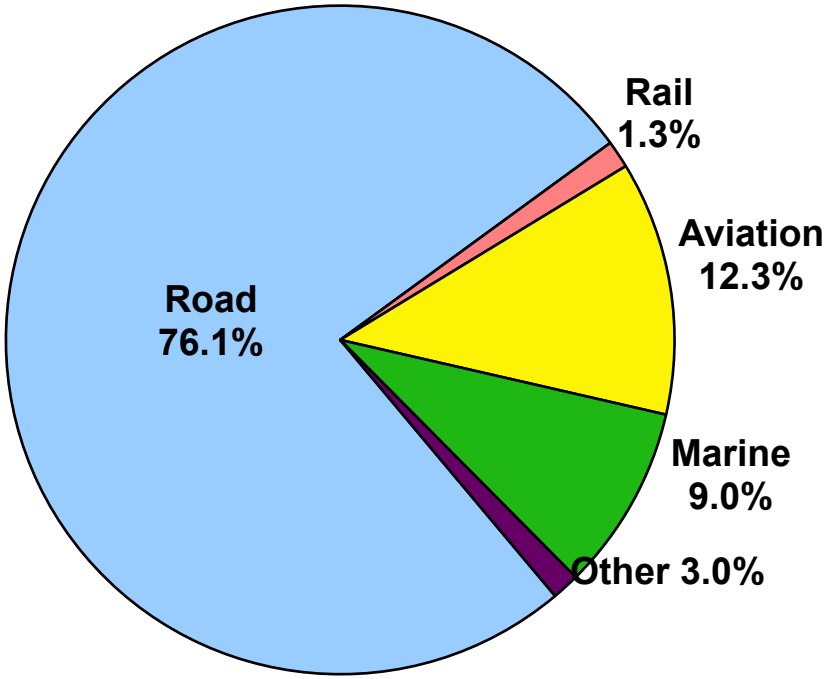

OECD Publishing 2008

Environment & Aviation– ACARE2050

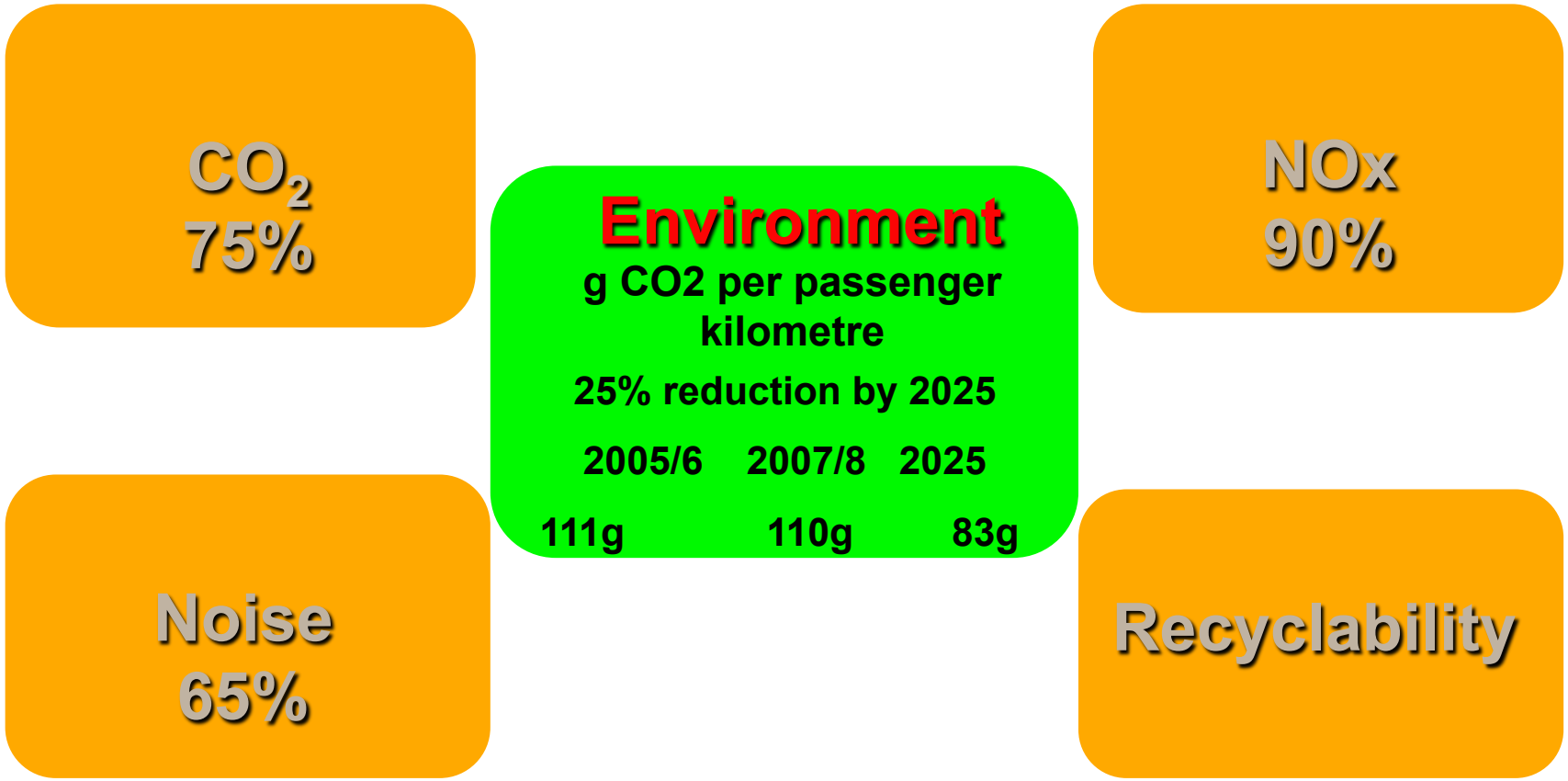

BA Carbon Reduction Goal

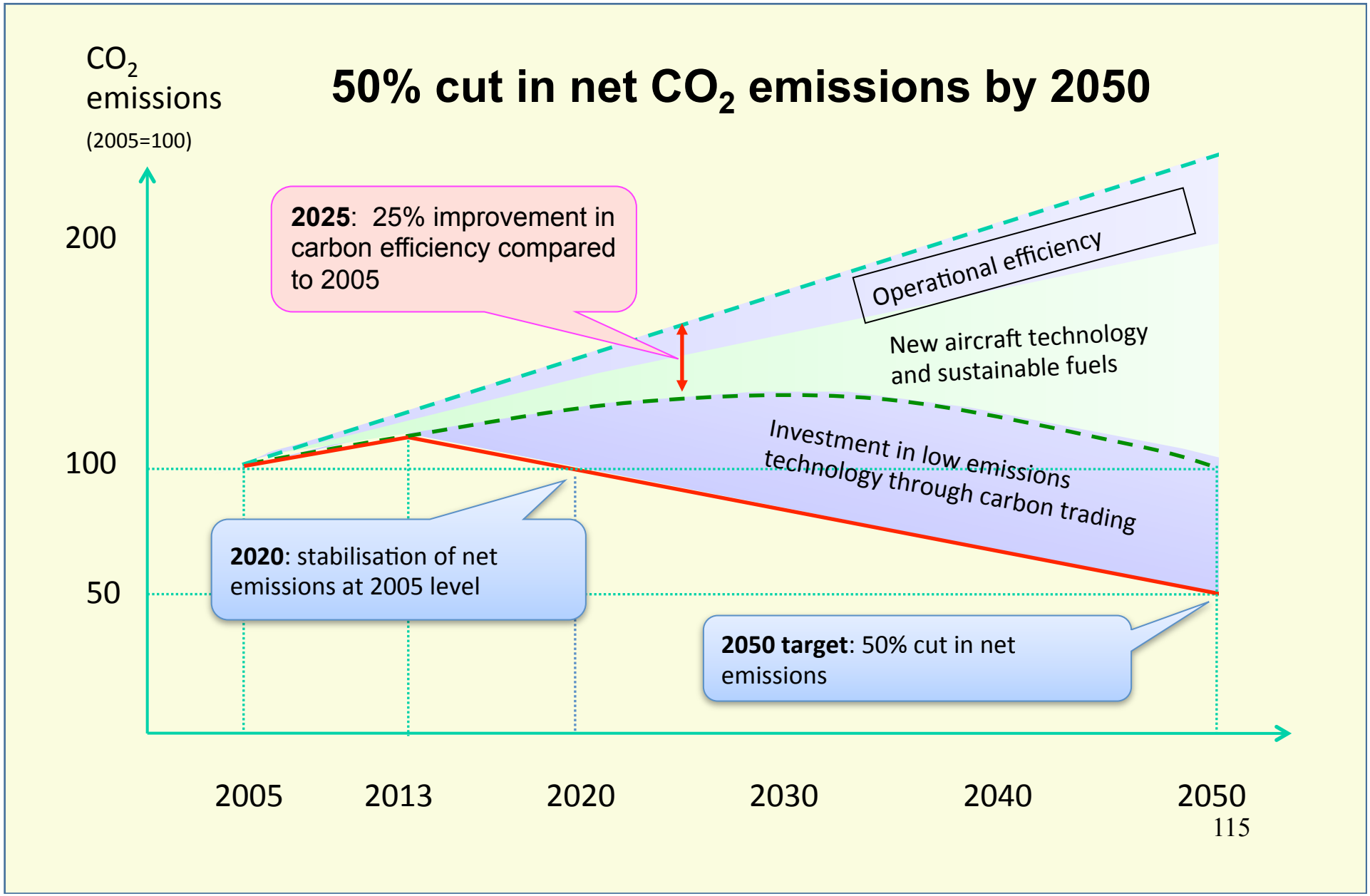

Drag

Green Aviation 2011

The need

A single trans-Atlantic flight consumes 60,000 litres of fuel, more than the average motorist uses in 50 years, producing 140 tonnes of CO2. Over 85,000 flights takes off daily from airports around the world. Air travel is the fastest growing source of CO2 emissions.

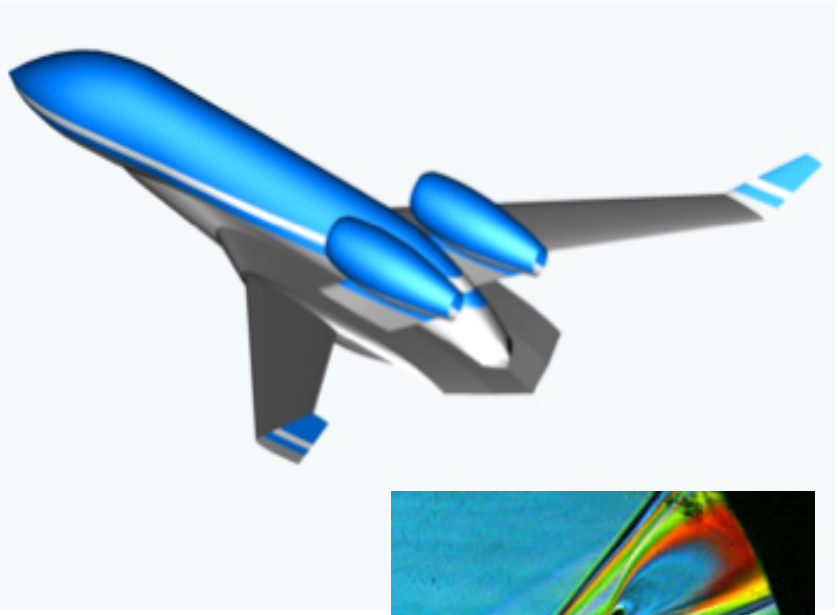

Aims

Engine thrust is used to overcome the drag generated by the motion of the aircraft through the air: at cruise, a 10% reduction, say, in drag leads roughly to a 10% reduction in emissions – CO_2 and NO_x – and fuel costs.

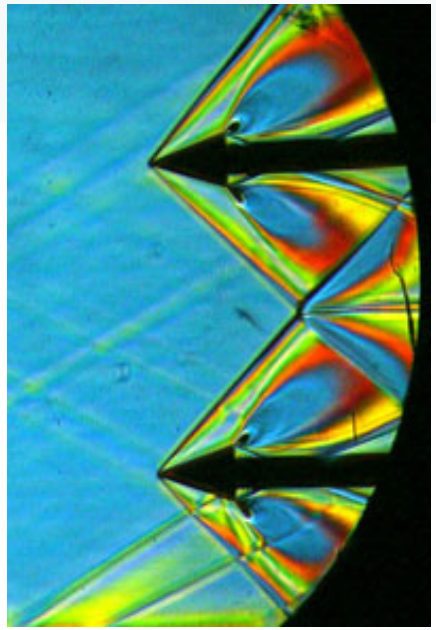

Drag

Green Aviation 2011

What is drag?

Air flow over the aircraft produces drag through surface friction, the generation of shock waves, the generation of lift and flow separation. Surface friction accounts for roughly half the total drag. It is inevitable, but the drag generated by a turbulent flow on the surface is about 4~5 times that produced by laminar flow.

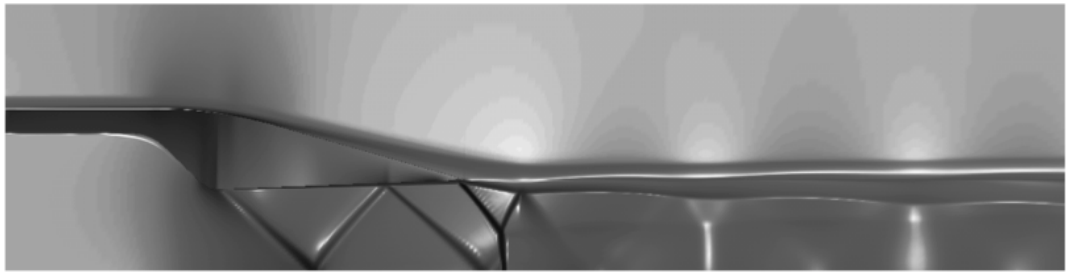

Aims

Half of friction drag is produced by the wings, the other half is produced by the fuselage. On the wings, the delay of transition onset reduces drag. On the fuselage, reducing the turbulent friction drag offers potentially huge drag and emissions reductions.

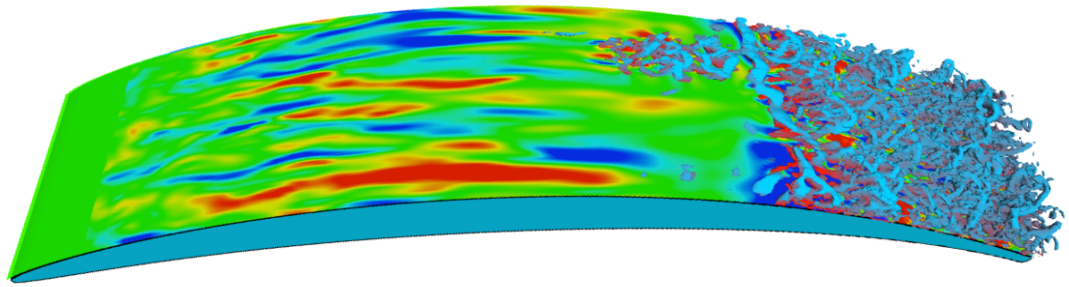

Can we control friction drag?

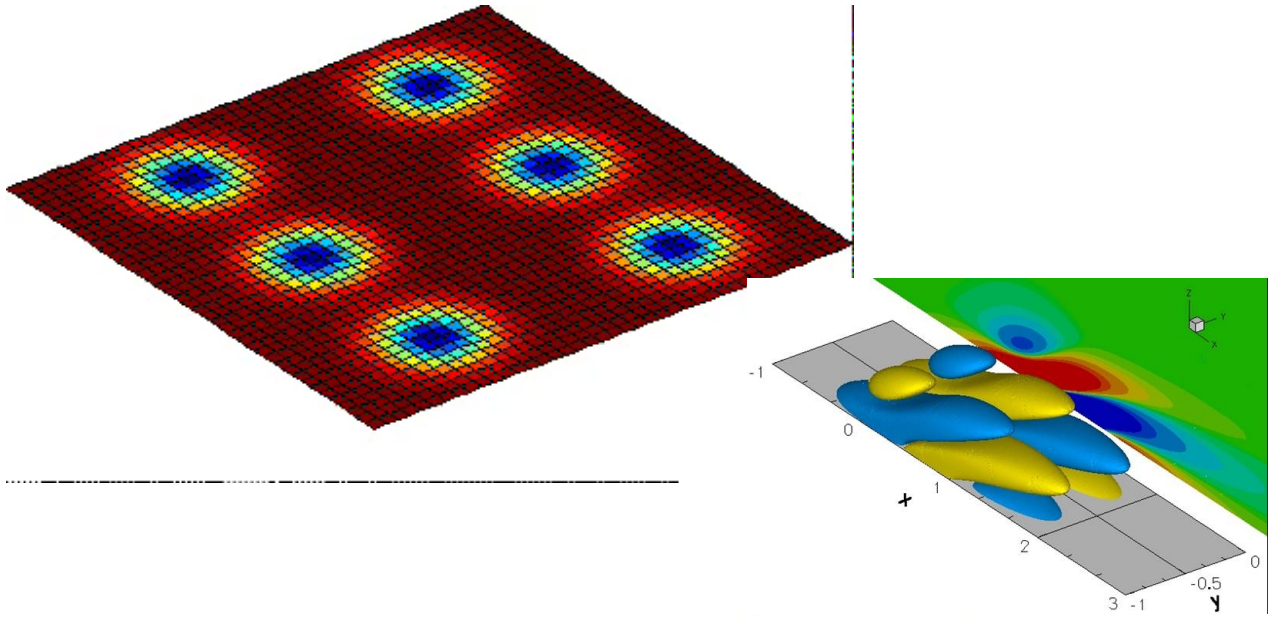

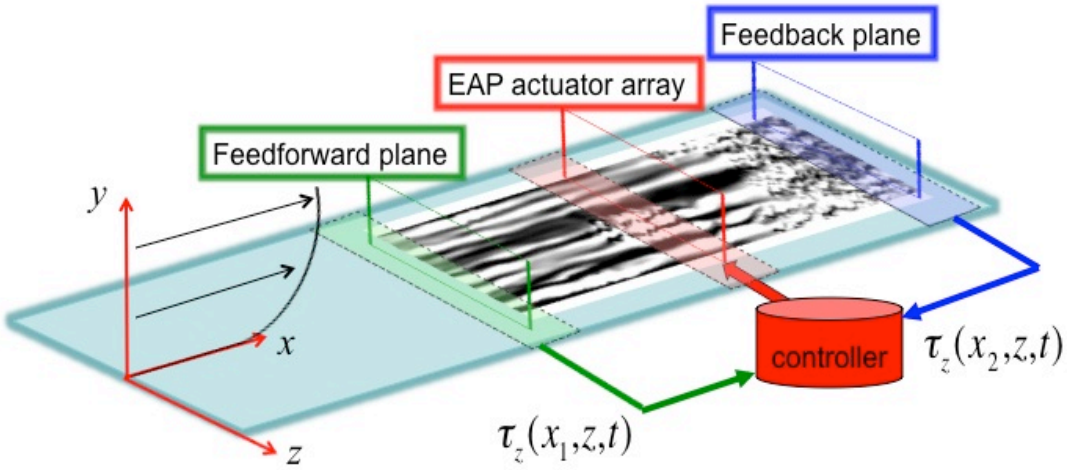

- Model: near-wall turbulence structure
- Wall-based sensing and actuation – the challenges of of estimation, observability and controllability
- Time-dependent moving surfaces – "dimples"
- Use of feedback to optimise efficiency of actuation

Observability

- Observability

  A linear system is observable if it is possible to determine its state through measurements of input *u(t)* and output *y(t)*. It is determined by *A* and *B*.

- Controllability

  A property of both actuator system and the plant state that determines whether all the state modes can be arbitrarily influenced by the actuators. It is determined by *A* and *C*.

Key concepts: observability & controllability I

- The following figure shows the first 25 eigenvectors of the Orr-Sommerfeld/Squire operator linearized about (a), the laminar flow profile and (b), the mean turbulent flow profile for channel flow.
- Real and imaginary components of w_y (blue) and v (red) plotted as a function of y (wall-normal).
- The laminar flow case, most of the modes are observable in the middle of the channel only – they have little support near the wall and are more-or-less unobservable with wall sensors and therefore uncontrollable with wall actuators.
- For turbulent flow case, larger fraction of unobservable, and uncontrollable modes. Situation becomes worse as Re increases.

Key concepts: observability & controllability II

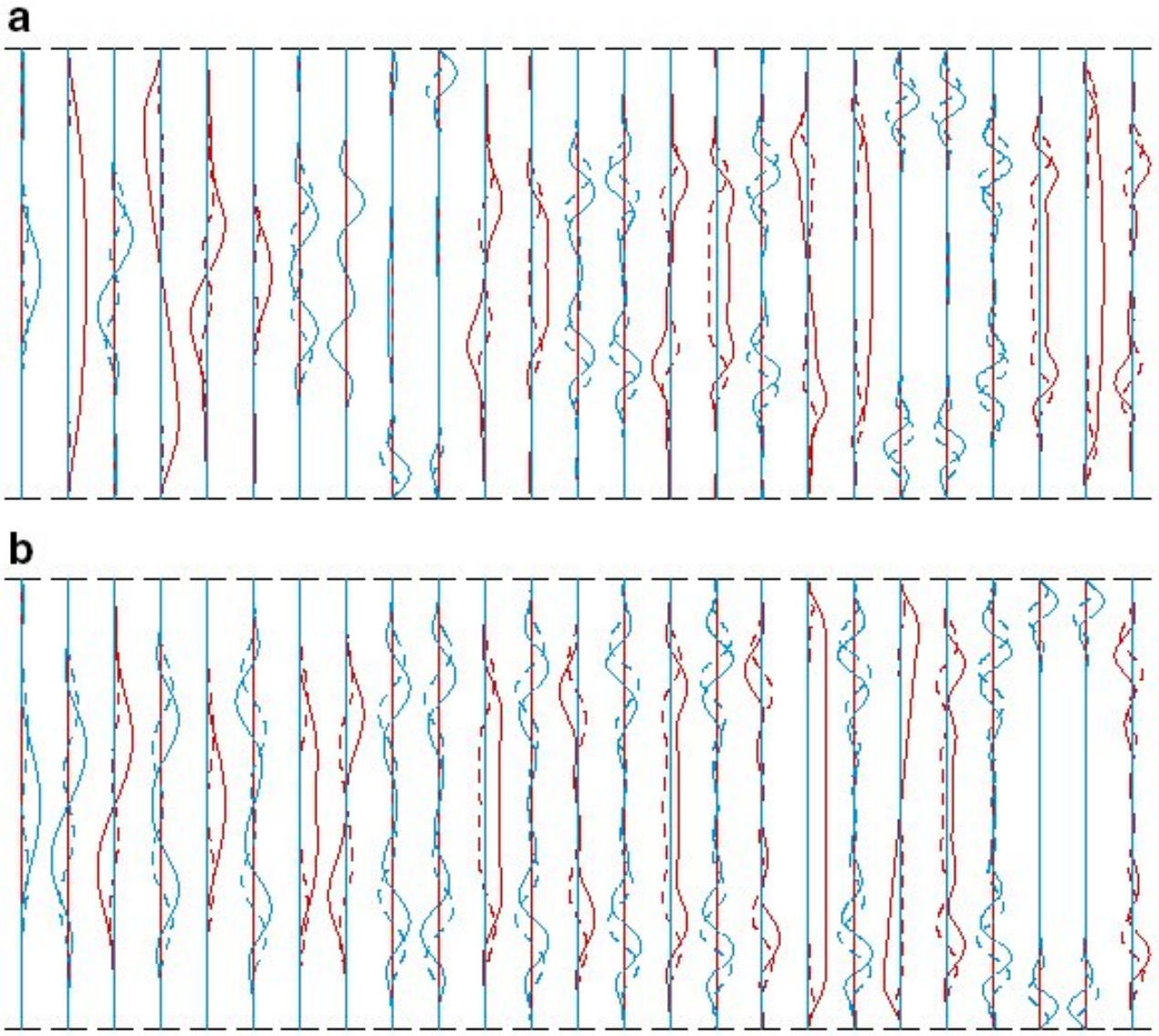

Figure 1

First 25 eigenvectors of Orr-Sommerfeld/Squire at $\{k_x, k_z\} = \{1, 0\}$ linearized about (*a*) the laminar flow profile at $Re_B = 1429$ ($Re_c = 2143.5$) and (*b*) the mean turbulent flow profile at $Re_B = 1429$ ($Re_\tau = 100$). Shown are the real (*solid*) and imaginary (*dashed*) parts of the ω component (*blue*) and v component (*red*) of the least stable eigenvectors, plotted as a function of y from the lower wall (*bottom*) to the upper wall (*top*).

v

ω_y

Solid: real
Dashed: imaginary

Sensing

- Sensing involves measurement of wall pressure and/or wall shear stress: in general, wall shear is a minimum requirement for a controller to be effective.
- You will have already been introduced to thermal anemometry techniques for measuring surface friction. These are non-linear. Conventional wall–pressure sensors are usually linear.
- It is easier to obtain accurate measurements of wall pressure than wall shear stress:

$$\sqrt{\frac{\overline{p_w^2}}{\overline{\tau_w^2}}} \approx \begin{array}{ll} 10 & \text{(lab)} \\ 20 & \text{(flight)} \end{array}$$

- We require robust transducers, preferably with a linear response.

Actuator requirements

Scaling of forces:

surface tension	L^1
electrostatic, pressure, biological	L^2
magnetic*	L^3
gravitational	L^4 (on earth L^3!)

- Thermal devices unattractive: much of the energy is wasted by forced convection
- Surface tension most attractive: largest force for a MEMS device
- Most MEMS devices use L^2: often pressure scales with area available – as in natural muscle
- Other requirements are deflection and speed of response – frequencies usually rise with miniaturisation
- An actuator of length, d, operating in a flow with velocity U will have a perceived frequency of U/d. How does this compare with the frequencies of the smallest scales of motion?

*depends on current density

Sensor & Actuator: size, d, & speed

- Size
  - At best, we want $d \approx \eta$ but dissipation spectrum peaks at about 10η so $d \approx 10\eta$ should be good enough
- Speed
  - distinguish smallest turbulence (Kolmogorov) timescale, $\tau = (\nu/\varepsilon)^{\frac{1}{2}}$
  - From eddy of size 10η being convected at speed $U \approx 10u$
  - It is this which determines required 'bandwidth'
  - Note $\varepsilon \approx u^3/\ell$ where u and ℓ are velocity and length scales for the energy-containing turbulence
- 'Bandwidth' =

$$\frac{\text{timescale of e-c eddies}}{\text{timescale of smallest scales to be resolved}} = \frac{\ell/10u}{10\eta/10u} \propto \mathrm{Re}^{\frac{3}{4}}$$

- Compare

$$\frac{\text{timescale of e-c eddies}}{\text{Kolmogorov timescale}} = \frac{\ell/u}{(\nu/\varepsilon)^{\frac{1}{2}}} \propto \left(\frac{u\ell}{\nu}\right)^{\frac{1}{2}} = \mathrm{Re}^{\frac{1}{2}}$$

Fundamental concepts: stability

$$v_p = \omega / k$$

$$v_g = \frac{\partial \omega}{\partial k} \sim \frac{\partial x}{\partial t}$$

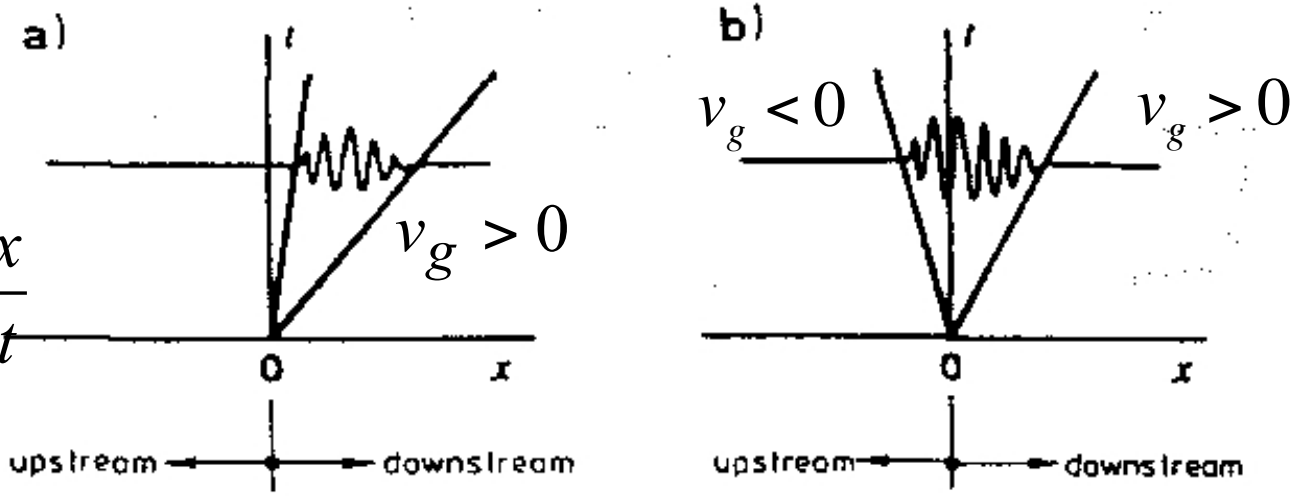

Fig. 8. Amplification of a perturbation at (a) convective- and (b) absolute instability.

- Most shear layers are convectively unstable: eg boundary layers, mixing layers – "amplifiers".
- Absolute instability: group velocity of any one perturbation has both positive and negative values such that disturbance grows in time at any *x*-location – "oscillators".
- Several separated flows have a "pocket" of absolute instability which, at sufficiently high Re can lead to a global instability – e.g. vortex shedding/ Kármán vortex street
- Group velocity, v_g, speed at which changes in the shape of the wave packet propagate – finite in a dispersive medium.

Fundamental concepts: receptivity

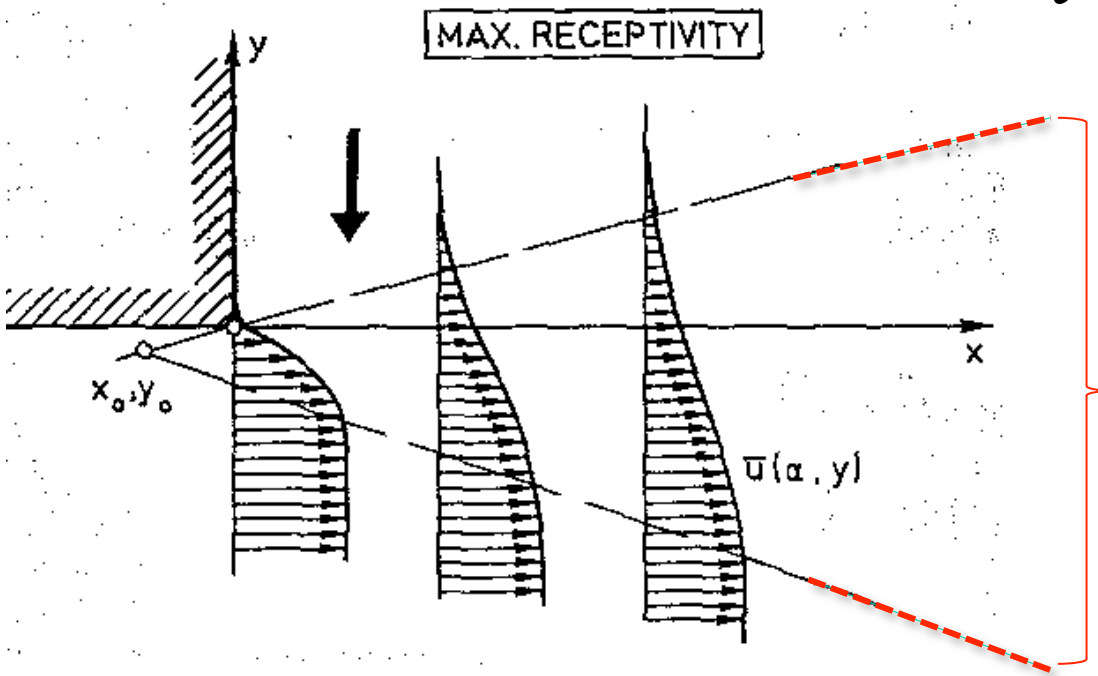

Fig. 9. *Locus of maximum receptivity in a mixing layer.*

- "Receptivity" points in flow particularly susceptible to forcing, i.e. from which disturbances will amplify.
- Requires impressing a constant frequency / wavelength so that this matches a dominant component of the base flow and there is an exchange of energy (see Brown Roshko structures, chapter 1).
- Typically these are points at which there are large gradients in the base flow and where a given perturbation provides maximum relative perturbation – *vU'*.

Attached wall eddies

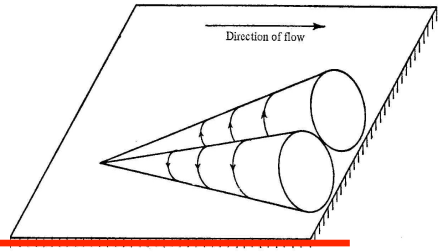

- Does top-down effect lead to:

  "modulation" of near-wall motion (Hutchins & Marusic 2007)?
  or streamwise vortices (Hunt & Morrison 2000) and hence –
  plane (oblique) waves (Sirovich 1990, Carpenter 2007)?

- Are viscous waves dynamically significant at high Re? – far too long a timescale?

- What is the role of wall-normal velocity and pressure fluctuations – "Anti-splats" as well as Splats (local surface stagnation points)?

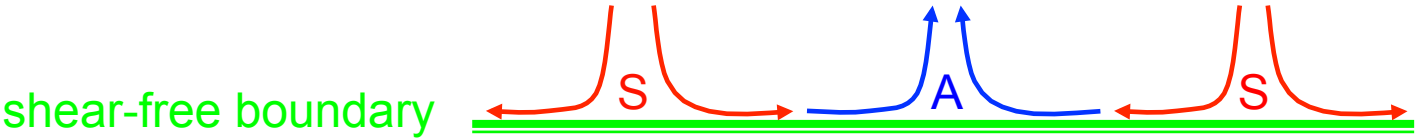

- Viscosity alters the balance between A and S: pressure-strain effects transfer of energy from v – component to u and w (Perot & Moin 1995)

Backup

- TS waves / receptivity

Results: One Actuator – Phase Lag

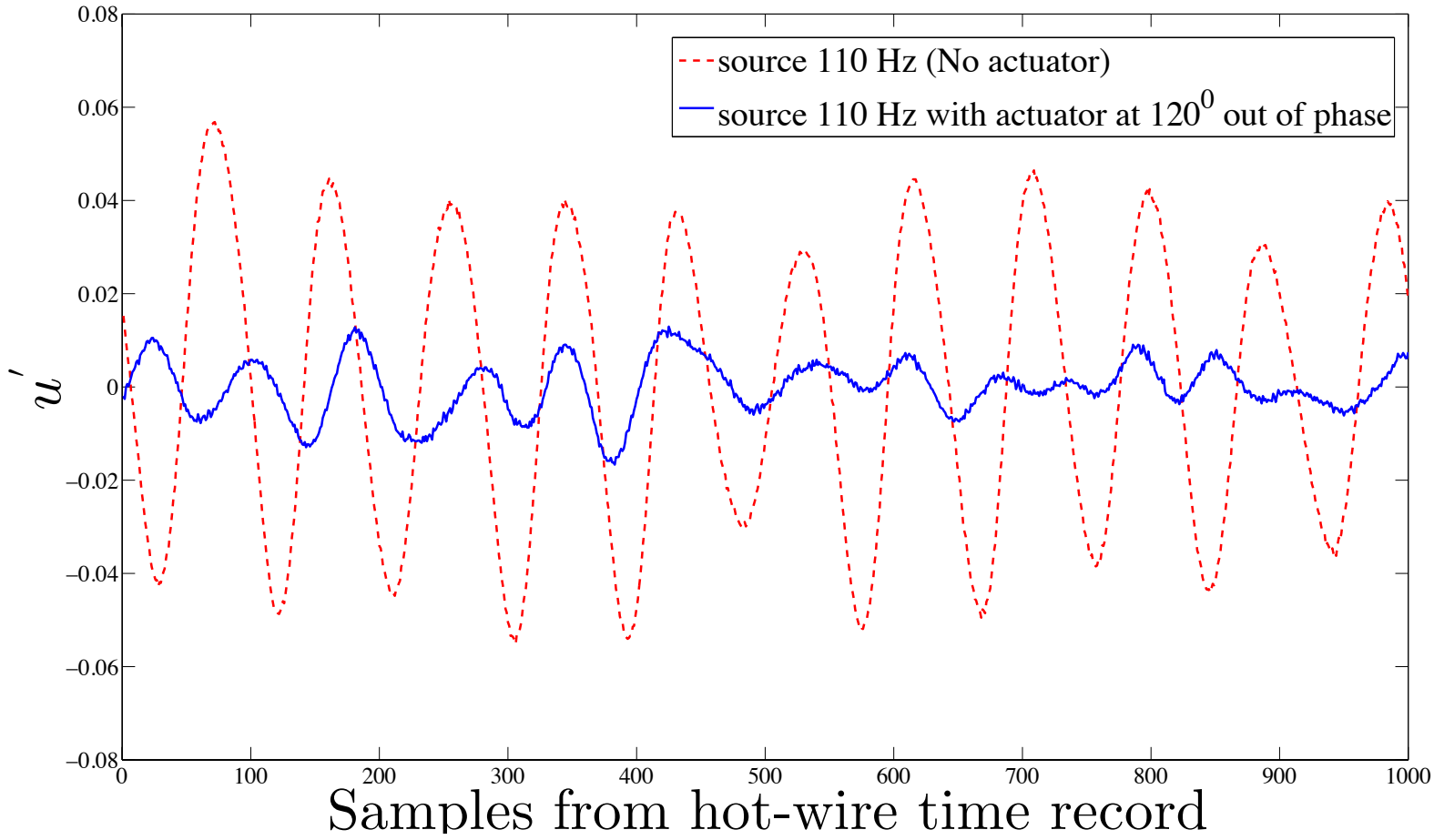

12 ms^{-1}, 83.5 cm from leading edge, 0.2 mm from plate

System ID: G_s

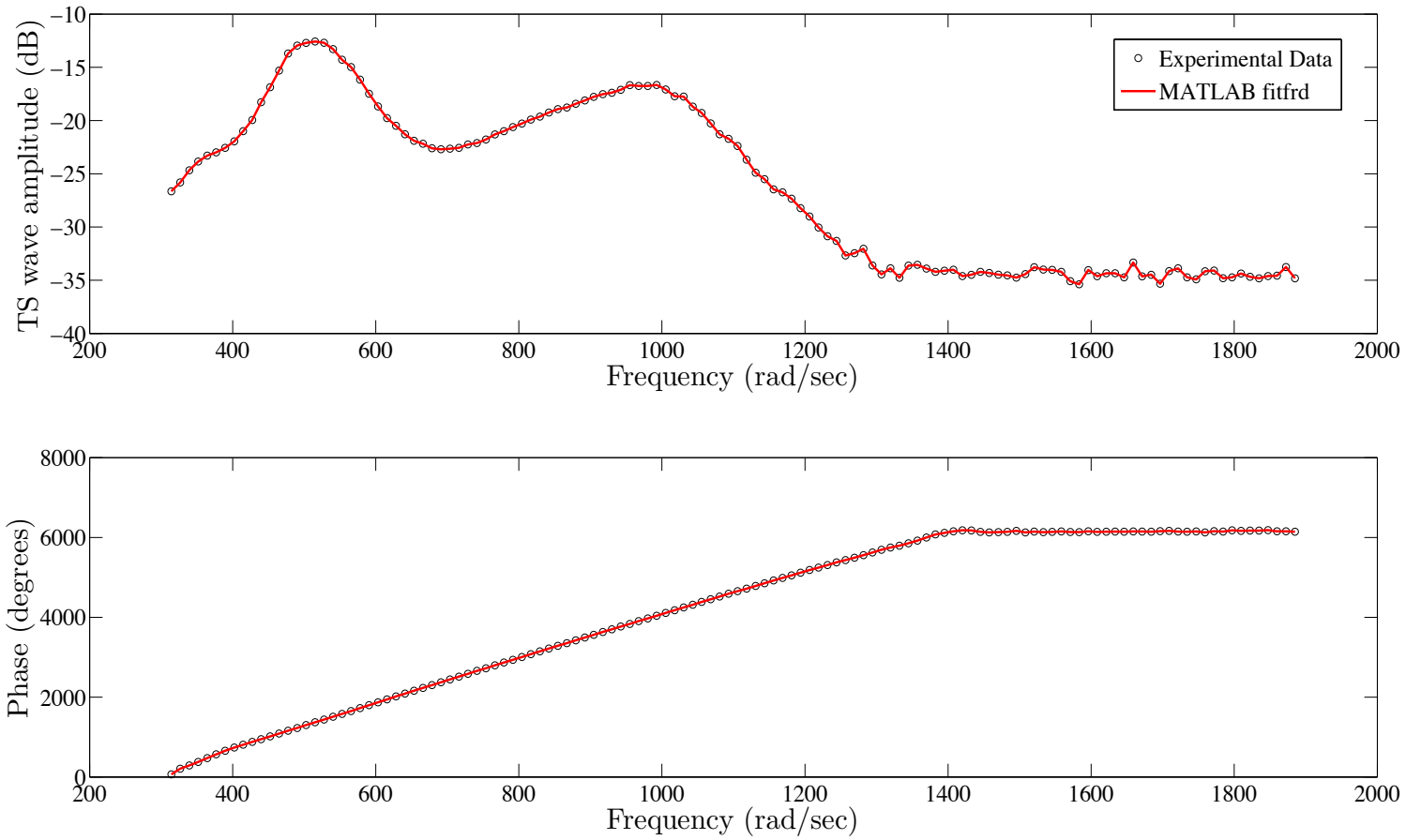

Frequency sweep for G_s at x = 697mm, 12 ms^{-1}

Transfer function G_a

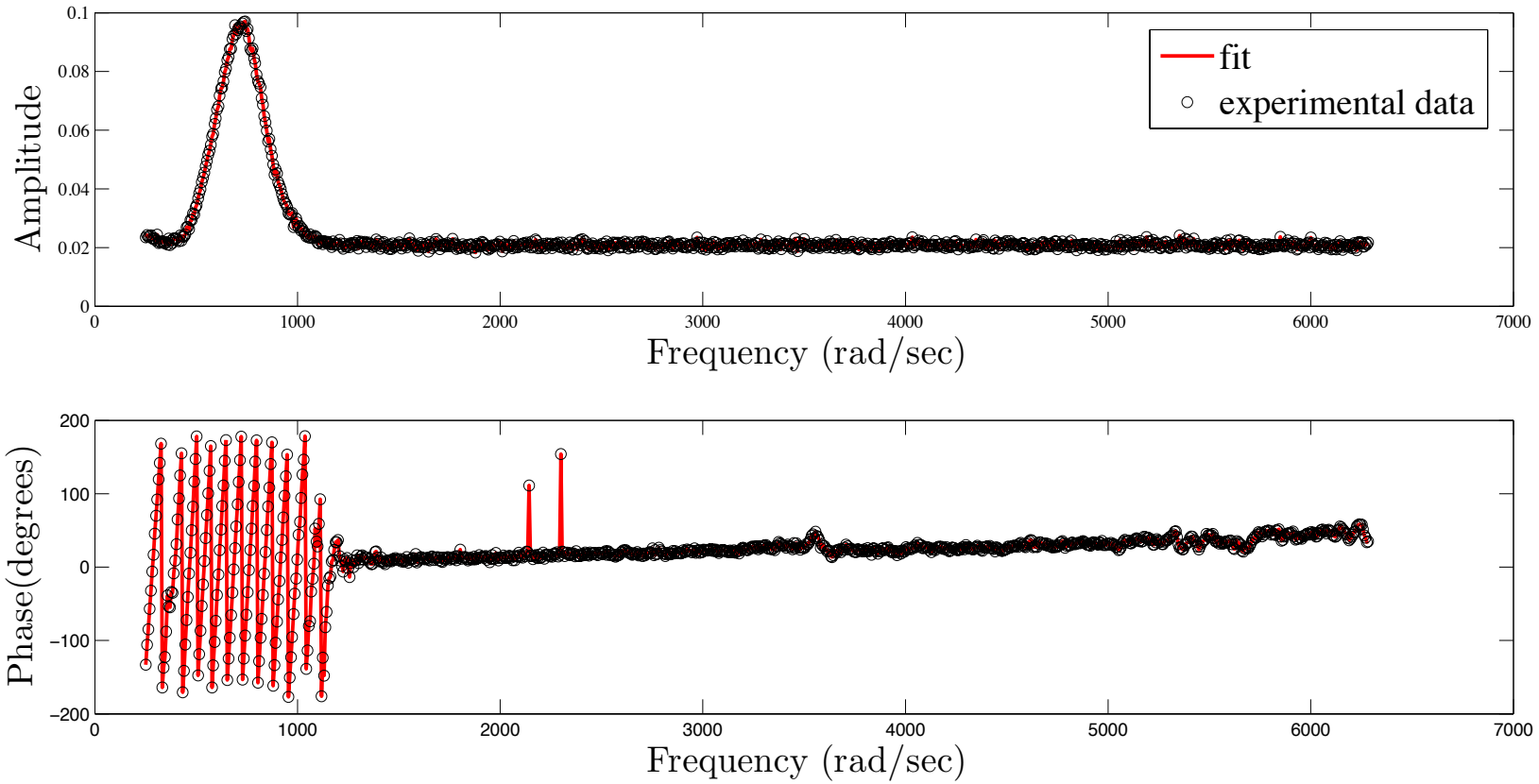

Frequency sweep for G_a at x = 800mm, 12 ms^{-1}

Summary – old

- System data shows a non-minimum phase system
- One actuator driven out-of-phase with the source is able to produce cancellation
- The controller is being designed and tested on various sensor-actuator configurations numerically to obtain the optimal one
- This controller will then implemented to perform real-time cancellation of TS waves with the optimal configurations experimentally
- Testing of configurations based on state-space methods with spatial discretisation of linearised N-S equations

Intensity Profiles with Subtraction

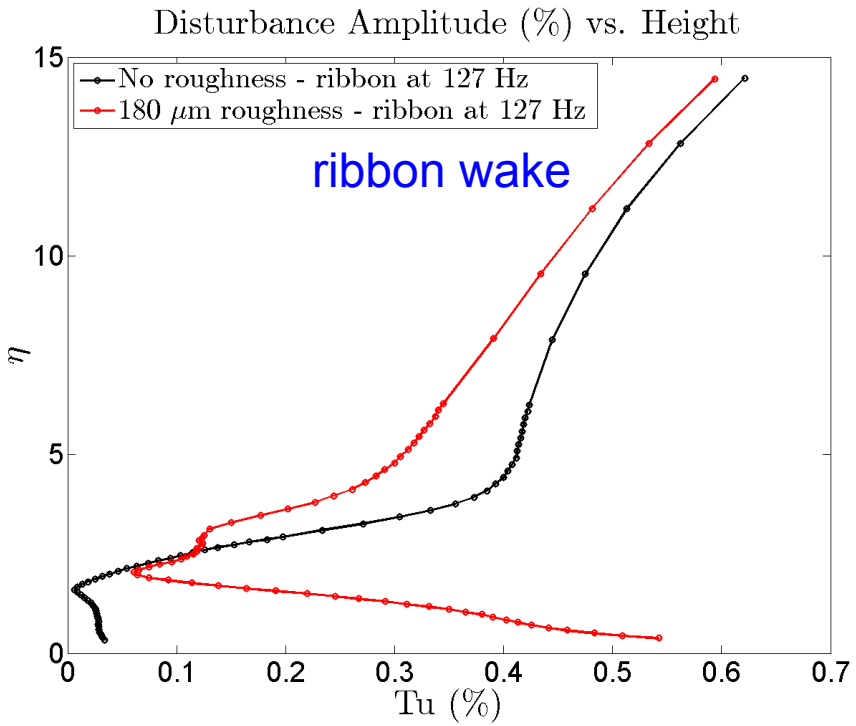

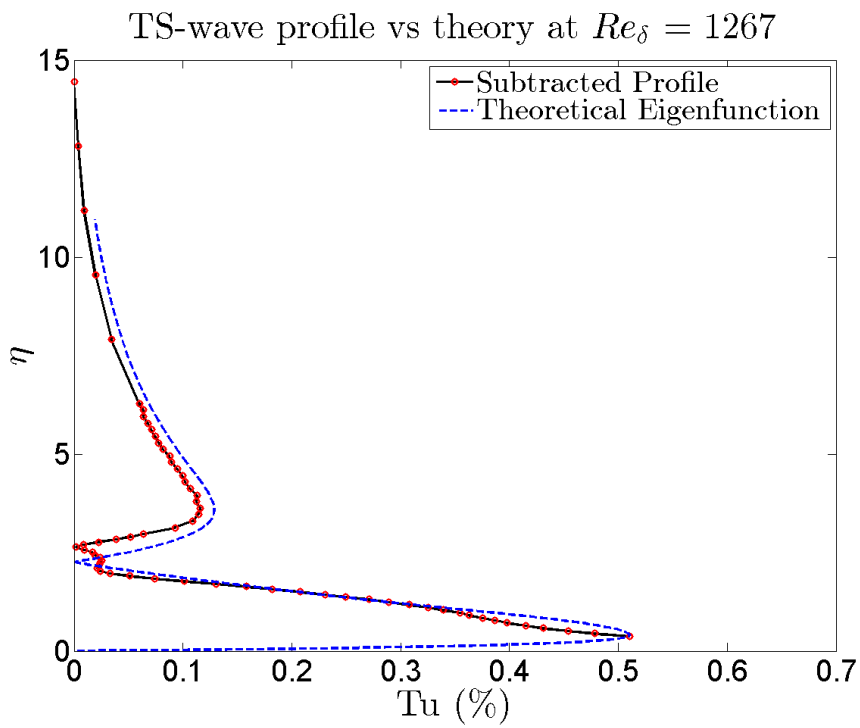

- Subtract 'no-roughness' amplitude profile from the roughness case
- The resulting profile compares well with the theoretical eigenfunction $\phi(y)$

Experimental Growth Rate *vs*. Theory

- Streamwise growth rates similar to 2D theory
- Closest fit to theory for a slightly adverse pressure gradient (β = -0.01)
- Falkner-Skan: $U(x) = U_1 x^m$

$$\beta = \frac{2m}{m+1}$$

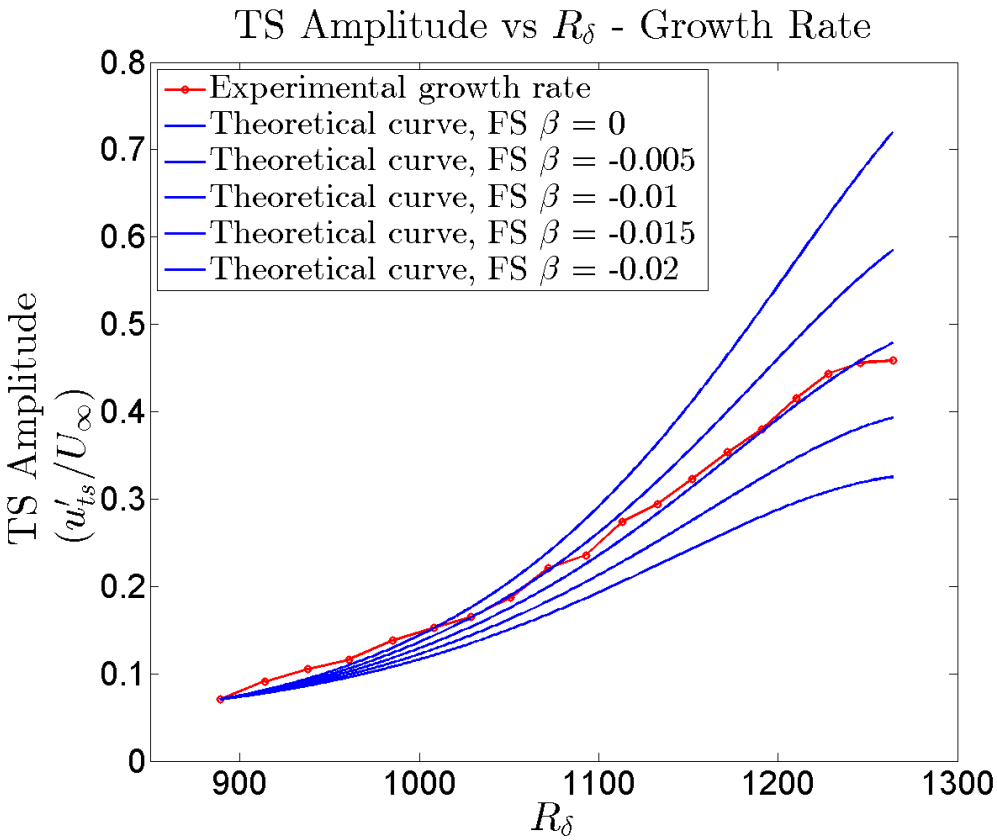

Linearity with Forcing Amplitude

- No roughness: increasing of forcing amplitude has very little effect
- Roughness: TS amplitude increases linearly with forcing amplitude
- Linear up to 0.8% − almost identical to Dietz (1999)

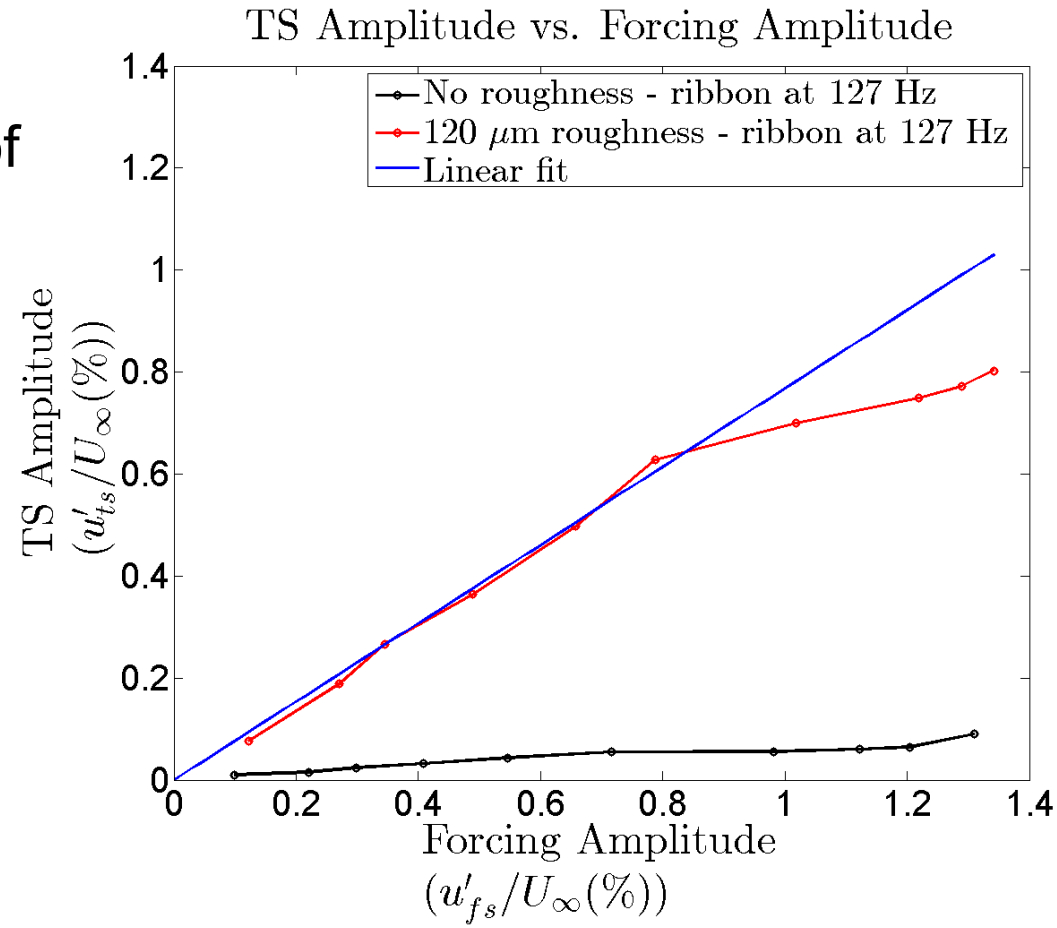

Linearity With Roughness Height

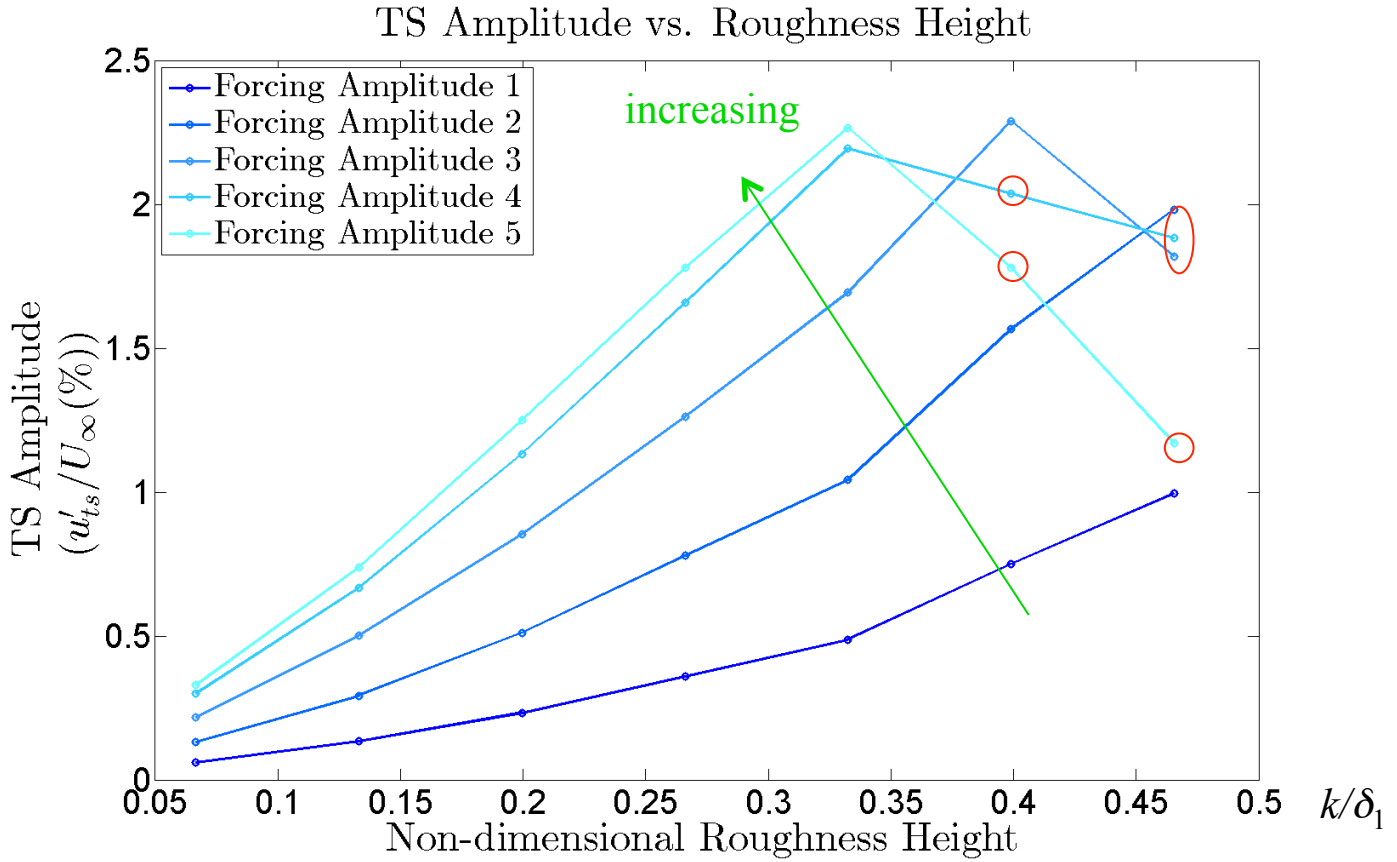

- Linear theory valid up to boundary layer inner deck height – $0.1\delta_1 \approx \eta \approx 0.2$
- Saturation / attenuation at high forcing amplitudes and roughness heights

Effects of variable forcing amplitude

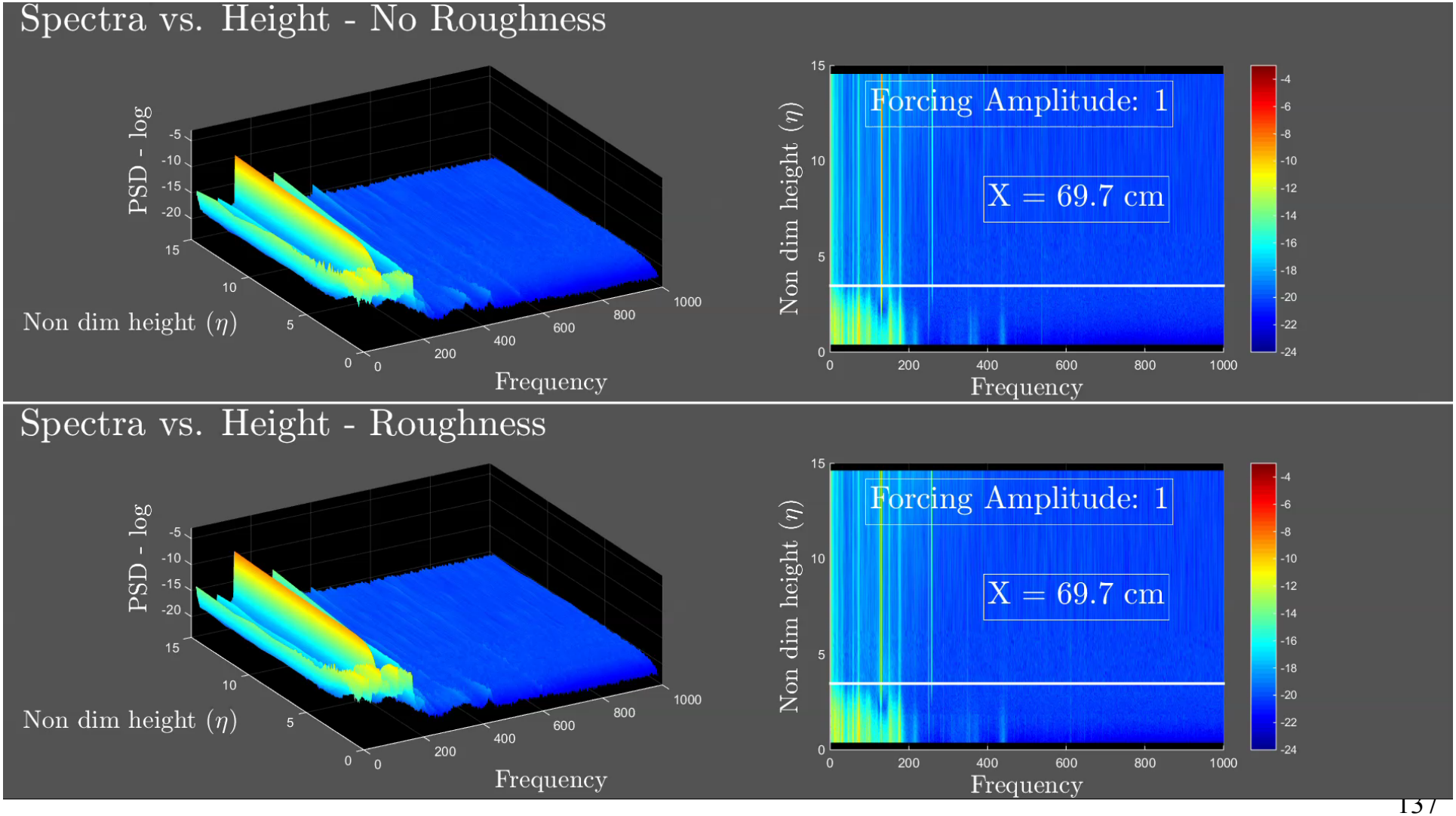

Backup

- Bypass

Feedback control - schematic

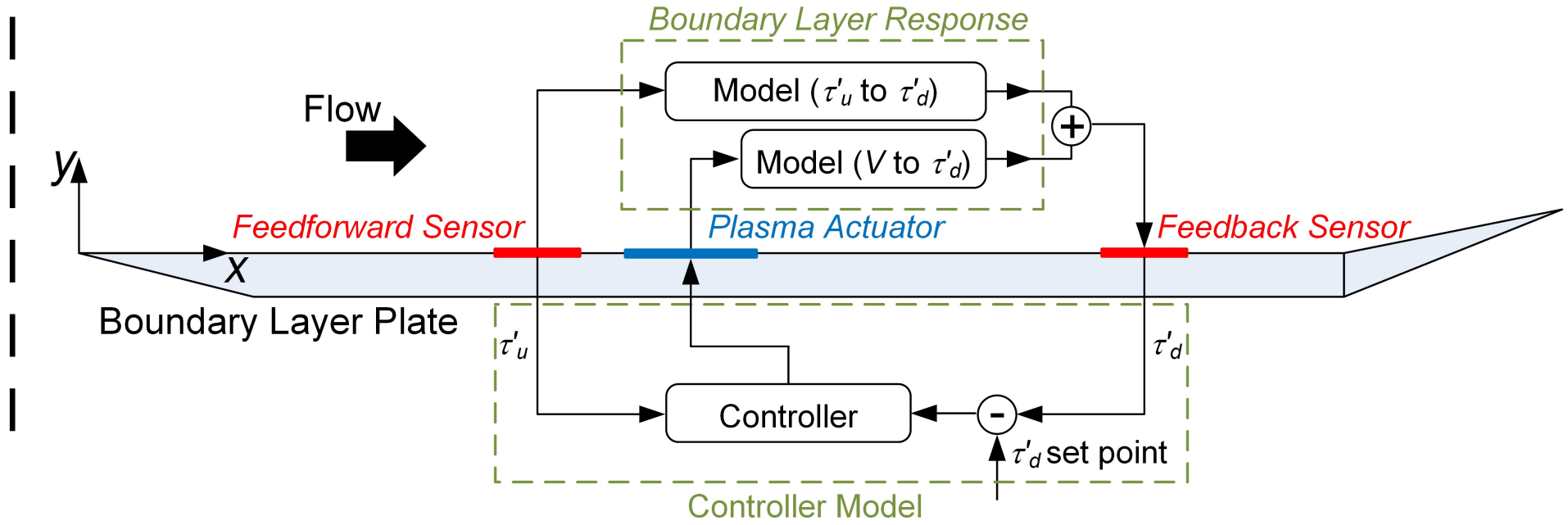

Schematic control diagram

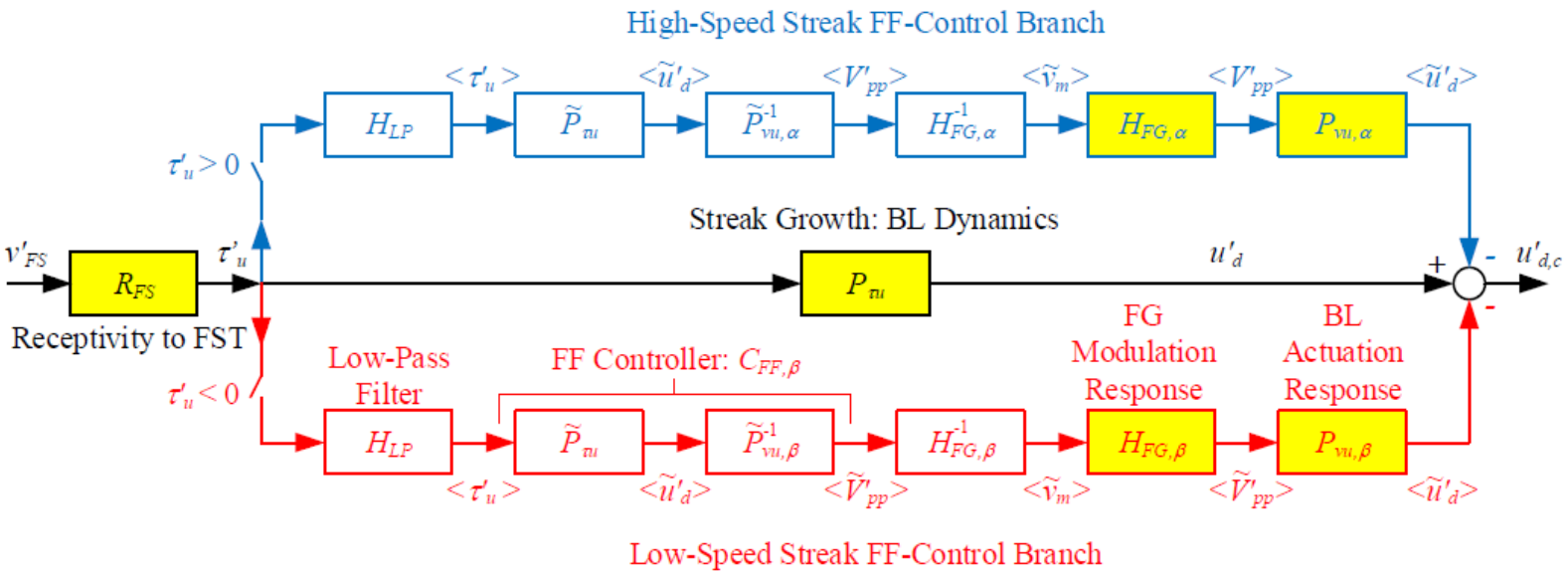

Naguib, A.M., 2015, Imperial-College Experiment on Localized Reactive Control of Streaks: A Brief Report on Sabbatical Work

Single-point LSE

Model for disturbance at downstream wall-shear sensor based on a measurement at the upstream wall-shear sensor

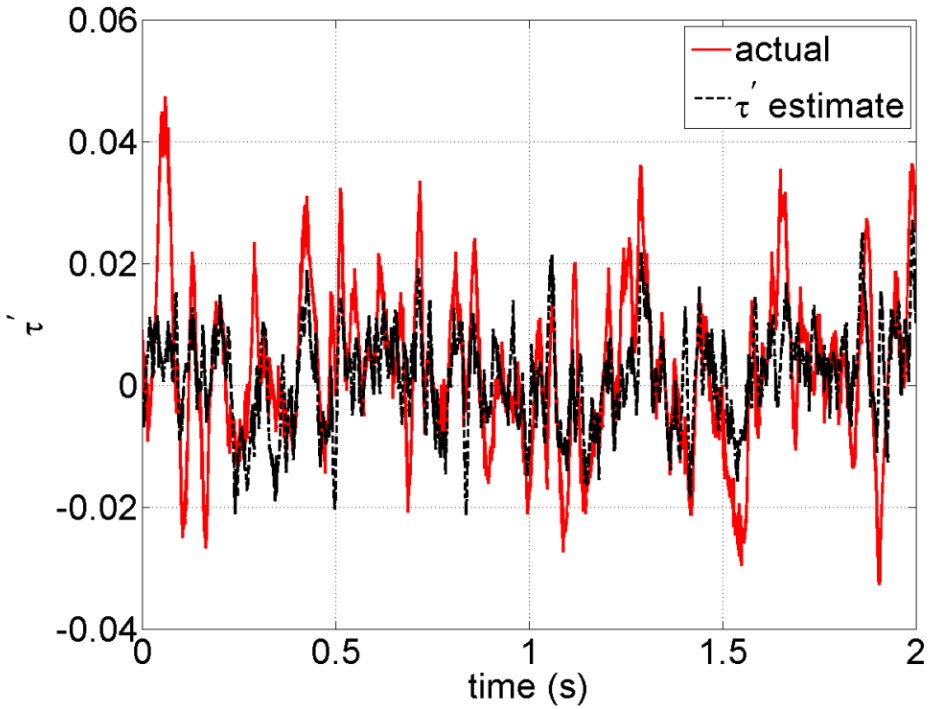

Feedforward control: hot-wire at peak r.m.s

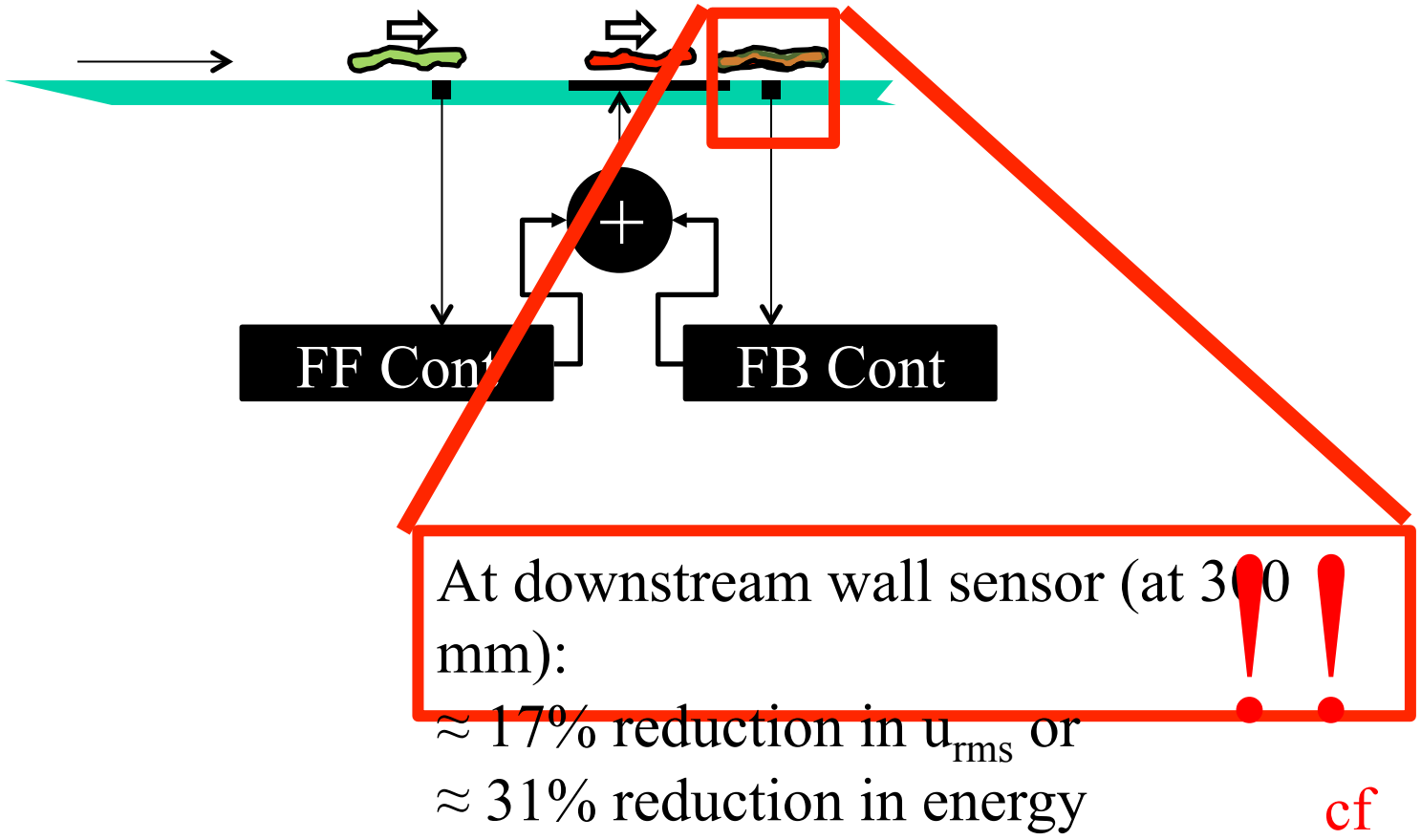

- Compute spectra of downstream (feedback) sensor data.
- Compute correlation coefficient between upstream and downstream sensors.

Generation of transient growth

$$\eta = y/\delta = y\Big/\sqrt{x\nu/U_\infty},\ \beta = 2\pi\delta/\Delta z$$

$$\mathrm{Re}_\delta = U_\infty\delta/\nu,\ \mathrm{Re}_k = u\big|_{y=k}\,k/\nu$$

Streak amplitude $\Delta u'\big|_{\max}/2U_\infty\ \%$

White (2002): < 4

Fransson *et al*. (2004). 5.5 – 11.5

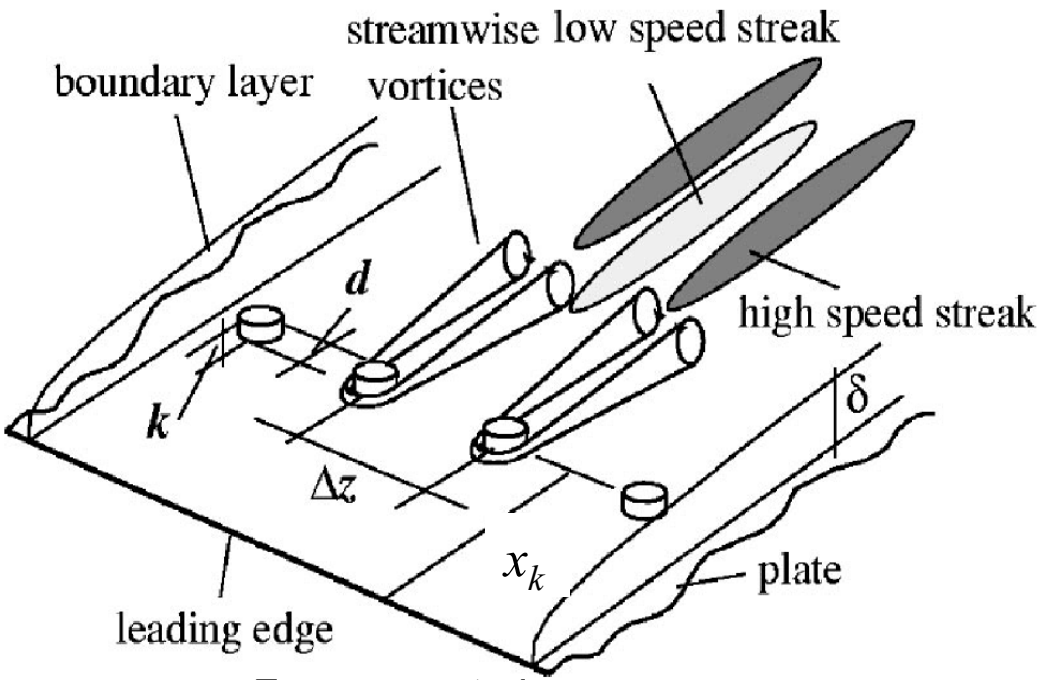

Fransson *et al*. (2004).

$2.5 \le U_\infty \le 12$ m s^{-1}

$x_k = 200$ mm

$0.14 \le \beta \le 0.53$

$162 \le \mathrm{Re}_{k,\infty} \le 498$

$36 \le \mathrm{Re}_k \le 336$

$1.5 \le \Delta u'\big|_{\max}/2U_\infty \le 13\%$

Experimental setup

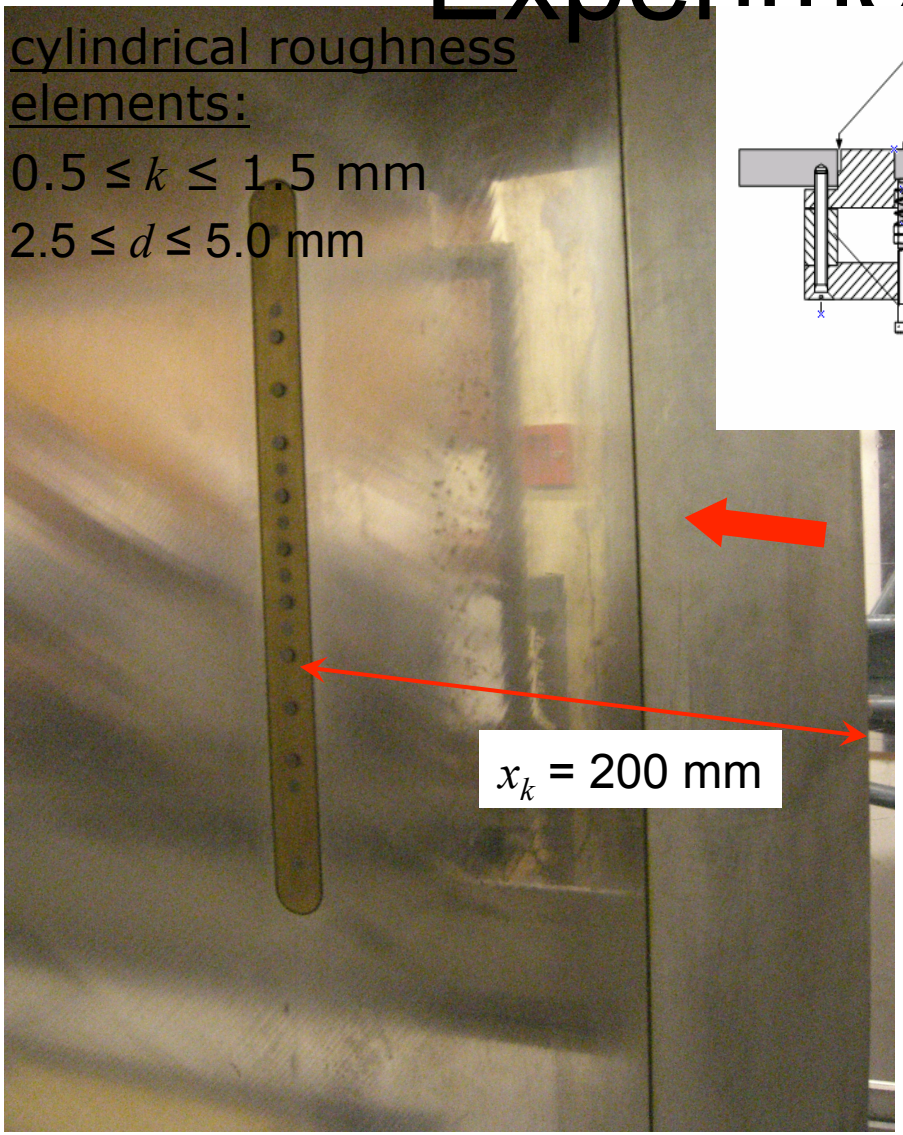

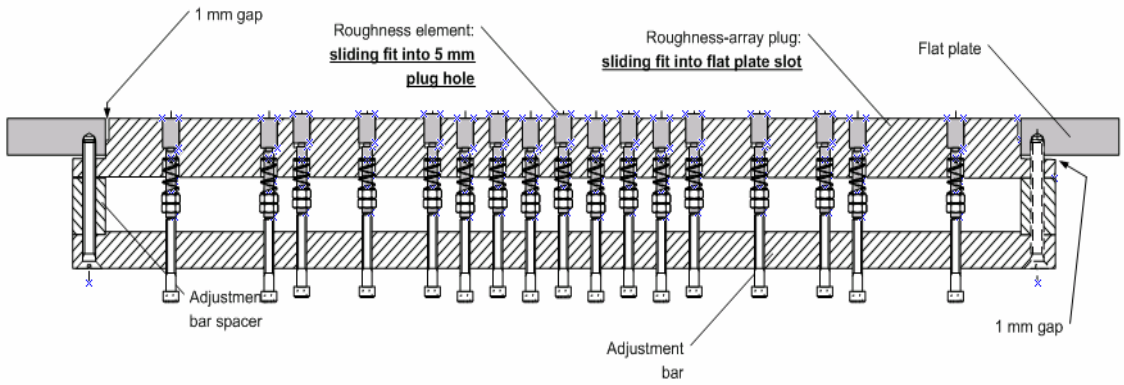

- Square contraction 9:1 – u turbulence intensity ~ 0.05%
- Vertical, polished cast aluminium plate at non-integer division of tunnel width (~ one third)
- Sharp leading edge
- Double-flap control of pressure gradient/leading-edge stagnation point

Hot-wire measurements

- Span = 8Δz: phase averaging over central 6 spaces
- u and w hot-wire measurements – co-located by interpolation
- Spanwise sampling with Δz/16 increments
- 250 ≤ x ≤ 700 mm

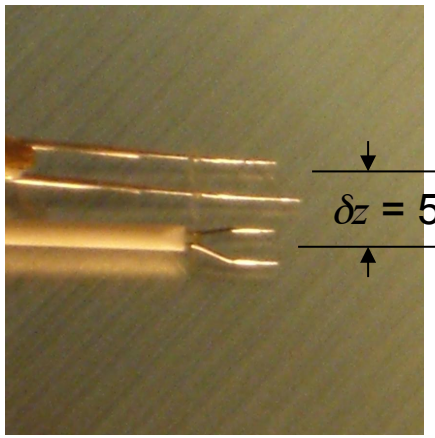

	U_∞ ms^{-1}	Δz mm	k mm	d mm	k/δ	β	Re_k	$Re_\delta\|_{x_k}$
1	5.0	10.0	0.50	5.0	0.7	0.48	35	262
2	5.0	10.0	1.00	5.0	1.3	0.48	141	262
3	5.0	10.0	1.50	5.0	2.0	0.48	313	262
4	5.0	10.0	1.50	2.5	2.0	0.48	301	262
5	10.0	10.0	0.71	5.0	1.3	0.34	200	370
6	2.5	20.0	1.42	5.0	1.3	0.34	98	185

$\beta_{opt} \approx 0.45$

Case 4: u'/U_∞

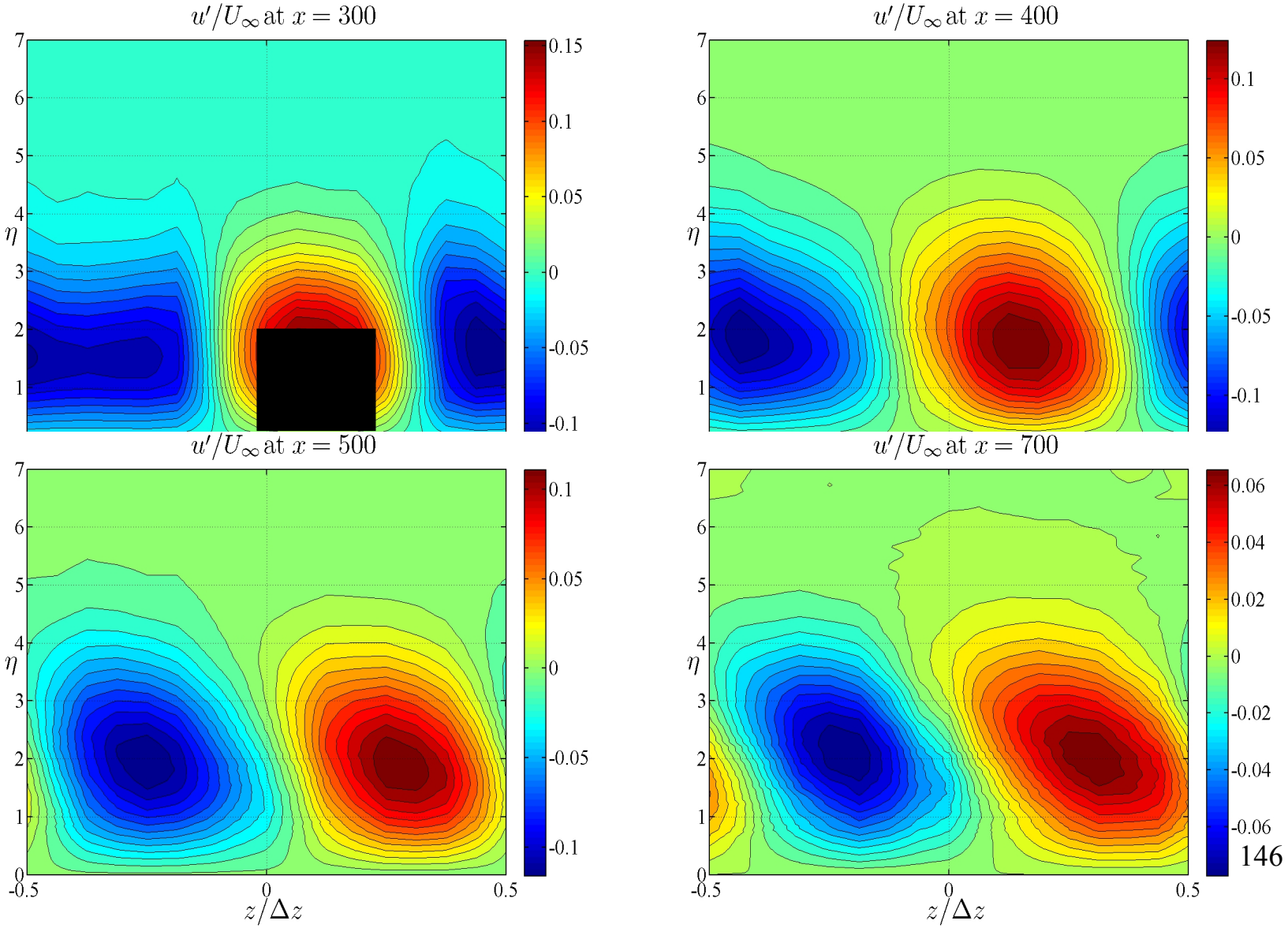

x/d=120

u'/U_∞

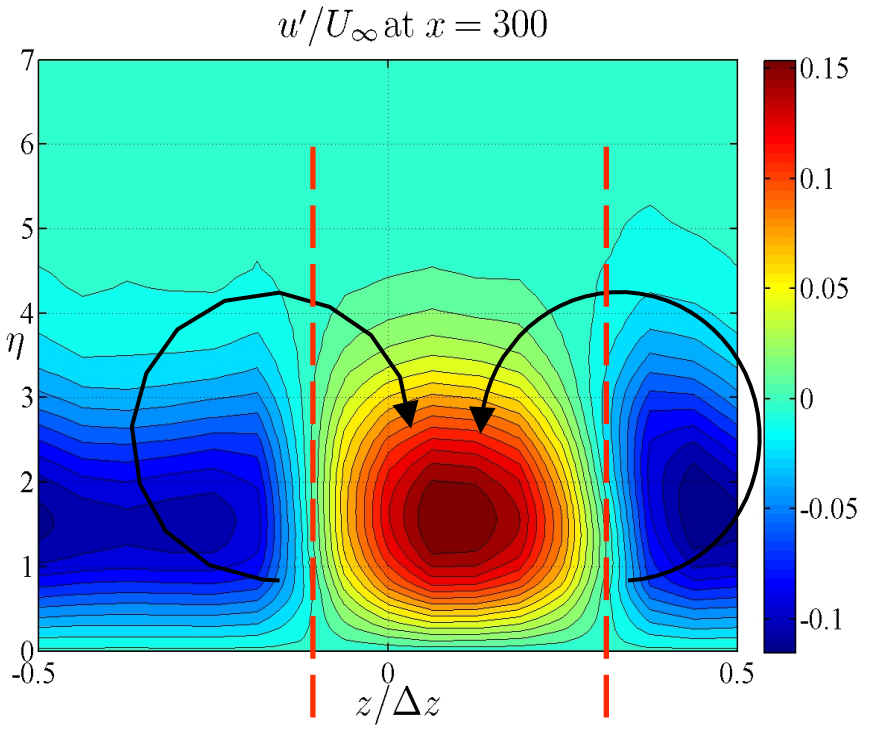

$w'/U_\infty = W/U_\infty$

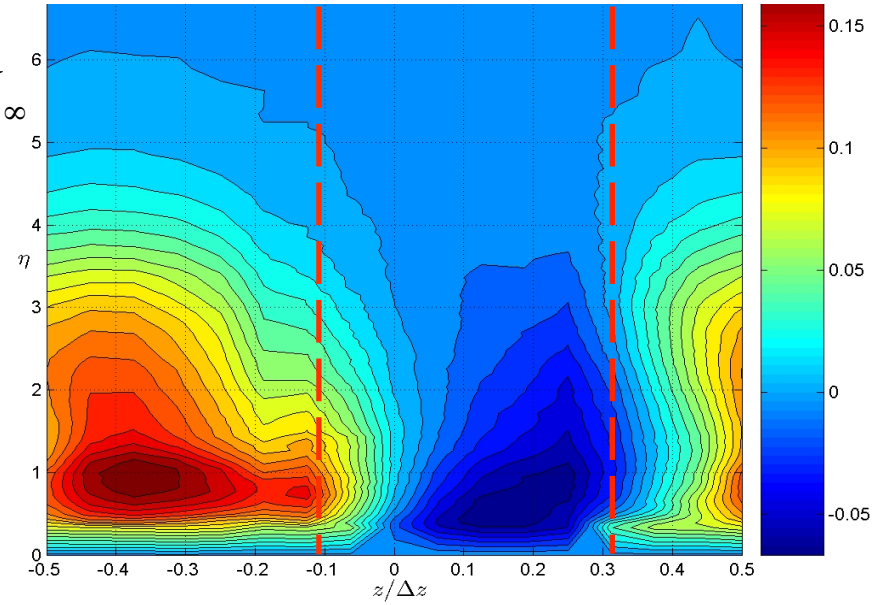

2-component LDA

Case 4 (β =0.48) x/d=120

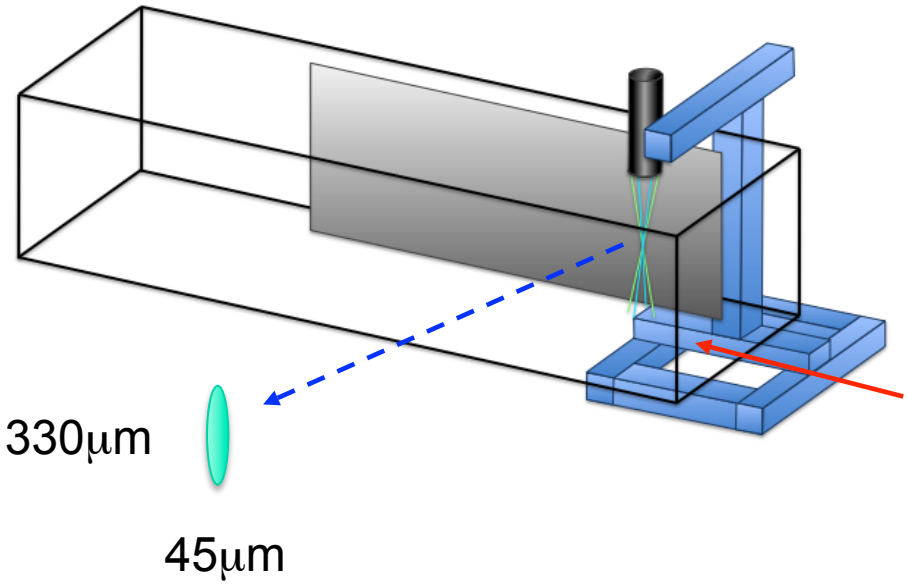

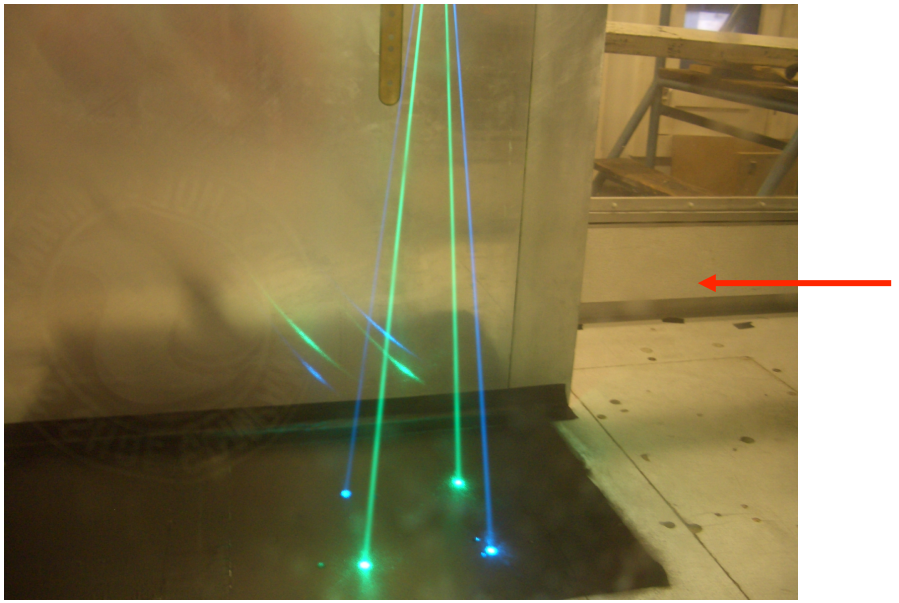

- Laser beams polarised to give *u, v*
- Two sets of fringes generate ‘bursts’ of reflected light
- Doppler shift gives particle velocity

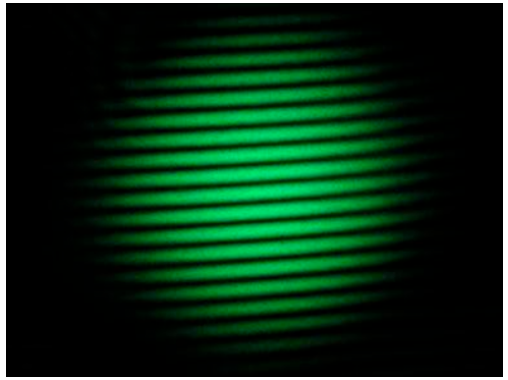

2-component LDA

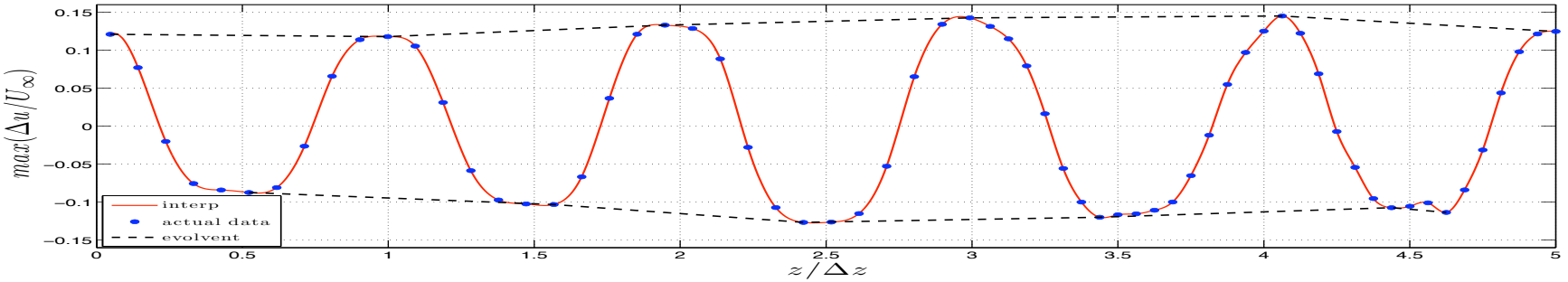

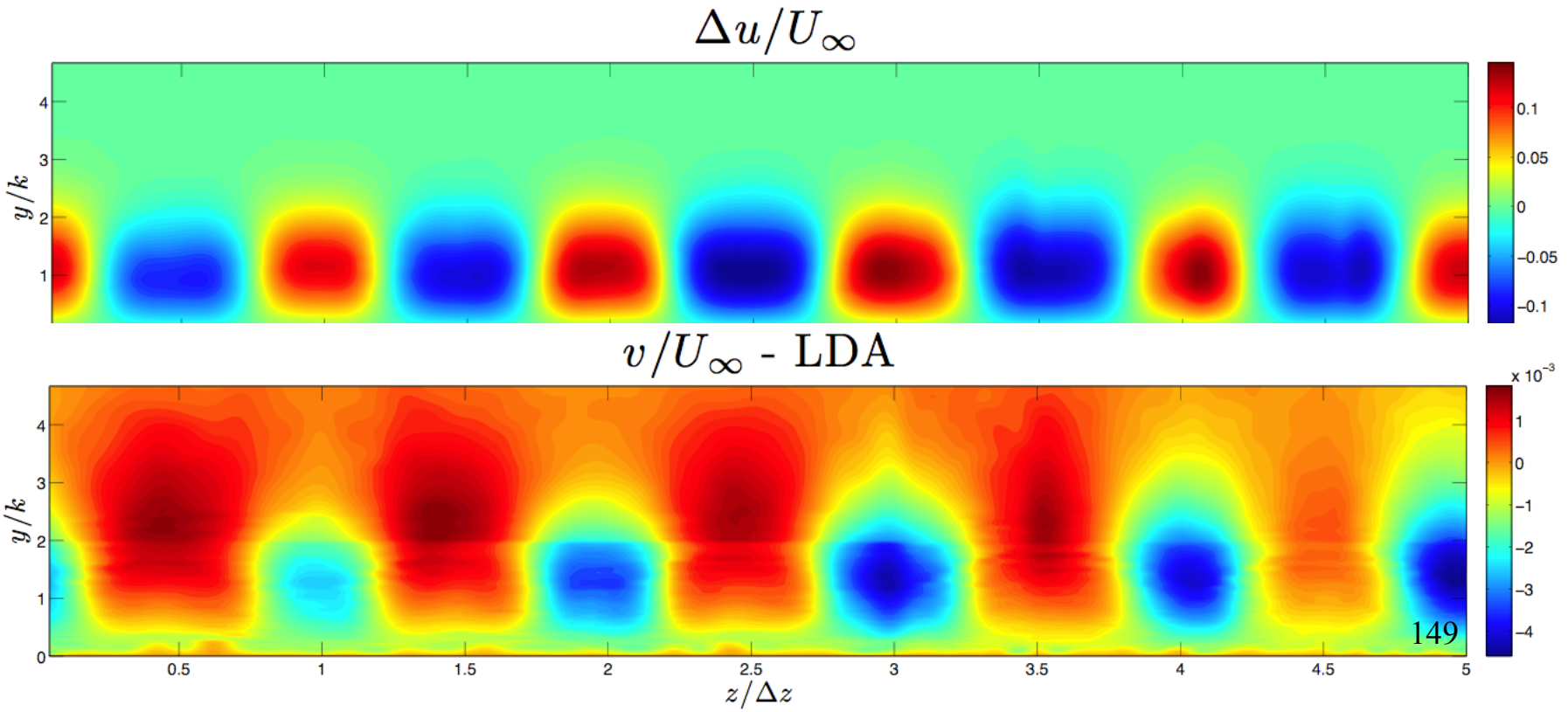

Disturbance profiles and spectra: hot wire

Case 4 (β =0.48)

x/d=120

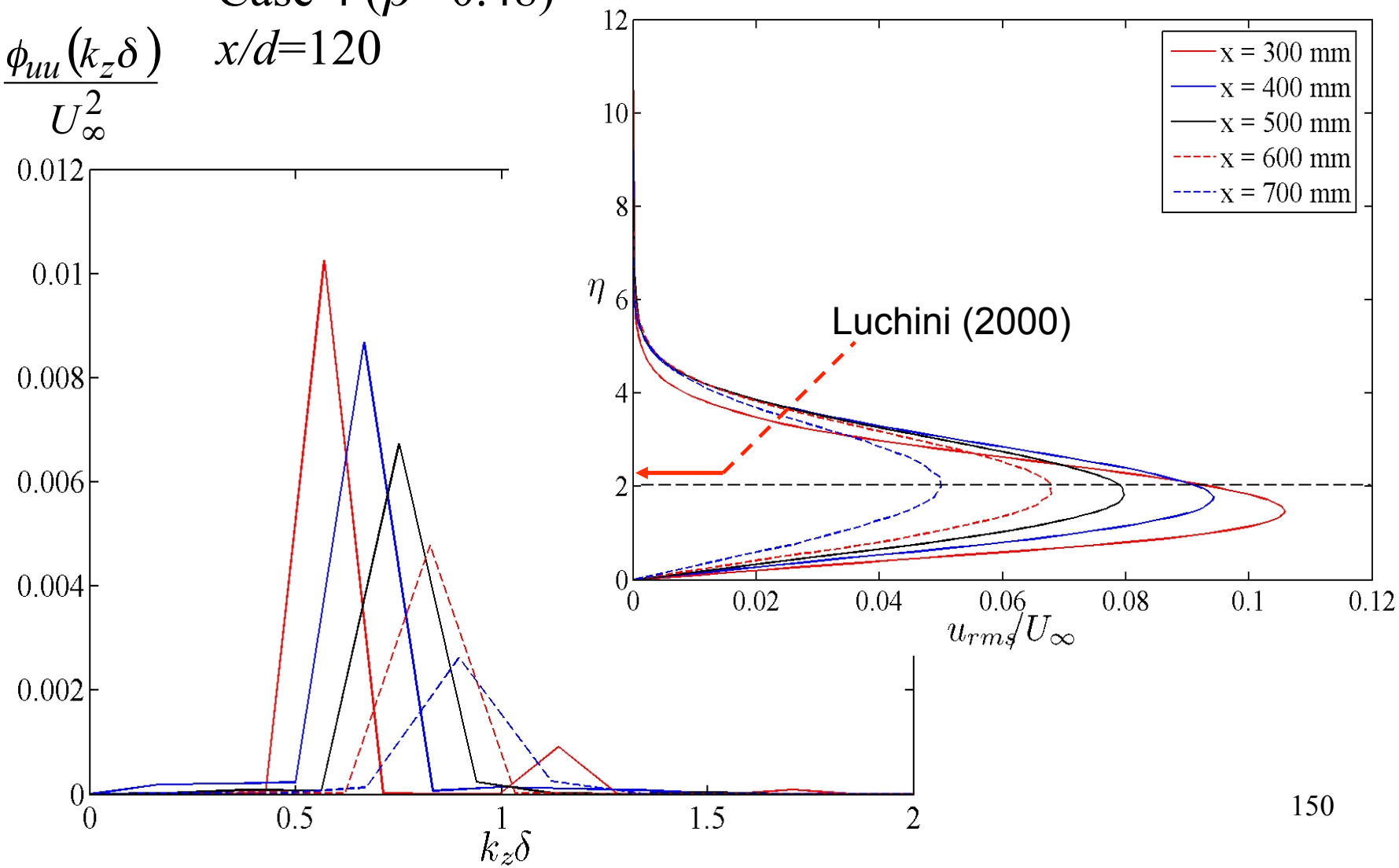

Disturbance spectra: hot wire

Case 15 (β =0.22)

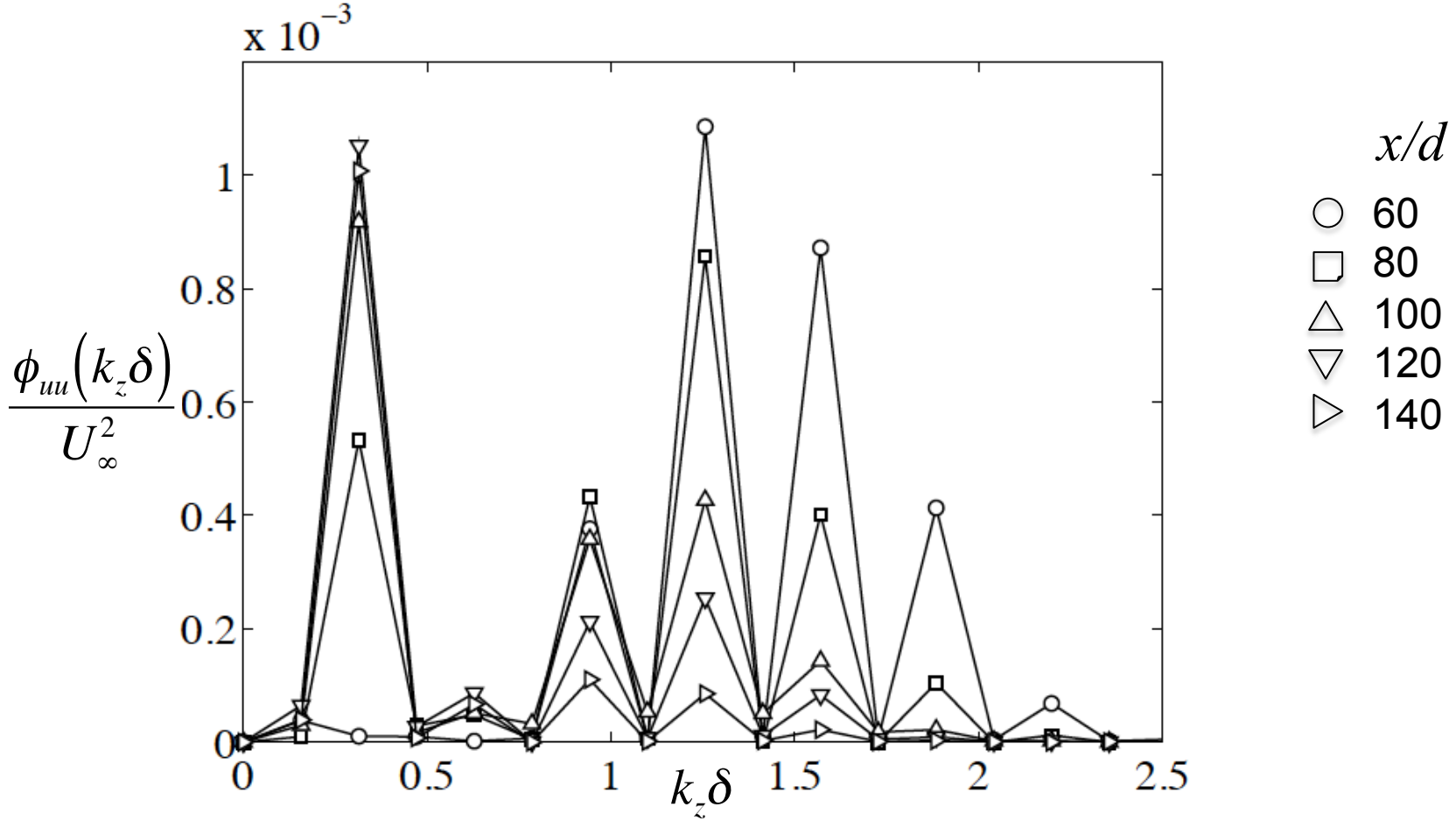

Case 15 ($\Delta z/d = 4$)

Actuators based on electro-active polymers

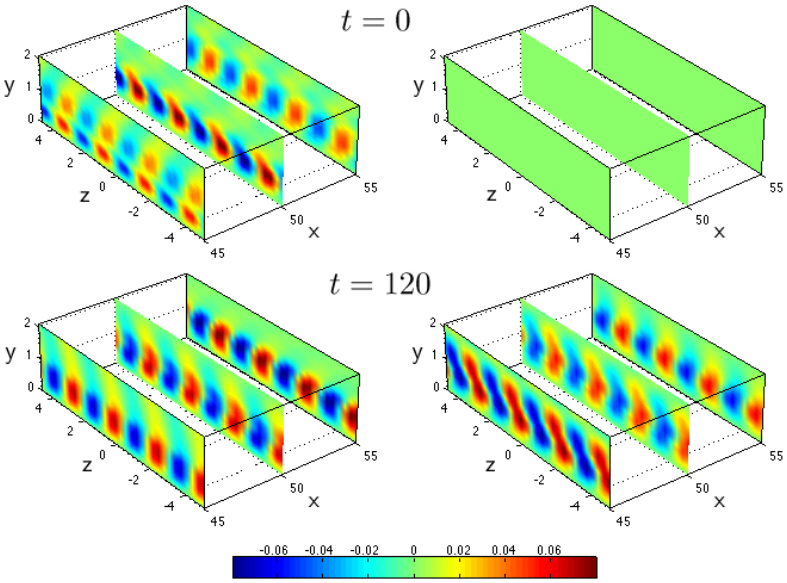

(a) u' - left: DNS data; right: reconstruction using Kalman filter estimates

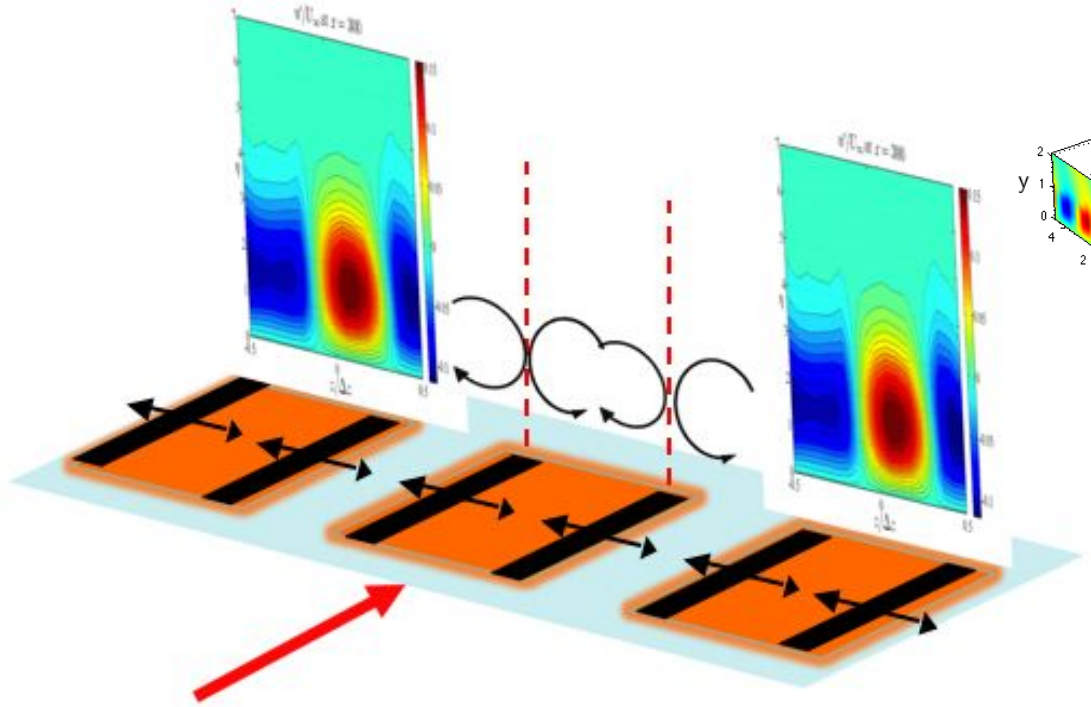

(b) Detail of EAP actuator arrays (orange with black electrodes), in which actuators at resonance with in-plane motion induce streaming motion towards surface indicated by circular arrows. Red/blue contours show low/high velocity regions respectively arising from steady forcing.

Non-normality

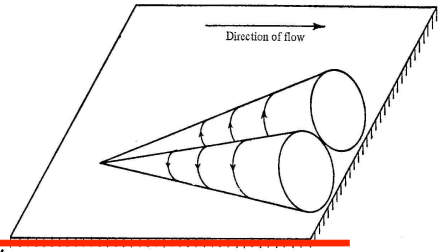

Sketch from

Rempfer (2003)

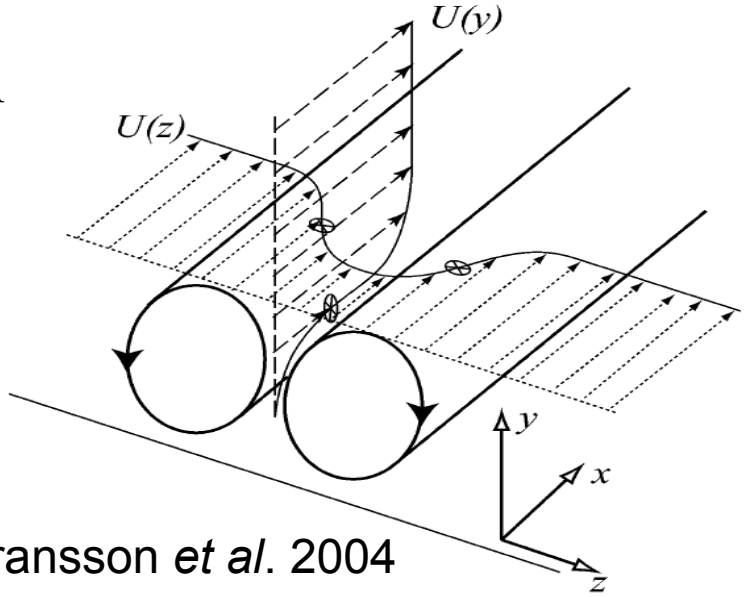

Sketch from Fransson *et al*. 2004

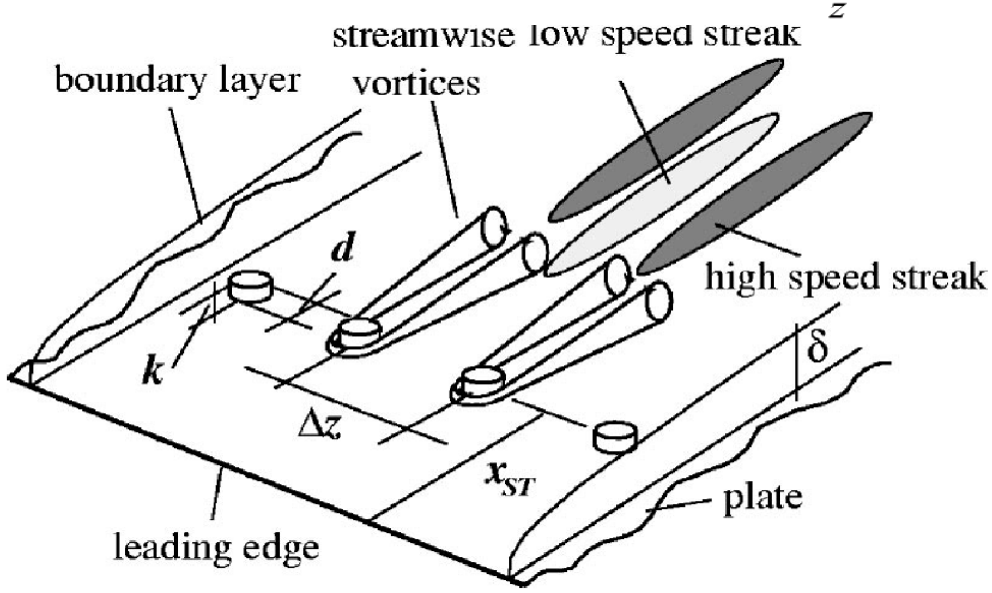

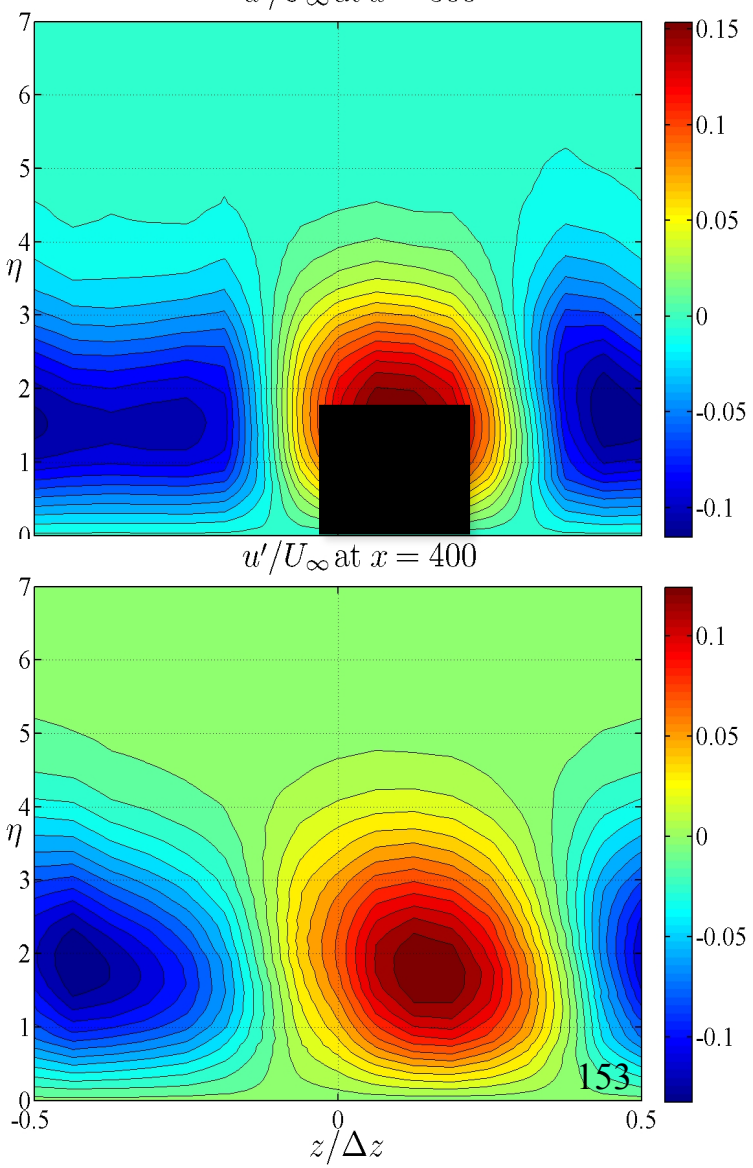

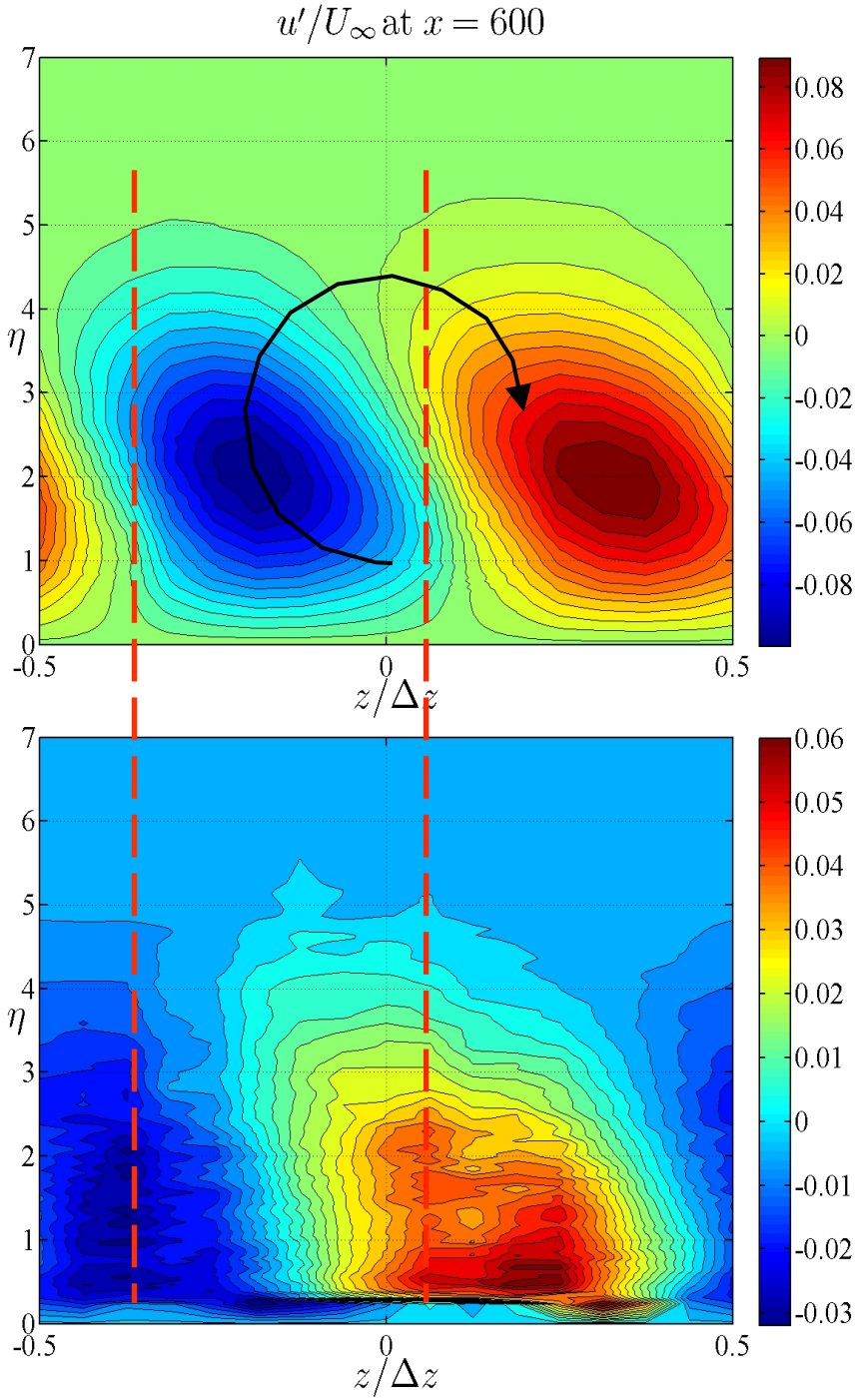
u'/U_∞ at $x = 600$
η
$z/\Delta z$
0.08
0.06
0.04
0.02
0
-0.02
-0.04
-0.06
-0.08
0.06
0.05
0.04
0.03
0.02
0.01
0
-0.01
-0.02
-0.03

The energy balance

Advection= $$\frac{D\left(\frac{1}{2}\overline{u_i^2}\right)}{Dt} = \frac{Dq}{Dt} = P_{ii} + T_{ii} + D_{ii} + \Pi_{ii} + \varepsilon_{ii}$$

- Production $$P_{ii} = -\overline{u_i u_j}\frac{\partial U_i}{\partial x_j} = -\overline{uv}\frac{\partial U}{\partial y}$$
- Turbulent transport $$T_{ii} = -\frac{\partial\left(\overline{qu_j}\right)}{\partial x_j} = -\frac{\partial\left(\overline{qv}\right)}{\partial y}$$
- Viscous transport $$D_{ii} = 2\nu\frac{\partial^2 q}{\partial x_j \partial x_j} = 2\nu\frac{\partial^2 q}{\partial y \partial y}$$
- Pressure transport $$\Pi_{ii} = -\frac{1}{\rho}\frac{\partial\left(\overline{u_i p'}\right)}{\partial x_i} = -\frac{1}{\rho}\frac{\partial\left(\overline{vp'}\right)}{\partial y}$$
- Dissipation $$\varepsilon_{ii} = \nu\overline{\left(\frac{\partial u_i}{\partial x_j}\right)^2}$$

The energy balance

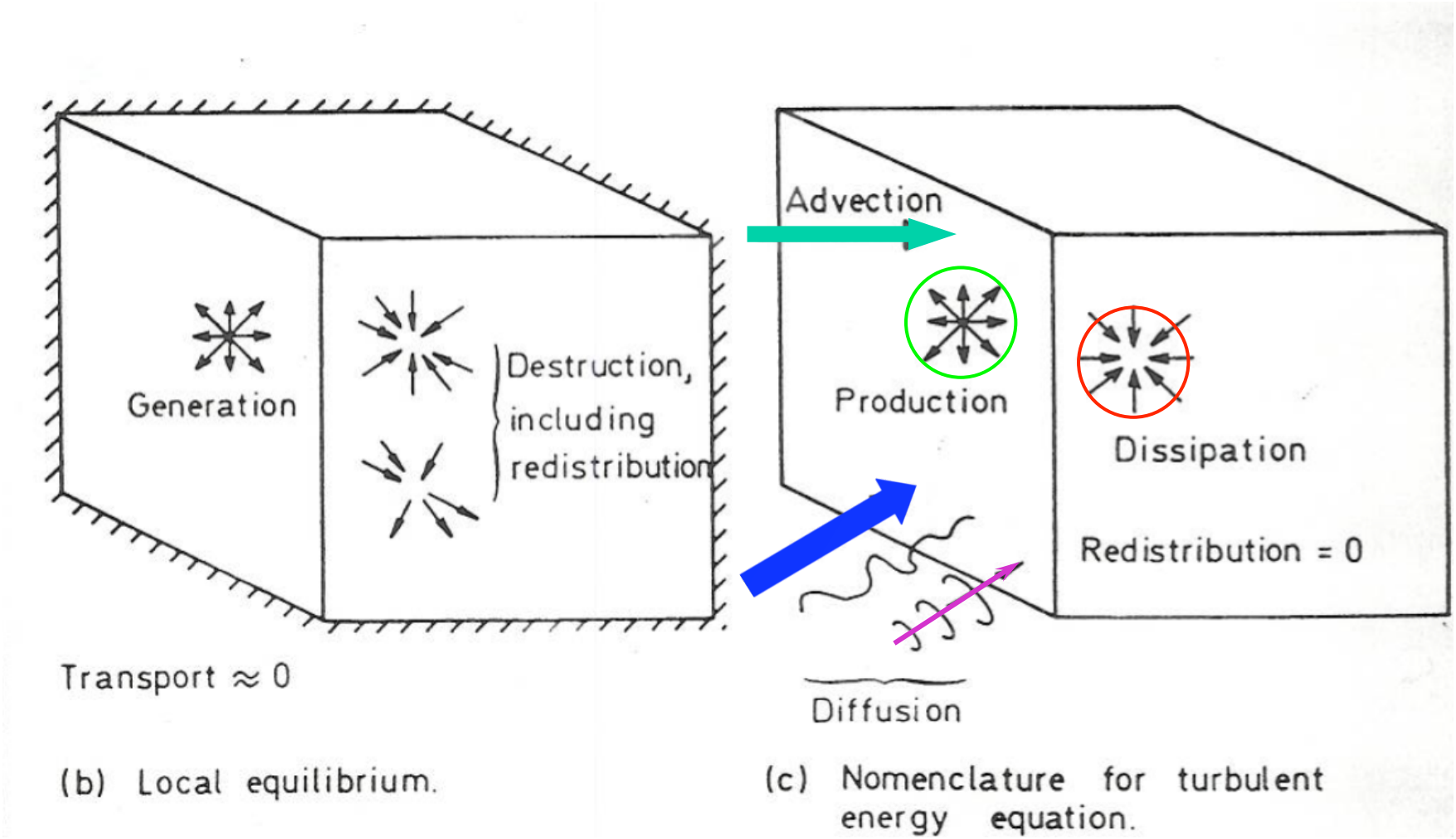

The energy balance

• Left-hand side: "Advection" – the rate of transport of q by the mean flow

•P_{ii}: "Production" – the rate at which the mean velocity gradients do work against the Reynolds stresses

•T_{ii}: "Turbulent transport" – the rate of transport by the turbulent velocity fluctuations

•D_{ii}: "Viscous transport" – the rate of transport by viscous stresses, diffusion

• Π_{ii}: "Pressure transport" – the rate of tranport by pressure fluctuations

• ε_{ii}: Dissipation rate" – the rate at which viscous stress fluctuations do work against the fluctuating rate of strain

Mathematical representation: the energy balance for channel flow (a thin shear layer)

$$\frac{D\left(\frac{1}{2}\overline{u_i^2}\right)}{Dt} = -\overline{uv}\frac{\partial U}{\partial y} - \frac{\partial}{\partial y}\left(\frac{\overline{p'v}}{\rho} + \overline{qv}\right) - \varepsilon$$

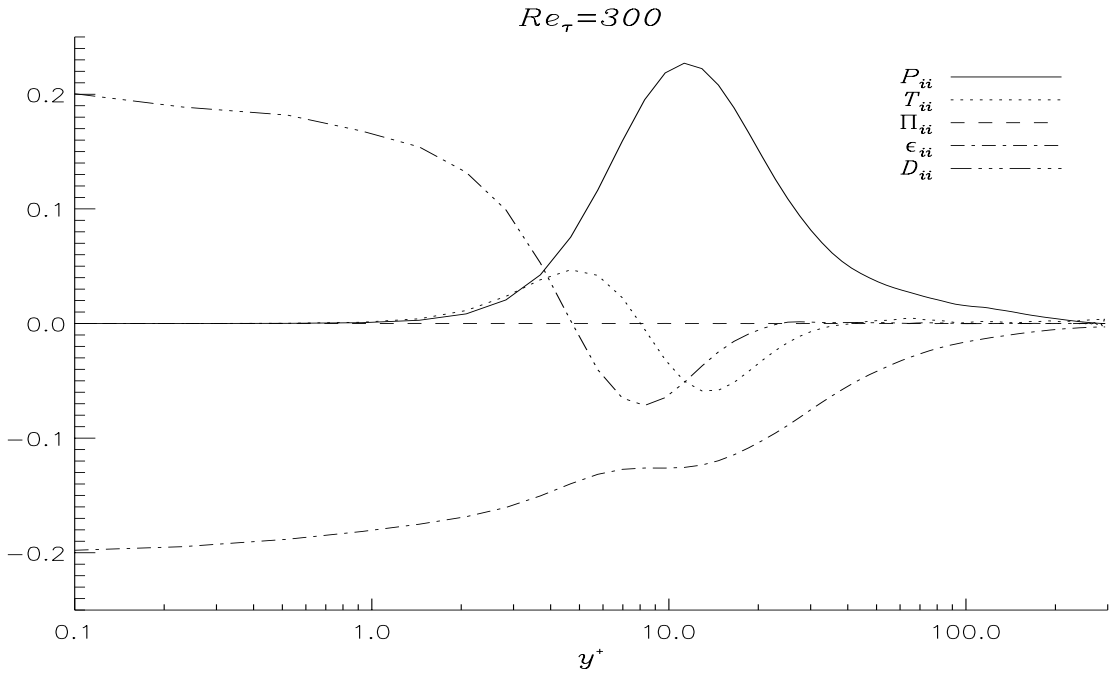

Module 2 – 20Hz

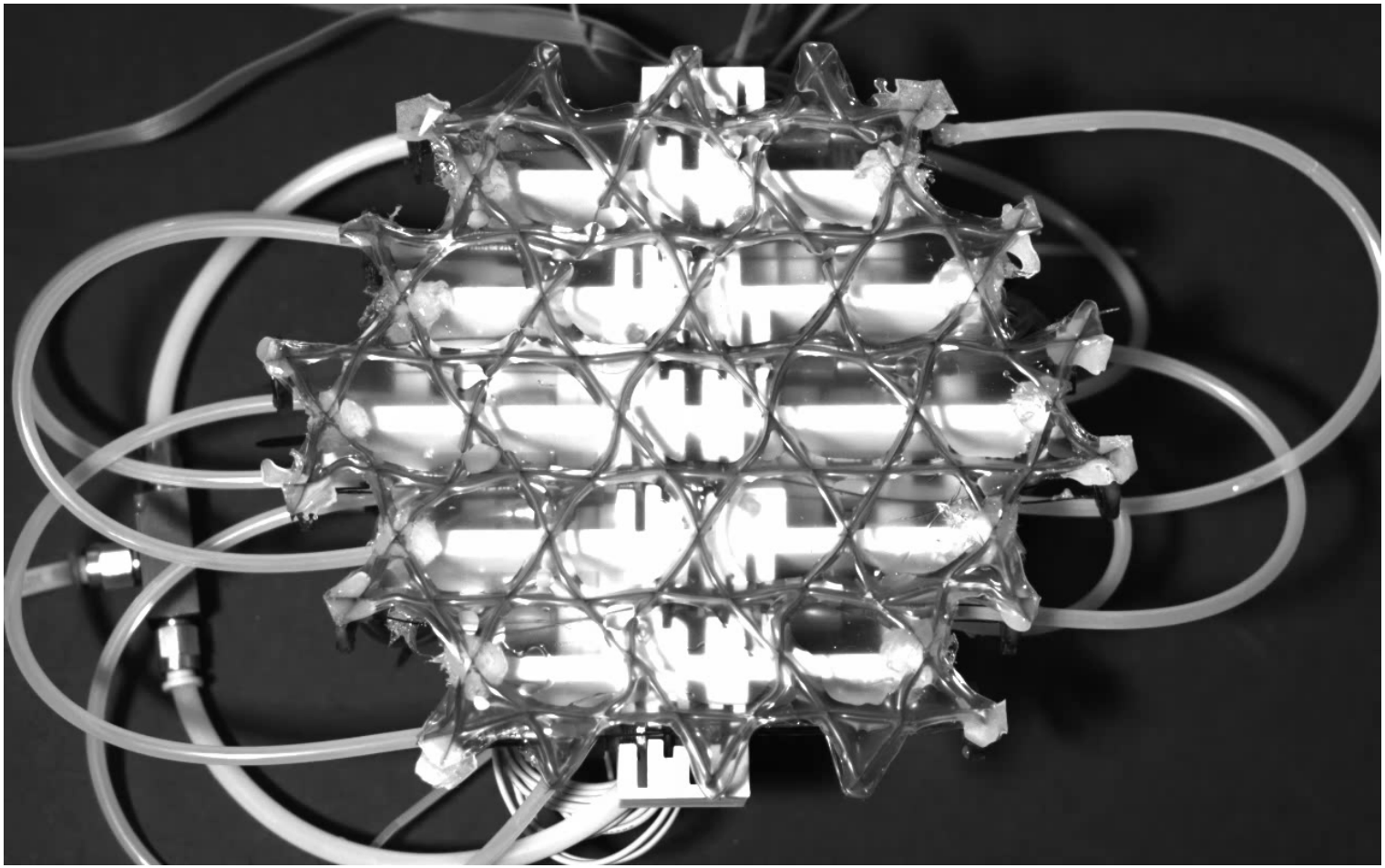

Module 2 – 55Hz

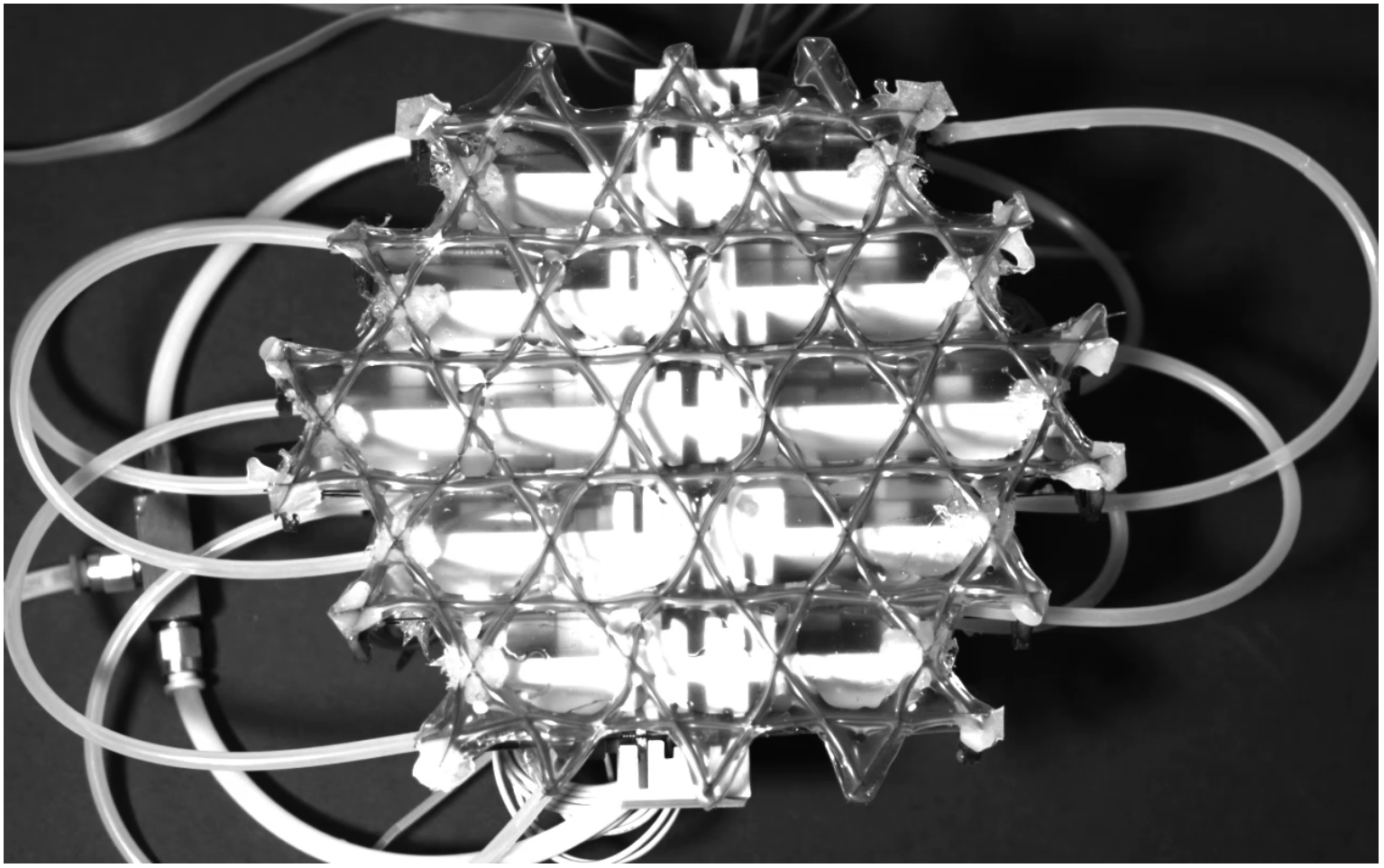

Latest module – with skin 40 Hz

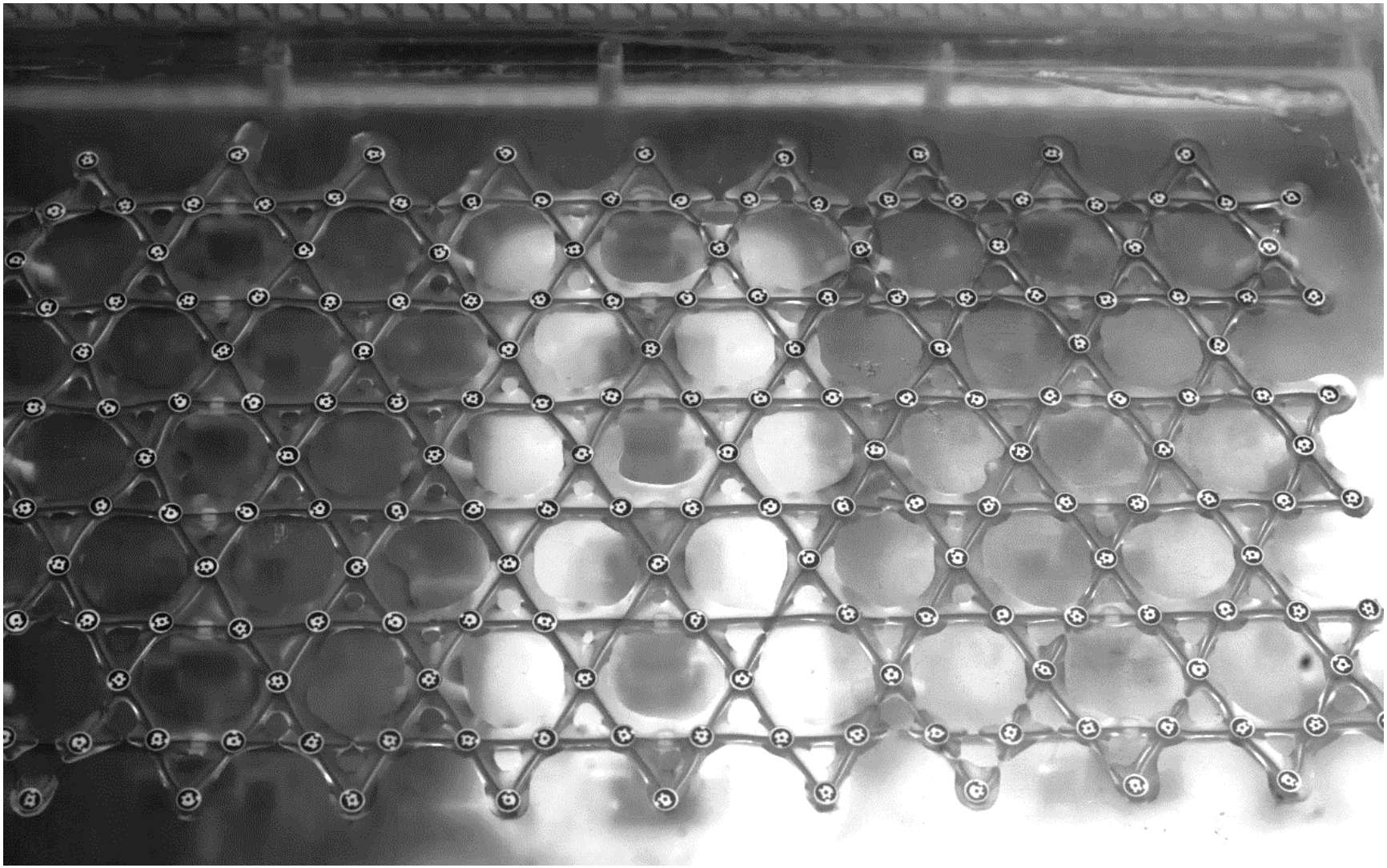

Latest module – with skin 50 Hz